BNL-52351-2007

Laboratory Directed Research & Development Program Activities For FY 2007

Annual Report

BROOKHAVEN NATIONAL LABORATORY
BROOKHAVEN SCIENCE ASSOCIATES
UPTON, NEW YORK 11973-5000
UNDER CONTRACT NO. DE-AC02-98CH10886
UNITED STATES DEPARTMENT OF ENERGY

December 2007

Acknowledgments

The Laboratory Directed Research and Development (LDRD) Program is managed by Leonard Newman, who serves as the Scientific Director, and by Kevin Fox, Special Assistant to the Assistant Laboratory Director for Finance (ALDF). Preparation of the FY 2007 report was coordinated and edited by Leonard Newman who wishes to thank Sabrina Parrish for her assistance in organizing, typing, and proofing the document. A special thank you is also extended to the Production Services Group for their help in publishing. Of course, a very special acknowledgement is extended to all of the authors of the project annual reports and to their assistants.

Table of Contents

Introduction 1

Project Summaries 3

Complex Thin Films and Nanomaterial Properties 4

Heavy Ion Physics with the ATLAS Detector 5

Behavior of Water on Chemically Modified Semiconductor Surfaces: Toward Photochemical Hydrogen Production 6

Multifunctional Nanomaterials for Biology 8

Intense THz Source and Application to Magnetization Dynamics 10

Nanoscale Imaging of Whole Cells with Hard X-Ray Microscopy 12

Development of Methodologies for Analyzing Transcription Factor Binding in Whole Genomes 14

Positron Labeled Stem Cells for Non-Invasive PET Imaging Studies of *In Vivo* Trafficking and Biodistribution 16

Novel Multi-Modality MRI and Transcranial Magnetic Stimulation To Study Brain Connectivity 18

Feasibility of CZT for Next-Generation PET Performance 20

Biology on Massively Parallel Computers 22

Giant Proximity Effect in High-Temperature Superconductors 23

Study of High-T_c Nanostructures 25

Lattice Studies of QCD Thermodynamics on the QCDOC 27

Detector Development for Very Long Baseline Neutrino Experiments 29

Detector for High Quality Imagers of Electron Microscopy 31

Table of Contents

Transparent Photocathode Development 33

Synthesis and Characterization of Band-Gap-Narrowed TiO_2 Thin Films and Nanoparticles for Solar Energy Conversion 35

Multiscale Analysis of *In Vivo* Nanoparticle Exposure 37

Development of Gadolinium-Loaded Liquid-Scintillators with Long-Term Chemical Stability for a New High-Precision Measurement of the Neutrino Mixing Angle, Theta-13 39

Electronic Properties of Carbon Nanotubes and Novel Multicomponent Nanomaterials 41

Growth and Characterization of CdZnTe Crystals for Improved Nuclear Radiation Detectors 43

Design, Synthesis and Characterization of a New Class of Hydrocarbon Polymers Containing Zwitter Ions and Nano-Structured Composites for High Temperature Membrane in PEM Fuel Cells 45

Novel Materials for Hard X-Ray Optics 47

Nano-Crystallography of Individual Nanotubes and Nanoparticles 49

High-Temperature Superconducting Magnet Development 51

Epigenetics: Methamphetamine (MAP)-Induced Brain Dysfunction and Methylation of DNA 53

Molecular Mechanism of Chromosomal Replication Initiation in Eukaryotic System 55

Diversification of Isoflavonoid Biosynthesis 57

Metabolic Flux Analysis in *Arabidopsis Thaliana* 59

Transformation and Fate of Nanoparticles in the Environment 61

Development of a Cloud Condensation Nucleus Separator 63

Aluminum Hydride – An Ideal Hydrogen Source for Small Fuel Cells 65

Gamma Ray Imager for National Security Applications 67

Table of Contents

Neurogenomics: Collaboration Between the Biology Department and the Brookhaven Center for Translational Neuroimaging to Investigate Complex Disease States.....69

Nanoparticles Labeled Neural Stem Cells Tracking *In Vivo* by Magnetic Resonance Microscopy (MRM).....71

MicroCT Methods of Quantitative Adipose Imaging: Development of a Long-Term Assessment Technique for Studying Obesity in a Rodent Model 73

Photocatalytic Reduction of CO_2 in Supercritical CO_2 75

QCD Thermodynamics at Non-Zero Temperature and Density.....77

Lattice QCD Simulations on BlueGene/L 79

Proof-of-Principal Laser System for ILC Positron Source.....80

Sensitive Searches for CP-Violation in Hadronic Systems 82

Feasibility and Design Study for a Detector for e+p, e+A, p+p, p+A and A+A Collisions at BNL 83

A Novel and Compact Muon Telescope Detector for QCD Lab.....85

Design Optimization of a Reactor Neutrino Experiment.....87

Development of Laser Beam Shaper for Low Emittance Electron Beams.....89

Surface Engineered and Core Shell Nanowires: Nanoscale Building Blocks For Third Generation Photovoltaics 91

Precision Assembly of Nano-Objects – Approaching Artificial Photosynthesis 93

Photocatalytic Carbon Dioxide Reduction to Methanol using Metal Complexes with an NADH Model Ligand 95

Structure of Mass-Size Selected Nanoparticles by Scanning Transmission Electron Microscopy.....97

Table of Contents

Synthesis of Conjugated Polymers for Fundamental Questions in Solar Energy.....99

Ultra-Thin Graphite Analog Compounds 101

Lipid-Coated Nanoparticles and Their Interactions with Lipid Membrane Surfaces.....103

Angle-Resolved Time-of-Flight Ion Scattering Spectroscopy from MBE-Grown Oxide Thin Film Surfaces.....105

Genome Analysis of Endophytic Bacteria that Promote Growth of Poplar For Biomass Production.....107

Structural Features of the Oxygen Tolerant Hydrogenase from *Thermatoga Neapolitana* 109

Characterization of Enzymatic O-acylation to Facilitate Biomass and Bioenergy Production.....111

Functional Neurochemistry.....113

Miniaturized RF Coil Arrays for MicroMRI 115

Neurocomputation at BCTN: Developing Novel Computational Techniques To Study Brain Function in Health and Disease.....117

A Non-Fermentation Route to Convert Biomass to Bioalcohols 119

Fate and Reactivity of Carbon Nanoparticles Exposed to Aqueous Environmental Conditions 121

Development of Room-Temperature CdMnTe Gamma-Ray Detectors.....123

Development a New Framework for Investigating Earth's Climate and Climate Change.....125

A Novel Approach for Efficient Biofuel Generation.....127

Investigations of Hygroscopic Growth and Phase Transitions of Atmospheric Particles by Noncontact Atomic Force Microscopy.....129

Chemical Imaging of Living Cells in Real Time.....131

Table of Contents

Coherent Bragg Rod Analysis of High-Tc Superconducting Epitaxial Films.....133

Development of a Planar Device Technology for Hyperpure Germanium X-Ray Detectors.....135

Study of Epigenetic Mechanisms in a Model of Depression.....136

Polarized Electron SRF Gun.....138

New Approach to H_2 Production, Storages and Use.....140

Increasing the Capability and Reliability of Small Diameter Direct Wind Multi-Layer Coil Magnets.....142

High End Scientific Computing.....144

Introduction

Brookhaven National Laboratory (BNL) is a multidisciplinary laboratory that carries out basic and applied research in the physical, biomedical, and environmental sciences, and in selected energy technologies. It is managed by Brookhaven Science Associates, LLC, (BSA) under contract with the U. S. Department of Energy (DOE). BNL's Fiscal year 2007 budget was $515 million. There are about 2,600 employees, and another 4,500 guest scientists and students who come each year to use the Laboratory's facilities and work with the staff.

The BNL Laboratory Directed Research and Development (LDRD) Program reports its status to the U.S. Department of Energy (DOE) annually in March, as required by DOE Order 413.2B, "Laboratory Directed Research and Development," April 19, 2006, and the Roles, Responsibilities, and Guidelines for Laboratory Directed Research and Development at the Department of Energy/National Nuclear Security Administration Laboratories dated June 13, 2006. In accordance this is our Annual Report in which we describe the Purpose, Approach, Technical Progress and Results, and Specific Accomplishments of all LDRD projects that received funding during Fiscal Year 2007.

BNL expended $10.2 million during Fiscal Year 2007 in support of 82 projects. The program has two categories, the annual competed LDRDs and Strategic LDRDs, which combine to meet the overall objective of the LDRD Program.

Proposals are solicited annually for review and approval concurrent with the next fiscal year, October 1. An LDRD Selection Committee, comprised of the Associate Laboratory Directors (ALDs) for the Scientific Directorates, an equal number of scientists recommended by the Science Council, plus the LDRD Scientific Director, and the Assistant Laboratory Director for Policy and Planning, review the proposals submitted in response to the solicitation. This competed LDRD category emphasizes innovative research concepts with limited management filtering to encourage the creativity of individual researchers. The competition is open to all BNL staff in programmatic, scientific, engineering, and technical support areas. Researchers submit their project proposals to the LDRD Scientific Director.

A portion of the LDRD budget is held for the Strategic LDRD (S-LDRD) category. These funds are used to establish and enhance initiatives that are consistent with Laboratory priorities. Projects in this category focus on innovative R&D activities that are likely to develop new programmatic areas within BNL's mission responsibilities and enhance the Laboratory's science and technology base. The Laboratory Director entertains requests or articulates the need for S-LDRD funds at any time. The Director selects two people to provide written reviews of the proposals.

These Projects are driven by special opportunities, including:

- Research project(s) in support of Laboratory strategic initiatives as defined and articulated by the Director.

- Research project(s) in support of a Laboratory strategic hire,
- Evolution of Program Development activities into research and development activities,
- ALD proposal(s) to the Director to support unique research opportunities,

The goals and objectives of BNL's LDRD Program can be inferred from the Program's stated purposes. These are to (1) encourage and support the development of new ideas and technology, (2) promote the early exploration and exploitation of creative and innovative concepts, and (3) develop new "fundable" R&D projects and programs. The emphasis is clearly articulated by BNL to be on supporting exploratory research "which could lead to new programs, projects, and directions" for the Laboratory. We explicitly indicate that research conducted under the LDRD Program should be highly innovative, and an element of high risk as to success is acceptable. In the solicitation for new proposals for Fiscal Year 2007 we especially requested innovative new projects in support of RHIC and the Light Source and any of the Strategic Initiatives listed at the LDRD web site. These included support for NSLS-II, RHIC evolving to a quantum chromo dynamics (QCD) lab, nanoscience, translational and biomedical neuroimaging, energy and, computational sciences.

As one of the premier scientific laboratories of the DOE, BNL must continuously foster groundbreaking scientific research. At Brookhaven National Laboratory one such method is through its LDRD Program. This discretionary research and development tool is critical in maintaining the scientific excellence and long-term vitality of the Laboratory. Additionally, it is a means to stimulate the scientific community and foster new science and technology ideas, which becomes a major factor in achieving and maintaining staff excellence and a means to address national needs within the overall mission of the DOE and BNL.

LABORATORY DIRECTED RESEARCH AND DEVELOPMENT

2007 PROJECT PROGRAM SUMMARIES

Complex Thin Films and Nanomaterial Properties

LDRD Project 04-038
Jim Misewich

PURPOSE:
The purpose of this LDRD is to develop state-of-the-art tools for high sensitivity probing of nanomaterials and thin films. The ultimate limit we seek is a capability to probe multiple properties of a single nanowire. The properties we wish to measure include transport properties as well as optical properties such as Rayleigh, Raman, electroluminescence and photo-conductivity spectroscopies. It is highly desirable to integrate these capabilities with other capabilities at Brookhaven for the structural characterization of the same individual nanomaterial sample.

APPROACH:
Our approach starts with the nano-lithographic capability at the CFN to fabricate test structures with the nanometer scale dimensions necessary for contacting ultra-small structures. This is combined with dispersion techniques to enable the fabrication of a single nanowire in a specially designed test structure with electrical contacts. With these samples we will use high sensitive electronics to measure the transport properties, and optical techniques including emission spectroscopy, nonlinear spectroscopy, laser spectroscopy and broadband spectroscopy at the NSLS to get a complete picture of the optical properties. Finally, we will determine the physical structure of the same single nanowires.

TECHNICAL PROGRESS AND RESULTS:
Previously we established our ability to fabricate the test structures, to disperse single nanowires in our test structures, to measure the transport properties of these test structures, and to do optical studies on individual nanowires. This includes photo-conductivity on single nanowires as well as electroluminescence from single nanowires. We have subsequently have been able to extend these studies to include Rayleigh spectroscopy characterization and for the first time to connect these capabilities with the ability to measure the physical structure of the *same* single nanowires. This has been done via collaboration with the advanced electron microscopy group at Brookhaven. In FY07, we extended these capabilities by designing experiments to measure the broadband IR optical properties of single nanowires at NSLS. This resulted in the development of a new technique—Fourier Transform Photoconductivity Spectroscopy which allowed us to determine the photoconductivity response of individual nanowires from the mid-infrared to the visible, and provides new insights into the photo-properties of nanowires.

Our work has led to an FWP on nanomaterial synthesis and characterization from the Division of Materials Science and Engineering of DOE Basic Energy Sciences.

Heavy Ion Physics with the ATLAS Detector

LDRD Project 05-006

Helio Takai

PURPOSE:

The ATLAS detector now under construction and early commissioning will be one of the two major experiments at CERN's Large Hadron Collider (LHC). This accelerator is designed for proton-proton collisions but will also collide heavy ions such as Lead (Pb) to study Quantum Chromodynamics (QCD) at temperatures never before achieved. At these temperatures it is expected that quarks and gluons approach asymptotic freedom and it will be a unique opportunity to study QCD in the laboratory. RHIC has shown a range of interesting science and provides a strong motivation to study nucleus-nucleus collisions at the LHC. ATLAS with its large coverage and excellent calorimeter coverage will allow us to study how partons interact in the hot matter, via jets. This LDRD focuses on establishing a heavy ion physics program for ATLAS with a strong foundation on RHIC results.

APPROACH:

The success of the RHIC program indicates that at higher partonic matter temperatures interesting phenomena is expected. To prepare the experiment for the initial round of experiments it is important to simulate its behavior to the high particle multiplicity environment of nucleus-nucleus collisions. Dr. Arthur Moraes who was hired in this project as a research associate to provide enough manpower for the first phase of studies of the ATLAS performance detector in the heavy ion environment.

TECHNICAL PROGRESS AND RESULTS:

Dr. Arthur Moraes contribution has been essential to create the ATLAS heavy ion physics group in BNL and also to start new initiatives within the ATLAS experiment. Thanks to his initiative, we fully migrated to the ATLAS software framework and all simulations are done using full detailed detector information. This is a giant leap forward when compared to previous results with partial simulations. We have also started to use GRID Computing for simulations to take advantage of the vast network of computers within the ATLAS collaboration. The ATLAS heavy ion group has also initiated a program to study minimum bias proton-proton collisions at the LHC. This group is co-led by Dr. Arthur Moraes and the studies will provide invaluable information for the most basic of the collisions for the heavy ion physics. This new initiative will also allow for the ATLAS heavy ion group to be fully integrated with the experiment. The ATLAS effort has grown in size with a well established group in BNL (and in the US) who is carrying out further studies. Unfortunately Dr. Moraes left our group before the end of this grant to take on a permanent position at University of Glasgow.

Behavior of Water on Chemically Modified Semiconductor Surfaces: Toward Photochemical Hydrogen Production

LDRD Project 05-028

Etsuko Fujita, José Rodriguez and James T. Muckerman

PURPOSE:

Photochemical water splitting to hydrogen, a renewable and non-polluting fuel, and oxygen using energy from solar radiation is extremely important for a sustainable source of energy. Hydrogen and oxygen have been successfully produced by UV irradiation of aqueous suspensions of various semiconductor catalysts including TiO_2 (and transition metal-loaded TiO_2) and $SrTiO_3$, but a detailed mechanism of the conversion at the active catalytic center remains unclear. Recently nitrogen and carbon doped materials, $TiO_{2-x}N_x$, and $TiO_{2-x}C_x$, have been synthesized and used as photocatalysts that utilize visible light (> 420 nm). We are carrying out coordinated experimental and theoretical studies on the electronic properties of N-doped rutile TiO_2(110) with an emphasis on attaining a fundamental understanding of the first elementary step in the water oxidation processes.

APPROACH:

The key issues associated with the doped semiconductors are their controlled synthesis, and characterization of band gaps, electronic properties, stability, and reactivity with water in ultrahigh vacuum (UHV). We prepare N-doped films of TiO_2 by modifying single-crystal semiconductor surfaces, characterize them by surface/materials science techniques under UHV conditions, and elucidate the electronic and proximal structures at the atomic level through both experiments and theory.

TECHNICAL PROGRESS AND RESULTS:

N-doping of TiO_2(110): Photoemission and Density Functional Studies. The electronic properties of N-doped rutile TiO_2(110) have been investigated using synchrotron-based photoemission and density-functional calculations. The doping via N_2^+ ion bombardment leads to the implantation of N atoms (~5% saturation concentration) that coexist with O vacancies. Ti 2p core-level spectra show the formation of Ti^{3+} and a second partially reduced Ti species with an oxidation state between +4 and +3. The valence region of the $TiO_{2-x}N_y$(110) systems exhibits a broad peak for Ti^{3+} near the Fermi level and N-induced features above the O 2p valence band that shift the edge up by ~ 0.5 eV. The magnitude of this shift is consistent with the "redshift" observed in the ultraviolet spectrum of N-doped TiO_2. The experimental and theoretical results show the existence of attractive interactions between the dopant and O vacancies. First, the presence of N embedded in the surface layer reduces the formation energy of O vacancies. Second, the existence of O vacancies stabilizes the N impurities with respect to N_2(g) formation. When oxygen vacancies and N impurities are together there is an electron transfer from the higher energy 3d band of Ti^{3+} to the lower energy 2p band of the N^{2-} impurities.

Investigation of Chemical Vapor Deposited N-doped TiO_2 Film. An N-doped TiO_2(110) ($TiO_{2-x}N_x$ or $TiO_{2-x}N_y$) film prepared by PNNL was studied by NEXAFS in order to determine the chemical state of the implanted nitrogen. The O K-edge and Ti L edge spectra indicated that the film retained a rutile structure with the nitrogen dopant. Using two detection modes of NEXAFS with different depth profiling ability (electron *versus* fluorescence yield), it was possible to distinguish the chemical state between surface and bulk nitrogen. The surface-sensitive partial electron-yield gave N K edge NEXAFS data which indicate that the nitrogen in

the surface region was in a similar chemical condition to TiN, while the bulk-sensitive fluorescence-yield gave N K edge NEXAFS spectra which showed the presence of molecular N_2 besides the species found in the surface (See figure at right).

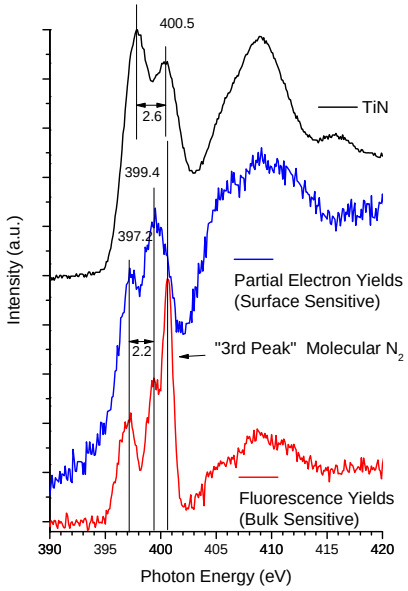

Preparation of N-doped TiO_2 particles.

We have prepared N-doped TiO_2 by reacting Degussa TiO_2 (15-20 nm particles) in triethylamine for over 4 days at 90 °C, followed by washing twice with fresh triethylamine. Upon vacuum drying at room temperature tan crystallites were obtained. While this material is air stable, the color changes to almost black upon heating to 330 °C. Using TEM we determined the doping profile and the associated morphology changes in comparison with the undoped nanoparticles. An energy loss spectrum of N-doped TiO_2 shows a clear N signature (left figure, below). Using real-time, high-resolution observations at variable temperature and electron intensity, we have investigated the oxygen loss from surfaces of undoped and N-doped TiO_2 nanoparticles in the TEM. We have obtained preliminary evidence that the rate of oxygen loss in N-doped nanoparticles exceeds that of undoped particles as seen in TEM images of unreacted and etched surface boundaries of undoped and N-doped TiO_2 in the figures below. (with E. Sutter)

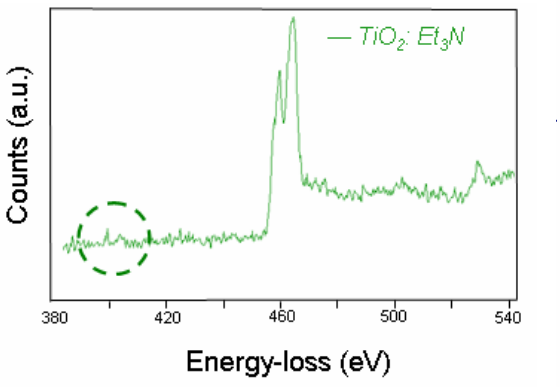

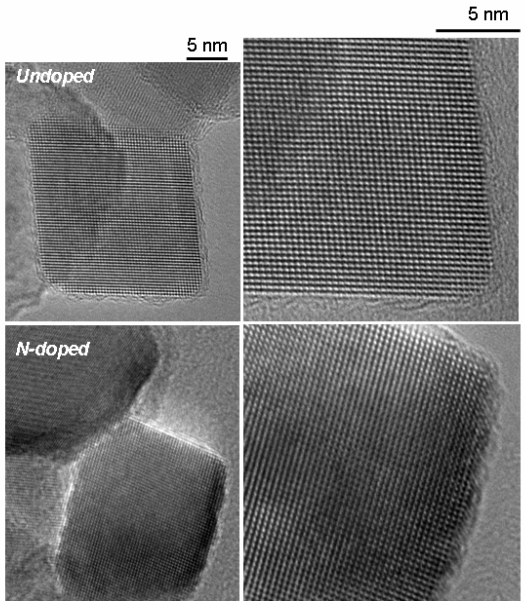

Conclusions. Our studies have demonstrated that the maximum N-doping level is 5 and 1% for film and single-crystals, respectively, and that an interstitial N-atom can easily escape as N_2, especially at high temperature. Such a low dopant level, its instability, and its low absorptivity in the visible region make this material less promising than we originally considered. We have changed our research direction to use GaN:ZnO solid solutions as a visible-light photocatalyst. Particles of this material have successfully been shown to lead to direct water splitting without using any sacrificial reagent.

Multifunctional Nanomaterials for Biology

LDRD Project 05-41
Stanislaus S. Wong

PURPOSE:
We would like to synthesize nanomaterials with simultaneous biological and physical function for application in life sciences. As a starting point we explored the use of carbon nanotubes as a platform for integrating biological specificity with physical function such as fluorescence or conductivity. We seek to put Brookhaven in a position of leadership in biochemical detection.

This will allow us to probe biological systems in ways that are not readily accessible using other methods. Although this project has risk since no laboratory has yet demonstrated nanotube based biosensing with high biochemical specificity, the proposed team has combined broad interdisciplinary expertise in nanomaterial synthesis and functionalization, biology, nanoelectronics, photonics, and microfluidics. These projects advance the application of physical methodologies to biological sciences.

APPROACH:
In the present study, we demonstrated a simple, fast-response, highly sensitive, real-time biosensor composed of a ligand-receptor protein complex covalently attached by a diimide linker to oxidized SWNTs via a mild, ambient, straightforward, and economical protocol. That is, we not only retained the intrinsic biological activity and specificity of the attached complex but also conserved the highly favorable electronic properties of SWNTs in these bio-functionalized single-tube devices. The proteins we used were the adenovirus protein, Ad12 Knob, and its complementary human 'coxsackievirus and adenovirus receptor', CAR.

Adenoviruses are one of many subclasses of viruses that cause infections, such as the common cold and mild ailments of the upper respiratory and gastrointestinal tracts. Infection is initiated by the formation of a high affinity complex between the Knob trimer and its complementary adenovirus CAR receptor present in human cells. Upon binding CAR, the Knob-coated virus replicates within the cell nucleus, triggering infections. Currently, adenoviruses are the leading candidates as vectors for gene therapy. In our work, we used 6 mg/mL of purified Knob and 2.5 mg/mL CAR protein, as verified using a BCA assay kit.

TECHNICAL PROGRESS AND RESULTS:
We measured current-gate voltage (I-V) data on a dozen nanotube devices to explore the effect of the attachment process and of protein binding on the SWNTs' electronic properties. Nanotube devices were of high quality; they consisted of individual SWNTs with ON/OFF ratios exceeding 1000, and possessed on-state resistance values of 100 – 500 kΩ. Findings discussed below were reproduced in all the devices, although there was some scatter in individual responses.

All devices showed a hysteretic I-V response, as is typical of nanotube FETs on untreated silica substrates. This response results from charge injection from the nanotube into nearby regions due to the substantial electric field (~ 10 V/nm) existing at the SWNT surface associated with a large gate voltage. The electric field of this injected charge and of other charge traps near the SWNT is partially screened when the FET is in its ON state, while almost no screening occurs when the FET is in the OFF state. Hence, in the following discussion, we assumed that the left-most (ON-

to-OFF) transition of the I-V characteristic is more reproducible than the OFF-to-ON transition in the presence of unavoidable charge switching, and is, therefore, more amenable to interpretation.

The oxidation process typically either increased the ON state current of the device (by 10-25 %) or left it unchanged. We concluded that mild oxidation created a low density of defect sites that did not degrade electron transport in the device; we attributed the small increase in the ON-state current to contact annealing. Oxidation also generated a reproducible increase of 0.5-3 V in the ON-OFF threshold voltage, consistent with the notion that defect sites created by oxidation are functionalized with oxygenated moieties that become deprotonated in the presence of adsorbed water. This change leaves the groups negatively charged, so that a more positive gate voltage is needed to turn the device OFF. Assuming a typical backgate capacitance of 25 aF/μm for this geometry, this shift in Vg corresponds to an increase in the carrier density of 80 – 400 holes/μm. Subsequently incubating the device in EDAC/NHS solution engendered a negative shift of the threshold voltage to its original value or to an even more negative voltage, in agreement with the expectation that the proton had been replaced by a stable active ester. CAR protein attachment led to a 1-2 V decrease in the ON-OFF threshold voltage, and a corresponding 20-40 % decrease in the ON state current. These observations are consistent with the FET experiencing a positive charge and enhanced carrier scattering due to the presence of the protein. Finally, exposing the CAR-SWNT hybrid to the complementary Knob protein further suppresses the ON state current; the molecular recognition event was thus fully detectable in this system.

In a separate control experiment, CAR-functionalized devices showed no evident change in I-V response, as expected, after exposure to (non-complementary) YieF, implying that the in vivo chemical specificity of the CAR protein is retained even when it is immobilized on the SWNT surface. In another experiment, we noted that the electrical profile of SWNTs, that had been non-covalently functionalized with CAR proteins, reverted to its original signal upon extended washing with phosphate buffer and water; these data highlighted the importance of covalent protein binding in our experiments and implied that weakly bound, physically absorbed proteins were lost upon washing of the SWNTs.

The present study provided proof-of-concept for developing a simple, efficient, sensitive, fast-response, and real-time miniaturized nanotube FET biosensor for detecting the Ad 12 Knob virus using CAR-Knob specificity. Moreover, this methodology can be extended to uncover the presence of serotype12 and all other possible CAR-binding adenoviruses, as well as subgroup B coxsackie viruses. This is the first evidence of straightforward, ambient covalent immobilization of a viral ligand-receptor protein system onto individual SWNTs and SWNT bundles, and of our subsequent confirmation of the bound proteins' retention of biological activity and specificity, as revealed by systematic electrical measurements. Our future goal will be to develop a single molecule biosensor based on the conductivity change of a single SWNT by adding a discrete CAR domain to the nanotube.

Intense THz Source and Application to Magnetization Dynamics

LDRD Project 05-44
G. Lawrence Carr, Darío A. Arena and X.-J. Wang

PURPOSE:

Coherent THz pulses are typically half, single, or few cycle electromagnetic pulses with time duration on the order of 1 picosecond or less. When the pulses are produced by ultra-short relativistic electron bunches from an accelerator, the transient field strength and energy should be sufficient to induce novel dynamical phenomena in materials. A key application of these pulses is for the study of ultrafast switching in ferromagnets, ferroelectrics and superconductors. This LDRD project intends to fully characterize coherent THz pulses from the NSLS Source Development Lab (SDL) linac and develop tools for utilizing the pulses in the study of dynamical processes in magnetic and other thin film systems.

APPROACH:

The SDL linac provides ultra-short (~350 fs) bunches containing up to $5x10^9$ electrons. These electrons are used to produce coherent THz pulses in the form of "transition radiation" by directing the electron bunches onto an aluminum mirror. The resulting pulses span the frequency range up to about 2 THz and the energy per pulse can be 100 μJ. When focused to a small spot, the electric field is expected to peak near values of 1 MV/cm, with a correspondingly strong magnetic field of B = E/c ~ 3kG. An important characteristic of these THz pulses is their temporal waveform, to be measured using time-domain electro-optic (EO) methods. This involves co-propagating the focused THz and chirped laser pulses through a ZnTe crystal while monitoring the change in the laser's spectral content. A schematic of this setup is shown in Figure 1, along with a plausible single-cycle THz pulse.

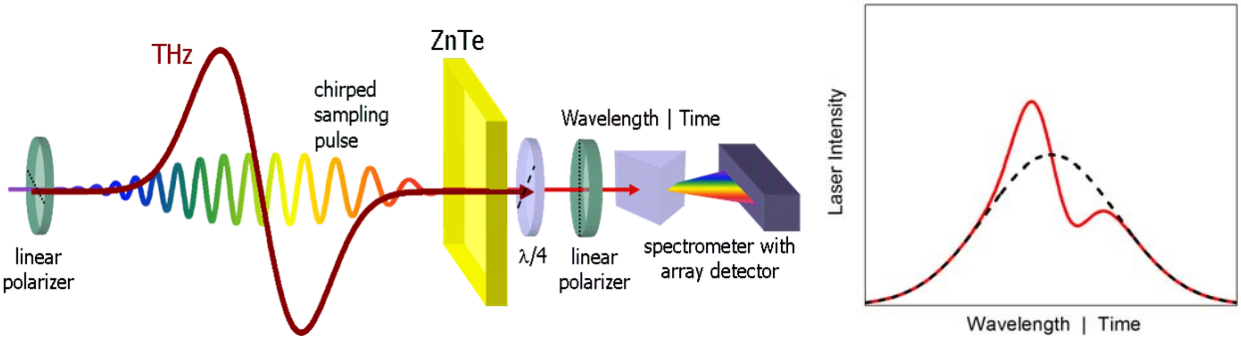

Figure 1. Left: Single-shot EO sampling setup of coherent THz pulses using a chirped laser pulse and spectrometer. Right: Schematic laser spectral intensity for no THz (dashed black) and with THz (solid red).

Once the THz waveforms and methods for measuring them are well-characterized, a specimen is placed at the ZnTe location. The transmitted THz can then be collected and focused to another EO setup for detection. In this manner, the response of a specimen to a particular THz waveform (shape and strength) can be measured. We envision that some specimen types, such as ferromagnetic films, will serve as their own detector (like a photographic recording medium). Other measurements will analyze the THz pulse after transiting the sample to sense evidence of switching or breakdown phenomena as a function of field strength.

TECHNICAL PROGRESS AND RESULTS:

This final year of the LDRD project focused on refining the optical systems for both THz and laser propagation, designing the optical setup for accepting samples in a cryogenic environment, and completing the EO computation for strong THz pulses. We had observed that the standard single-shot EO technique, where a chirped laser pulse samples the entire THz waveform, was yielding anomalous results for strong fields. The cause was identified as time-dependent phase modulation of the laser pulse, confirmed by specific measurements and the results were published. A complete time-dependent EO calculation for chirped pulses was later found to account for the anomalous results of our earlier measurement (see Figure 2.)

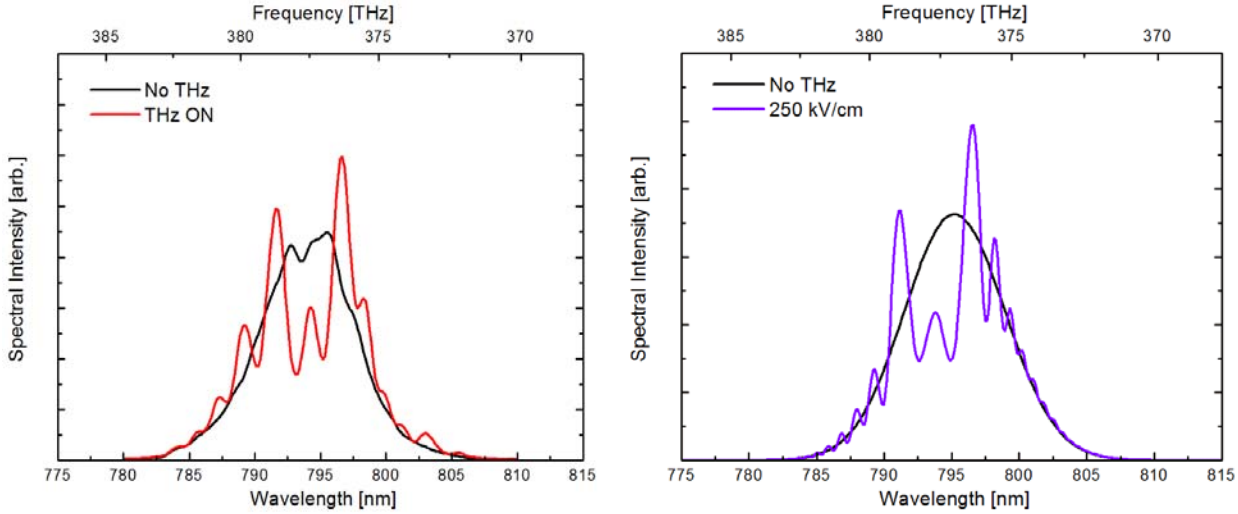

Figure 2. Left: Measured single-shot sampling of a strong THz pulse showing complex structure. Right: Full time-dependent EO analysis assuming a single-cycle THz pulse. The complex structure is a consequence of cross phase modulation and not inherent to the pulse waveform.

We also recognized that similarly strong fields exist near the electron bunches inside the linac, and therefore similar effects should be observable when applying EO methods to directly characterize the longitudinal bunch density. Calculations that included time-dependent phase modulation were found to explain anomalies observed by previous researchers. We also noticed that our THz measurement setup was particularly sensitive to beam steering errors, laser intensity fluctuations and aberrations in the THz optical system. To remedy this, much of this past year was spent on refining the relevant optical systems. The laser beam transport optic system was improved and motor systems were acquired to allow remote operation of the THz optical components and enable adjustments while the linac is operational. These systems are in the process of being deployed. A third activity was the optical design development for accommodating a specimen cryostat at the THz focus, as needed for the study of many ferroelectric systems as well as superconductors.

FUTURE:

This project served as the seed for a new program area in strong field physics of materials, and will continue to develop as a facility for materials research. We anticipate collaboration with the Condensed Matter Physics / Materials Science department for studies of ferroelectric and other systems of technological interest.

Nanoscale Imaging of Whole Cells with Hard X-Ray Microscopy

LDRD Project 05-048
Lisa M. Miller

PURPOSE:

The objective of this work is to develop 3-dimensional, high-resolution, hard x-ray imaging for the study of whole living (frozen) cells. This project takes advantage of the high brightness and coherence of synchrotron light and recent advances in new x-ray imaging technology (i.e. hard x-ray zone plates). To date, other imaging techniques are limited by sample thickness, e.g. soft x-ray microscopy is limited to <1 μm and electron microscopy is limited to < 100 nm. We aim to improve the sample penetration depth to 50 – 100 μm (the thickness of typical cells), and the spatial resolution to <20 nm by using hard x-rays for 3-D imaging. The NSLS has several beamlines that are well suited for developing hard x-ray microscopy, and also has an accomplished user base in the development and implementation of x-ray zone plates.

APPROACH:

Currently, confocal microscopy with visible light is the most common method of imaging biological processes in living cells. However, the primary drawback to this technique is the diffraction-limited spatial resolution of ~300 nm. This resolution can be used to image large sub-cellular organelles, but cannot be used to study smaller sub-cellular structures such as cell membranes and individual protein complexes. Other imaging techniques with higher spatial resolution, such as electron microscopy and soft x-ray microscopy, have limited sample penetration depth, so that only small cells and/or particles can be studied.

We are working towards the development of an x-ray microscope that surpasses any other at the NSLS in both spatial resolution and sample penetration depth. This type of spatial resolution will enable cellular processes, such as apoptosis and mitosis, to be studied in the native cellular environment, to provide new insight into the way cells behave as "molecular machines." Moreover, the development of this nanoscale tool will not only be applicable to biological systems, but will be valuable for the study of numerous other nanoscale structures in the chemical, materials, and environmental sciences fields.

The specific aims of this proposal are: (1) to customize and test a hard x-ray zone plate to an NSLS bending magnet beamline, (2) to develop cryogenic cooling techniques, (3) to adapt current electron microscopy biochemical tags for hard x-ray microscopy, and (4) to apply the newly developed technique to image cellular processes such as mitosis or apoptosis.

TECHNICAL PROGRESS AND RESULTS:

In FY 2005, Meghan Ruppel (LDRD graduate student) developed methods for combining epifluorescence microscopy with hard x-ray microprobe in collaboration with Dr. Antonio Lanzirotti (University of Chicago). In FY 2006, in collaboration with Dr. Yen-Fang Song at the National Synchrotron Radiation Research Center (NSRRC) in Taiwan, we collected hard x-ray microscopy images of microdamaged bone samples in both absorption and phase contrast mode. These experiments were performed to test the technology on samples that were not radiation-sensitive. The results demonstrated ~30 nm spatial resolution and high mineral-to-matrix contrast.

In FY 2006, Ms. Ruppel set up a cell culture laboratory at the NSLS and tested methods for growing fibroblasts (human skin melanoma cells) and osteoblasts (bone cells) on x-ray transparent materials including formvar, silicon monoxide, and silicon nitride. We began to adapt immuno-fluorogold tags (standard antibody-conjugated labels) for x-ray microscopy and tested them at the NSRRC and NSLS. Results collected in early FY2007 showed that the labeling of the cytoskeleton in the cells was successful, as indicated by bright green fluorescence (**Figure 1**). However, the 3 nm gold particles were too small to provide enough contrast with 8 keV x-rays in absorption or phase contrast mode. Thus, future experiments will be required to either use larger gold nanoparticles, or silver-enhance the 3 nm particles after binding.

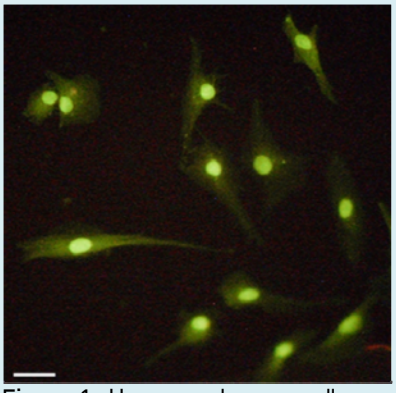

Figure 1. Human melanoma cells were labeled in the cytoskeleton with immuno-fluorogold and grown on SiN film. The gold nanoparticles were 3 nm in diameter. The bright green fluorescence indicates successful labeling. Scale bar is 20 microns.

Also in FY 2007, we examined mineralizing osteoblasts with the hard x-ray microscope. Specifically, mineralized nodules produced by 28-day cultured osteoblasts (MC3T3-E1 cells) were examined. The nodules are surrounded by confluent cells (**Figure 2A)**, which are not visible in the phase contrast image (**Figure 2B**). The gray scale of the phase contrast image gets darker from the edge to the center of the nodule, indicating that the nodule is denser at its center. The mineral also appears disorganized, suggesting that it is ectopic mineral, which has a granular appearance. Ectopic mineral is not associated with any collagen matrix. Thus, these results indicate that the collagen produced by these osteoblasts in culture is disordered and does not have the correct fibrous structure to initiate proper mineralization. These findings are consistent with earlier work on the characterization of these mineralizing osteoblasts [Wang et al., JBMR, 14:893, 1999]

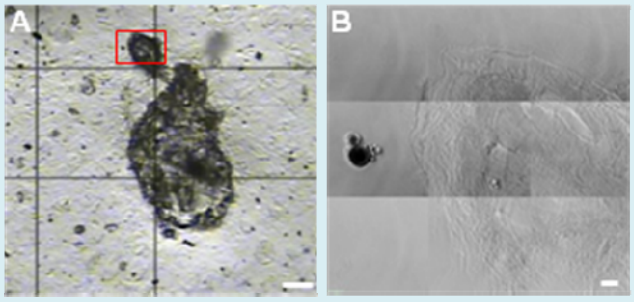

Figure 2. (A) Visible image 50X of MC3T3-E1 mouse osteoblasts, grown for 28 days in osteogenic media. Scale bar is 50 microns. (B) A mineral nodule was imaged in phase contrast mode and demonstrates the disorganized nature of cell culture bone mineral. The dark circle in center, left part of the image is a 3 nm gold sphere used as a fiducial marker for tomography. The scale bar is 2 μm.

Development of Methodologies for Analyzing Transcription Factor Binding in Whole Genomes

LDRD Project 05-058
Carl W. Anderson

PURPOSE:
Goal is to develop a robust method for identifying and characterizing protein binding sites and epigenetic markers in whole genomes of eukaryotic cells. The technology is relevant to developing systems to understand the cellular responses of human cells to low doses of ionizing radiation for DOE's Low Dose Radiation Program. This will require determining how and where ionizing radiation induces changes in transcription factor binding, chromosome structure and whether epigenetic changes, such as methylation of cytosine residues, occurs in the DNA. The methodology also is applicable to understanding the complex physiological and behavioral systems coordinated by a central nervous system and the regulation of plant genes. Therefore, this project complements the BNL's Life Sciences Directorate strategic initiative to understanding brain function and the BNL initiative to develop sustainable biofuels.

APPROACH:
Two major principles underlie the Paired-End Serial Analysis of Chromatin Occupancy (PE-SACO). First, short DNA sequences (21 base-pairs) are sufficient to identify unique sites within a genome; second, short sequences from the ends of selected DNA fragments can be obtained economically using new, modern, DNA sequencers that obtain 100s of thousands or millions of short DNA sequences quickly. PE-SACO uses a technique called **ch**romatin **i**mmuno-**p**recipitation (ChIP), in which proteins bound to DNA are reversibly crosslinked to the DNA segment to which they are bound, the crosslinked chromatin is then fragmented into short fragments, and the DNA to which any given protein is bound is recovered using antibodies that specifically recognize that protein.

For PE-SACO, ~500 bp ChIP fragments are first cloned into a specially constructed vector that has MmeI restriction sites (or sites for other suitable restriction enzymes) flanking the cloning site. The MmeI restriction enzyme cleaves DNA 20 or 21 base-pairs (bp) away from its recognition site, thereby creating ~20 bp sequence tags from each end of each ChIP fragment. The cleaved vectors are then relegated to create a ~42 bp insert, a "di-tag," containing ~20 bp from each end of a ChIP fragment, or a ~60 bp di-tag, in which special barcoding sequences are inserted between the tags. The di-tags then may be amplified using the polymerase chain reaction (PCR) and sequenced with one of several, modern, high-throughput DNA sequencers. An advantage of the PE-SACO method is that for factor binding loci that are recovered many times, the factor binding site must be found with the segment that is common to all recovered DNA fragments corresponding to the locus. This feature reduces the segment that must be examined for factor binding sites from ~2000 bp to about 100 bp. The method also can be used to identify modified DNA segments in chromatin such as segments that are epigenetically marked with methylated cytosines. Chromatin segments containing methylated cytosines are recovered using a protein, such as the DNA binding segment of MeCP2, in place of an antibody to a protein that recognizes a transcription factor. Subtractive methods for the analysis of methylated DNA segments that would more readily permit identification of changes in epigenetic marks also can be explored.

To validate the PE-SACO technique, we proposed preparing and characterizing a PE-SACO library corresponding to the binding sites of the p53 human tumor suppressor protein in human epithelial cells following treatment with ionizing radiation. Genomic approaches have shown that p53 induces or inhibits the expression of more than 1500 human genes, but the identity of its binding sites has not been carefully explored in normal human cells or as a function of the type or dose or cellular stress. p53 specifically recognizes the consensus sequence 5'-RRRCWWGYYY (N = 0-14) RRRCWWGYYY-3' where R stands for a purine base (A or G), Y stands for a pyrimidine base (T or C) and W stands for either A or T. The degenerate nature of the DNA binding consensus sequence makes it difficult to predict and identify authentic binding motifs in whole genomes by simply scanning the sequence; in addition, not all consensus sites (p53 responsive elements, p53REs) are competent for p53 binding *in vivo*. The nuclear concentration of p53 increases about two orders of magnitude in response to certain genotoxic and non-genotoxic stresses. Protein modifications and the presence of binding partners and their concentration, also modulate p53's ability to specific response elements. Understanding which sites in chromatin are bound by p53 after genotoxic stress is critical for understanding how p53 prevents cancer and may lead to improved cancer treatments as well as an understanding of the cellular response pathways activated in response to low dose radiation.

TECHNICAL PROGRESS AND RESULTS:

During the first two years of this project, several technical improvements were made to the PE-SACO technique. The idea of barcoding libraries using a simple DNA sequence inserted between the paired di-tags was developed and tested. Barcoded PE-SACO libraries were prepared from presenescent IMR90 human fibroblasts that were untreated, or 4 hr after exposure to either 0.1 Gy or 8 Gy ionizing radiation. Quantitative polymerase chain reaction (PCR) analysis showed that fragments from the p21 gene promoter were enriched in the immunoprecipitates as expected compared to the input DNA. The libraries were prepared by sequential amplifications of 20 and 25 PCR cycles fragments and were processed for sequence analysis by the Joint Genome Institute (JGI) Life Sciences 454 DNA sequencer.

Sequencing revealed that PCR amplification had selectively amplified some DNA fragments much more than others such that the di-tags no longer were representative of the original ChIP fragments. During FY 2007, a large effort was made to examine in detail the PCR procedure and to develop a method that resulted in a more uniform amplification process. Recent sequencing by the JGI of a p53 library from IMR90 cells prepared with our improved procedure showed that the problem of PCR overamplification has been completely resolved and that over half of the barcoded di-tags (~15,000) could be mapped back to locations in the human genome. Known p53 binding locations were identified as well as locations that have not previously been identified.

Positron Labeled Stem Cells for Non-Invasive PET Imaging Studies of *In Vivo* Trafficking and Biodistribution

LDRD Project 05-068
S. Srivastava and L. Pena

PURPOSE:

The overall goal of this project is to develop methods for radiolabeling progenitor stem cells for noninvasively tracking their behavior and fate *in vivo* through PET imaging. If successful, these investigations would lead in the long run to the development of a generally practical, convenient, and reliable method for following the distribution, differentiation, and survival of stem cells in a quantitative fashion. This project has the potential to significantly enhance and broaden our understanding of the mechanisms of stem cell involvement in health and disease. It involves the use the very sensitive PET radiotracer imaging technique, which has derived DOE support at BNL for over four decades.

APPROACH:

The overall *rationale* derives from published reports that identify the need for a practical, reliable, and cost-efficient way of marking progenitor stem cells to non-invasively evaluate their distribution and survival following transplantation. Our preliminary results and work from multiple laboratories suggest that, radiolabeling antibodies that are specific to subpopulations of progenitor stem cells, with positron emitters to allow PET imaging, is perhaps the most efficient and economical way to follow stem cell trafficking, survival, and differentiation *in vivo*. The general approach for cell labeling involves preparing a radioimmunoconjugate of the appropriate cell-specific monoclonal antibody (MAb) first with the PET radionuclide (e.g, I-124 and Co-55 proposed in this investigation), and then stably and irreversibly attaching the resulting radioimmunoconjugate to the progenitor stem cell under study. The initially selected model was the bipotential glial stem cell line, CG-4, and the monoclonal antibody A2B5 which targets an antigen present specifically on the glial cell surface. After initial experimentation, it became clear that the level of A2B5 expression in these glial progentior cells (CG4) was rather low. We began looking for another cell type with high levels of A2B5 expression to use as a positive control. The best candidiate turned out to be the RIN-m5F cells. These cells are derived from a rat insulinoma model. This work is expected to accomplish the first steps towards fulfilling the above stated unmet need for a noninvasive imaging methodology for following stem cell trafficking, survival, and differentiation *in vivo*. Other investigators involved in this project were M. Rao (NIH, Consultant), G. Meinken, Scientific Associate, N. Medvedeva, Research Associate, and D. White, Technical Assistant.

TECHNICAL PROGRESS AND RESULTS:

Our efforts during FY 2006 involved improving the methodology for preparing mg amounts of MAb A2B5 from an appropriate hybridoma cell line and to label it with commercially available I-125 (as a surrogate for the positron emitter I-124) using increasing number of iodine atoms per MAb molecule (no-carrier-added, 0.5, 5, and 10 with carrier). The next step was to prepare a slot blot of cell lysates from test and control cell lines. The procedure for determining the binding efficiency and the retention of biological activity of the immunoconjugate included incubating the blots with the radioiodinated A2B5, and autoradiography using a Phosphor Imaging System.

During FY 2007, the preparation and purification of the MAb A2B5 and scaling up its production were successful. We grew hybridoma cells that secrete MAb A2B5 in cell culture and optimized conditions for cell growth and for harvesting the medium. We then carried out affinity purification #1

using a T-Gel column (that enriches thiophilic proteins including MAbs) and affinity purification #2 using a Protein L Column (to enrich immunoglobulins, particularly IgM). Following this, an ultrafiltration procedure (100K cutoff) was performed to accomplish concentration and buffer exchange in one step. While establishing the scaled up A2B5 production and purification procedures, we also optimized the iodination with I-125 using commercially available (very expensive) as well as locally prepared A2B5 achieving good labeling efficiency (50 – 80%).The retention of biological activity of radioiodinated A2B5 was determined using positive glial cell controls. The results confirmed successful radiolabeling and retention of biological activity (Fig.1). Biological activity as a function of increasing I-125:A2B5 molar ratios (up to 10) was not significantly different.

The *in vivo* behavior (organ uptake and kinetics) in mice, following i.v. administration of I-125-A2B5 antibody is shown in Fig. 2. A2B5 is specific to C-series gangliosides GT1, GT2, GT3 and GQ1. Therefore our target organ was pancreas, where most of these gangliosides are expressed. Some signal in liver, kidney and stomach, which also express small concentrations of these gangliosides was expected. It is clear that despite the fast degradation of the radiolabeled antibody *in vivo* it is still possible to receive a good signal in the pancreas. The whole body autoradiogram (Figure 3) confirms this conclusion: we can see a much brighter spot in the pancreatic area.

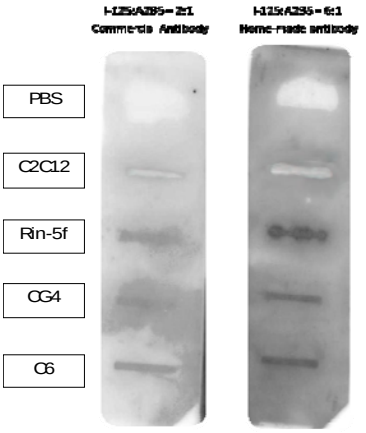

Fig.1.Retention of biological activity of commercial (left) and homemade (right) A2B5 labeled with I-125.

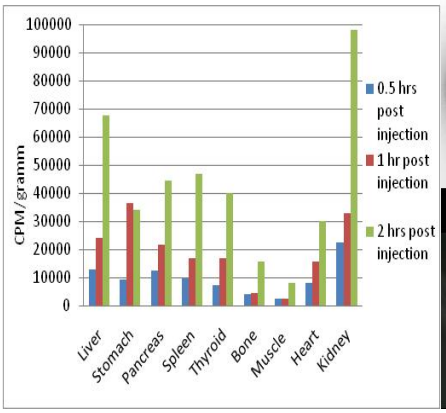

Fig. 2. Biodistribution and kinetics of I-125-A2B5 in mice after i.v. injection

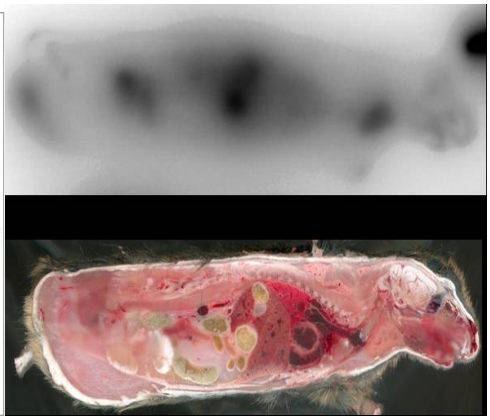

Fig.3. Whole body autoradiogram and scan of a mouse after i.v. injection of I- 125-A2B5.

In preparation for micro-PET experiment "homemade" A2B5 antibody was fractionated and labeled with I-124 under the conditions optimized for I-125. Mice were injected with iodinated antibody via the tail vein and PET images were taken immediately and with 1 hr intervals up to 6 hrs. At this point the results of the PET studies are at the stage of being processed and analyzed.

In conclusion, we were able to successfully demonstrate that: 1) it is possible to label stem cells with a radioiodinated cell-specific monoclonal antibody without affecting their biological activity; and 2) by using PET scanning with I-124, or in the future with other positron emitters, it should be possible to study the *in vivo* trafficking and biodistribution of stem cells in a non-invasive manner.

Novel Multi-Modality MRI and Transcranial Magnetic Stimulation to Study Brain Connectivity

LDRD Project 05-070
Elisabeth de Castro Caparelli

PURPOSE:

Propose to develop a revolutionary methodology integrating transcranial magnetic stimulation (TMS) and interleaved acquisition of functional magnetic resonance imaging (fMRI) and diffusion tensor imaging (DTI), using BNL's 4T MR scanner, so as to provide the unique windows on brain function and connectivity. TMS can, non-invasively and painlessly, transiently disrupt activity in focal brain regions; fMRI is a well established technique used to measure changes in blood oxygenation level dependent (BOLD) signal in brain regions, which reflects changes in neuronal activity; and DTI permits the visualization of the tracts or bundles of neuronal axons that connect different parts of the brain. Thus, with this novel combination of TMS and multi-modality of MRI techniques, in a high magnetic field, we will be able to answer fundamental questions relating to brain behavior and its anatomical basis, which will promote the conduct of highly innovative and exploratory research, and advance medical sciences at BNL.

APPROACH:

Background: Boning et al. (2000) applied single-pulses of TMS over the motor cortex in healthy volunteers during fMRI studies in a 1.5T MR scanner. They verified that interleaved TMS/fMRI can be used in averaged single-pulse trials, and BOLD responses to single-pulse TMS can be detected under the TMS coil. Guye et al. (2003) combined fMRI and DTI, to explore primary motor cortex (M1) connectivity in the human brain. The results demonstrated strong connections from M1 to the pyramidal tracts, premotor areas, parietal cortices, thalamus, and cerebellum, showing that the combination of fMRI and DTI is a promising tool to study the structural basis of functional networks in the human brain *in vivo*.

Aim: Integrate TMS and MRI technologies for the first time in a 4-T MRI scanner. Map brain activation produced by TMS-pulses, when applied over the motor cortex area using fMRI. Map structural connectivity within the TMS-activated neural networks using DTI.

Method: TMS will be applied through a nonferromagnetic double cone coil (70-mm outer wing diameter), connected to a Magstim Rapid stimulator (The Magstim Company, Wales, UK). The fixation and placement of the TMS coil will be done using a custom-made, adjustable coil holder that will attach to the MRI head coil. fMRI will be performed using an EPI-GRE sequences and data analysis will be performed in SPM2. DTI will be acquired using an EPI-SE sequence and data analysis will be performed using the medical imaging display and analysis group (MIDAG) package.

Collaborators: D. Tomasi, Ph.D., G.-J. Wang, M.D., F. Telang, M.D., D. Anschel, M.D., W. Backus, M.D. and R. Goldstein, Ph.D.

TECHNICAL PROGRESS AND RESULTS:

During the first and second year, the technical implementation of TMS inside the high field MRI scanner was successfully concluded. For this purpose the brain stimulator, Magstim Rapid, model 220, and the coils and an MRI compatible and standard, both 70 mm figure of eight TMS coils, were acquired. Quality tests and calibration of the TMS coil were performed with a pickup

coil. An adjustable holder was made with wood to attach the TMS coil inside of the RF-coil and tested for safety using piezoelectric to detect coil vibration. Imaging artifacts has started to be explored for the combination of TMS & MRI using a phantom. DTI technique has been incorporated in the 4 T MRI scanner including imaging acquisition and data post-processing. A new environmental safety review (ESR) was generated and approved. The protocol, to explore the motor? are in 20 adult, healthy volunteers, was initialized and modified to explore the primary visual (PV) area, since the coil holder was inappropriate to reach the motor cortex area.

During the third year, the renewed protocol was initiated and TMS stimulus paradigm was optimized to be a block design composed with three stimulus epochs of 30s, with TMS applied each 4 s, and three resting epochs. The technical developmental implementation of TMS in a high field MRI was validated with the first sample of data, which was composed of two groups: 1) able to see phosphenes and 2) unable to see phosphenes (see figure 1).

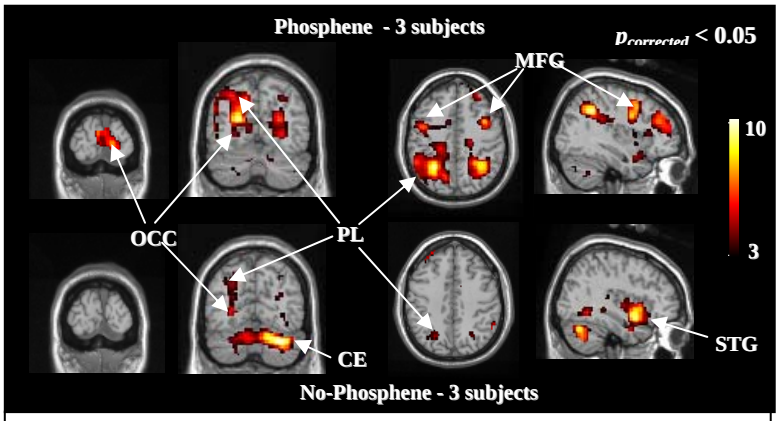

Figure 1: A) Statistical maps of BOLD signal, as a result of a fix-effect analysis for the two groups. The color bar shows the T-score window.

These preliminary results demonstrate the feasibility of combining TMS and fMRI in a 4 T MRI scanner, and that the TMS pulses activate an extended network of brain regions. Moreover, we observed that TMS pulses can modulate activity in brain areas interconnected with the stimulus site, even in the absence of phosphene sensations.

Finally, the protocol was modified to include a second session of simultaneous TMS-fMRI interleaved with a session of 1 Hz rTMS (15 min), which has shown to decrease cortical excitability. Thus, with this new study design, we were able to evaluate changes in brain function as a result of this inhibitory effect induced by the rTMS session. Finally, the preliminary result obtained has shown (see figure) that brain activation decrease on the subject that is able to see phosphenes, but presents a different pattern for the one who was unable to see phosphenes.

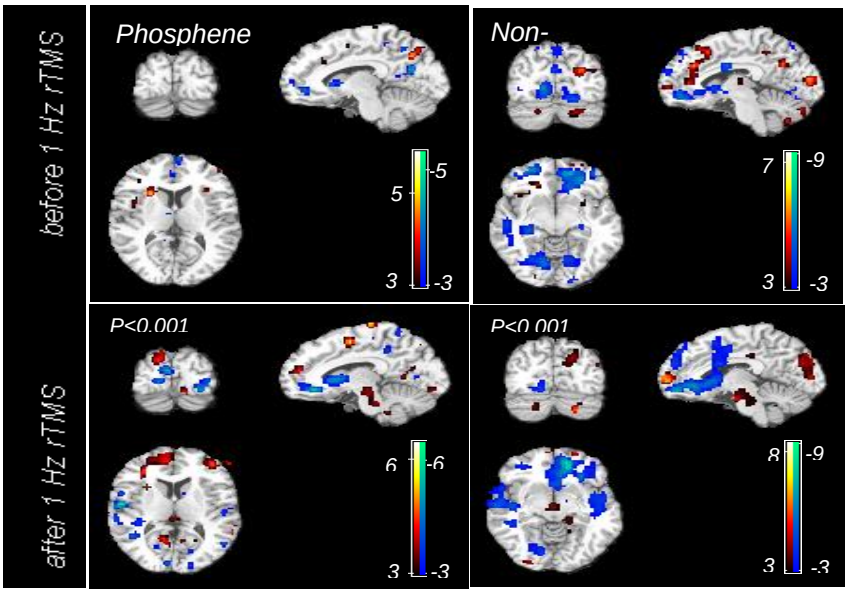

Feasibility of CZT for Next-Generation PET Performance

LDRD Project 05-072

Paul Vaska

PURPOSE:

Aim to demonstrate the feasibility of using cadmium zinc telluride (CZT) as a gamma-ray detector for medical imaging with positron emission tomography (PET). In particular, CZT provides the opportunity to achieve extremely high spatial resolution, a very important goal in PET because it will allow meaningful imaging of the mouse brain which opens up access to all the powerful transgenic models available in this species. CZT has been discussed in this context for years and the quality and availability of CZT detectors has steadily increased, but a diverse team of detector and imaging scientists is required to overcome a number of technical obstacles.

APPROACH:

CZT has great potential for PET because of its potentially high spatial resolution (1 mm or less, including in depth, which is important to minimize parallax problems), high energy resolution (to reject scattered radiation), favorable geometry (no photosensor, compact), and insensitivity to magnetic fields (to permit simultaneous imaging with PET and MRI, currently a very hot topic in nuclear medicine). The main hurdles are poor timing (required to reject random coincidences) and relatively low stopping power at 511 keV. The high risk element of the project is how well we can mitigate these shortcomings.

To demonstrate feasibility, we have developed methods to overcome these hurdles with an exceptionally qualified, interdisciplinary team of experts from the areas of solid state detector development and nuclear medicine research. The team includes members of world-leading research groups in CZT detectors (Aleksey Bolotnikov and Ralph James), low-noise electronics (J.-F. Pratte, Angelo Dragone, Yong-gang Cui, Jack Fried and Paul O'Connor), and imaging physicists (F. Avraham Dilmanian, Sang-June Park, Wonho Lee, and Paul Vaska). The general approach is to first develop methods to overcome the timing and sensitivity drawbacks of CZT using actual CZT devices, incorporate the optimized methods and measured detector performance into a realistic Monte Carlo simulation of a full PET system to estimate the ultimate performance of CZT for PET, and develop a prototype system for PET imaging.

TECHNICAL PROGRESS AND RESULTS:

The first portion of the grant period was dedicated to studying the basic detector characteristics of our CZT pixel detectors, developing methods to process the data for optimal timing and spatial resolution, and showing feasibility of a full PET imager composed of these detectors using Monte Carlo simulation.

In FY07, the main work consisted of designing and constructing a complete mouse brain PET scanner. The design shown in Fig. 1 employs a novel detector geometry which is covered under a provisional patent filed this year by the PI of this LDRD. This arrangement takes optimal advantage of the superb spatial resolution of these detectors in the cathode-to-anode direction, allowing very high resolution imaging with a minimal of readout channels. All CZT detectors are in hand and the electronics schematics are now complete. Printed circuit board layout is underway (~50% complete) and fabrication of all boards is expected by the end of CY07 with system integration and testing in early CY08.

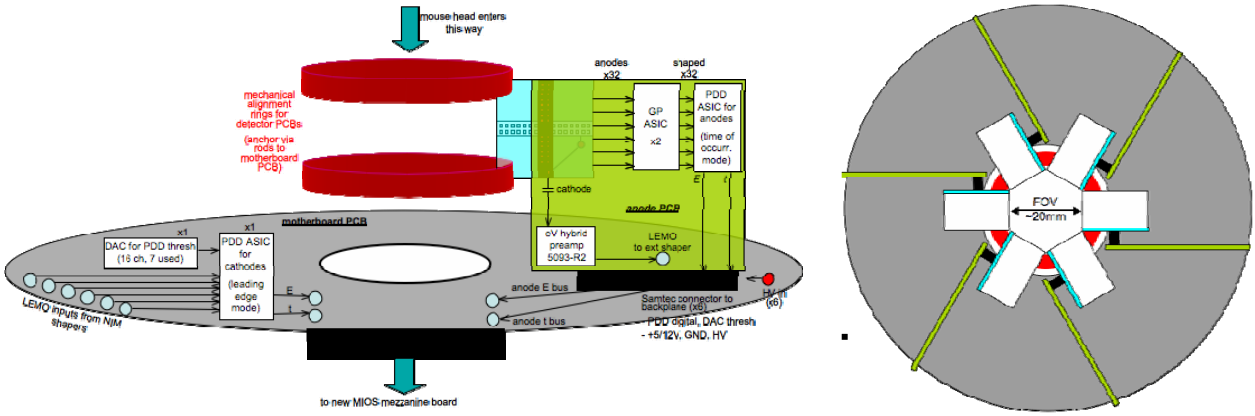

Fig. 1. Electronic architecture of CZT-based mouse brain PET imager with one detector in place (left), and end view including all 6 detectors (right).

Detector testing is ongoing, especially with respect to cathode-anode positioning. Fig. 2 shows the impact of depth measurement on the overall energy resolution. Data processing and image reconstruction algorithms have been developed in parallel based on both the traditional analytical approach of filtered backprojection as well as a more accurate maximum likelihood based method. They will be ready when the hardware is complete.

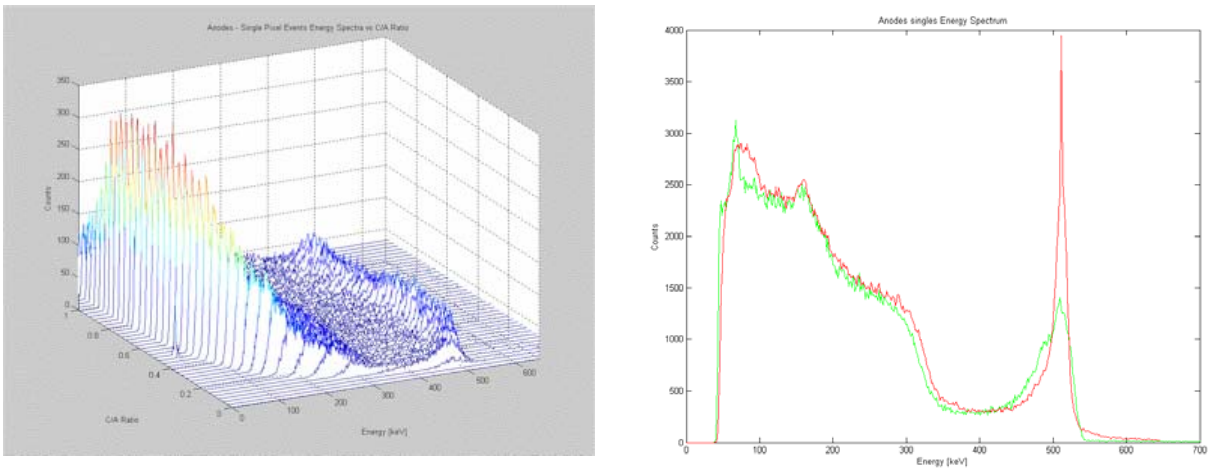

Fig. 2. Ge-68 energy spectra as a function of event depth (left), and summed spectra over all depths with and without depth-correction.

Biology on Massively Parallel Computers

LDRD Project 05-074
J. W. Davenport

PURPOSE:
This is a proposal to develop new algorithmic approaches for computational biology on massively parallel computers. The aim is to make effective use of machines such as the 12,000 processor QCDOC and the 131,000 processor BlueGene/L requiring a combination of algorithms and applications. The algorithmic research includes the development of efficient molecular dynamics (MD) codes which take account of data non-locality and apply explicit routing protocols suitable for both QCDOC and BG/L. The applications involve molecular dynamics simulations of several small proteins including the adenovirus protease studied structurally by Mangel and co-workers and Botulinum neurotoxin studied by Swaminathan and co-workers both at the NSLS.

APPROACH:
Molecular dynamics simulations require large amounts of computer time in addition to efficient algorithms. To deal with these a new MD code specifically adapted to QCDOC is being developed. The time limitations are usually due to the long range nature of the forces between atoms. These are evaluated by fast Fourier transforms (FFT's), which are known to be slow on massively parallel machines. Hence an important component of this research is the development of communication routines for FFT's which is being carried out by Y. Deng and students at Stony Brook. Application to the proteins mentioned above uses the AMBER suite of codes. The adenovirus work is being performed at BNL, the Botulinum at Stony Brook.

TECHNICAL PROGRESS AND RESULTS:
Results for the scaling of the FFT's and lengthy simulations of Botulinum have been published. Results for the adenovirus simulation are being continued with other funding.

Giant Proximity Effect in High-Temperature Superconductors

LDRD Project 05-104

Ivan Bozovic

PURPOSE:

We are investigating systematically the Giant Proximity Effect (GPE) in high-temperature superconductors (HTS) using the atomic-layer-by-layer molecular beam epitaxy (ALL-MBE) system at CMPMS department. The atomic-layer engineering capability allows us to synthesize atomically perfect HTS films and fabricate precise multilayers and superlattices. We have proved that GPE is real and intrinsic to HTS, and this imposed a new experimental constraint on the theory of HTS. We are tightening this further by determining quantitative dependence of the proximity-induced superconductivity on a number of parameters. This is expected to provide new insight into the mechanism of HTS as well as open prospects for new advances in superconducting electronics.

APPROACH:

Our strategy is to synthesize a series of SN' bilayers and SN'S junctions; here, S denotes an optimally doped HTS compound and N' an underdoped or overdoped HTS materials with a reduced $T_c^{'}$. [Note that the GPE is observed at temperature $T_c^{'} < T < T_c$.] We can vary systematically the doping level *x*, the temperature *T*, the external magnetic field ***H***, the power *P* of microwave radiation, etc. H. Shim, P. Chaudhari, G. Logvenov, V. Butko, A. Gozar and A. Bollinger are also participating in this project.

TECHNICAL PROGRESS AND RESULTS:

In FY 2007, we performed about 250 thin film synthesis experiments. Every film was characterized by Reflection high-energy electron diffraction (RHEED), transport measurements (resistivity and susceptibility as a function of temperature down to 4.2 K). Many of them were also characterized by atomic force microscopy and X-ray diffraction. We fabricated a range of HTS bilayer, trilayer, and superlattice films for a systematic study of proximity effects. Some of these were processed by lithography into sandwich-junction structures and studied in detail using our new Josephson Junction characterization setup; others were studied by our collaborators from Paul Scherrer Institute, Zurich, Switzerland by low-energy muon spin resonance spectroscopy and from University of Illinois at Urbanna by soft resonant X-ray scattering. All the findings so far are consistent with our original claims about Giant Proximity Effect in cuprate superconductors [I. Bozovic *et al*., Phys. Rev. Letters **93**, 157002 (2004)].

An unexpected bonus of these studies was the discovery of interface superconductivity [A. Gozar, G. Logvenov, A. T. Bollinger and I. Bozovic, "Interface superconductivity between a metal and a Mott insulator", submitted to Nature Physics (2007).]. We have synthesized a number of bilayers consisting of an insulator (La_2CuO_4) and a metal ($La_{1.55}Sr_{0.45}CuO_4$), neither of which is superconducting *per se*. However, in bilayers T_c is either ~15 K or ~30 K, depending on the layering sequence. The phenomenon is confined within 3 nm from the interface. Furthermore, if such a bilayer is exposed to ozone, T_c reaches 50 K – an enhancement of about 25% compared to the maximum we obtain in single-phase films, see Fig. 1. This approach opens prospects for manipulating interfacial charge and increasing T_c in known superconductors and/or finding new ones, e.g. as native or artificial superlattices. We hope to attract significant new funding to study this effect. A patent application has been drafted and will be submitted before long as well.

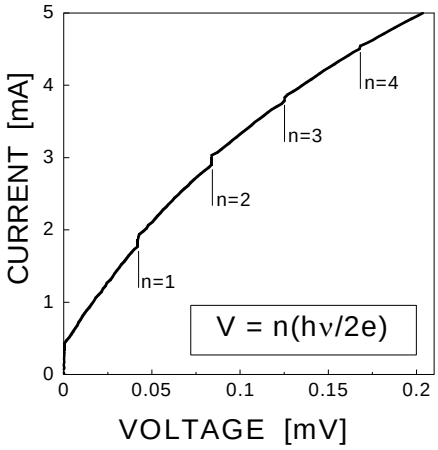

Figure 1. Shapiro steps induced by microwave (ν = 20 GHz) radiation in an SN'S device, at T = 30 K > T_c'. The steps occur exactly at the voltages given by $V = nh\nu/2e$, for n = 1, 2, 3, 4,..., as expected from a single Josephson junction. This project does not involve animal vertebrates and/or human subjects.

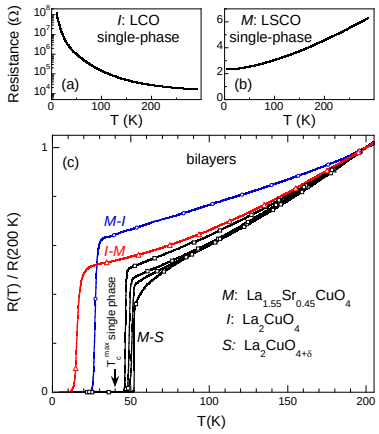

Figure 2. The dependence of resistance on temperature for single-phase and bilayer films. Here, *I* = La_2CuO_4, vacuum-annealed and insulating; *S* = $La_2CuO_{4+\delta}$, oxygen-doped by annealing in ozone and superconducting; *M* = $La_{1.55}Sr_{0.45}CuO_4$, overdoped and metallic but not superconducting. Panels (a) and (b): *R(T)* for single-phase layers of *I* (note the log scale) and *M*, respectively. Panel (c): *R(T)* normalized to *T* = 200 K for various bilayers. *I-M* and *M-I* bilayers both show robust and reproducible superconductivity even though neither of the two constituents does.

.

Study of High-T_c Nanostructures

LDRD Project 05-114

Ivan Bozovic

PURPOSE:

We are investigating systematically the effects of reduced dimensionality and confined geometries on high-temperature superconductors (HTS). This should allow us to attack some of the most basic questions in HTS physics such as what are the spin and the charge of free carriers, what is the nature of superconducting transition – do Cooper pairs form and condense at T_c or else the pairs formed at some higher temperature T^* undergo the Bose-Einstein condensation at T_c - and is the presence of dynamic stripes a necessary condition for HTS to occur. If we demonstrate that HTS can be sustained in mesoscopic samples (such as nanowires or nanodots), this would rule out a large class of theoretical models currently under active investigation and narrow down the playing field; this could be an important step towards elucidation of the mechanism of HTS.

APPROACH:

We use the state-of-the art atomic-layer-by-layer molecular beam epitaxy (ALL-MBE) system to synthesize atomically smooth HTS films, multilayers, and superlattices. Electron-beam nanolithography allows fabrication from such films of a variety of mesoscopic (nanoscale) devices such as nanowires, nanorings, and nanodots. Measurements of transport properties of these nanostructures reveal their critical temperature T_c, the critical current density j_c, etc. It is important to make as perfect samples as possible, in order to discriminate between extrinsic and intrinsic causes of T_c reduction. Apart from the PI, other participants in this project are G. Logvenov, A. Bollinger, A. Gozar and V. Butko.

TECHNICAL PROGRESS AND RESULTS:

In FY 2007, we performed about 250 thin film synthesis experiments. Every film was characterized by Reflection high-energy electron diffraction (RHEED), transport measurements (resistivity and susceptibility as a function of temperature down to 4.2 K), and many by atomic force microscopy and X-ray diffraction. We have achieved essentially 100 % yield of atomically smooth films, thus surpassing what used to be the state-of-the art anywhere in the world in this field. Many of these films were heterostructures – multilayers and superlattices – some of which included HTS layers only one-unit-cell thick. We have used electron-beam nano-lithography on such films to fabricate nanowires made out HTS compounds such as $La_{1.85}Sr_{0.15}CuO_4$. More recently, we have greatly developed our technical capabilities in optical lithography using interference techniques. This has enabled lithographic fabrication of unprecedented parallel arrays of several thousands of HTS nanowires, 10 mm long and typically about 100 nm wide, at high density. This is illustrated in Fig. 1a which shows a large field of view on such an array and in Fig. 1b where we have zoomed-in on a couple of wires.

In terms of new physics, the main new result is a discovery (in collaboration with the group of A. Zewail at Caltech) of colossal photo-induced expansion in $La_2CuO_{4+\delta}$ films grown by MBE, reported in the Science magazine in April 2007. The principle of the experiment and the key experimental findings are illustrated in Fig. 2. We found that upon intense photo-illumination, the film expands along the *c*-axis by as much as 0.3 Å (~ 2.5%). This is an unambiguous proof that electron-lattice coupling is very strong in cuprates. In order to achieve electron transmission,

we need HTS nanostructures, not thicker then few tens of nanometers. We have fabricated them using electron-beam lithography first, then developed a much more efficient optical lithography process described above. We are continued the experiments and expanding them to other materials.

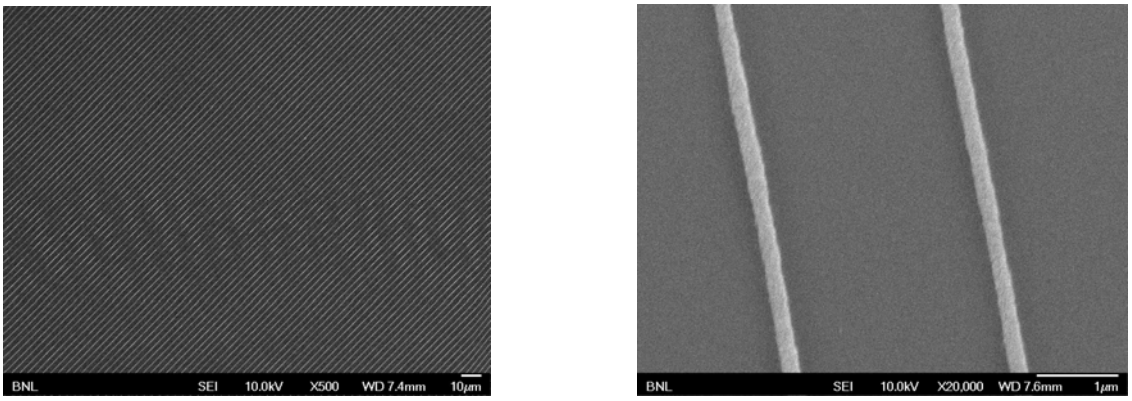

Figure 1. (a) Nanowire array fabricated out of a $La_2CuO_{4+\delta}$ film grown by MBE using optical lithography. The pattern extends over the entire film area, i.e. 10x10 mm^2. (b) A zoom-in on two nanowires.

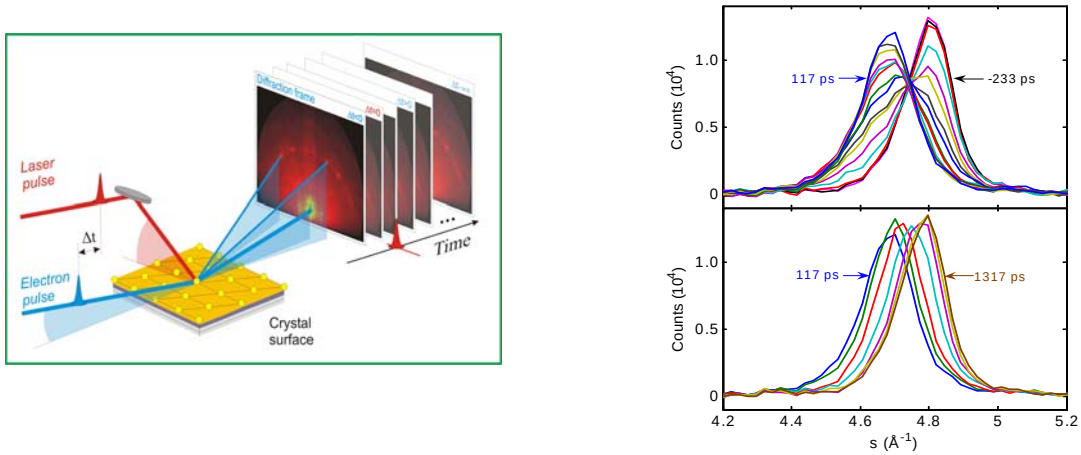

Figure 2. (a) Schematics of the ultrafast RHEED experiment described in N. Gedik, D.-S. Yang, G. Logvenov, I. Bozovic and A. Zewail, Science **316**, 425 (2007). An $La_2CuO_{4+\delta}$ film grown by MBE was photo-excited by intense short light pulses and the surface structure was analyzed using picosecond electron diffraction. By scanning the delay time one obtains RHEED 'movies' that show time-resolved changes in the crystal structure. (b) The main result: upon intense photo-illumination, the film expands along the *c*-axis by as much as 0.3 Å (~ 2.5%).

Lattice Studies of QCD Thermodynamics on the QCDOC

LDRD Project 06-001
Frithjof Karsch

PURPOSE:
Objective is to reach a better understanding of the thermodynamics of strongly interacting matter through large scale numerical simulations on the two QCDOC supercomputers operated at BNL. The main goals are a determination of the QCD equation of state with light, nearly physical quark masses and a strange quark mass as well as the parameters controlling the transition and a study of in-medium properties of hadrons.

APPROACH:
Numerical studies of the phase structure of QCD have in the past had to rely on approximations (unphysically large quark masses, crude discretization of the continuous space-time) in order to become feasible at all. New supercomputers like the QCDOC machines at BNL now allow calculations with a realistic quark mass spectrum to be performed with improved actions on lattices with strongly reduced discretization errors. Furthermore, newly developed simulation algorithms now also allow to perform simulations without intrinsic step-size errors inherent in previous discretization schemes for the molecular dynamics evolution of the QCD Hamiltonian. We perform a large scale simulation of QCD with light up and down quark masses close to their physical value and a strange quark mass value fixed to its physical value. For this purpose we use a lattice discretization scheme (improved staggered fermions) that has been optimized by us for thermodynamic calculations.

The numerical calculations are performed at BNL as well as on a supercomputer, apeNEXT, at Bielefeld University, Germany. The collaboration involves about 15 members from Bielefeld University (Prof. E. Laermann et al.), Columbia University (Prof. N.H. Christ, Prof. R.D. Mahinney et al.) and members of our BNL based Lattice Group (S. Ejiri, P. Petreczky, K. Huebner, C. Pica, C. Schmidt, W. Soeldner and myself).

TECHNICAL PROGRESS AND RESULTS:
During most of FY2006 we performed a detailed analysis of the QCD transition which led to a determination of the transition temperature. The continuum extrapolation of our results, which at present is based on results obtained at two values of the lattice cut-off, gave a transition temperature of about 190 MeV. In FY2007 we performed studies of the QCD equation of state at vanishing chemical potential. This new set of lattice calculations has been performed with a nearly physical spectrum of light and strange quarks. The high temperature behavior of the difference between energy density and three times the pressure was analyzed for the first time for three different choices of the lattice cut-off, which allowed to control systematic errors in this regime. This is the first calculation of the equation of state of QCD with a nearly physical quark mass spectrum that covers the entire energy density regime accessible in heavy ion collisions at RHIC and even further up to energy densities of about 1TeV/fm^3.

The data collected in this project will now be used for more detailed studies of properties of the high temperature phase, the determination of the bulk viscosity in the transition region and the calculation of the QCD equation of state at non-vanishing baryon number density.

A major result of these studies is the confirmation of the existence of large deviations of the QCD equation of state from ideal gas behavior in the entire energy density regime accessible to RHIC. This stresses the need of an accurate determination of the EoS through lattice studies as input for the hydrodynamic modeling of dense matter created at RHIC.

In FY 2007 we presented a systematic study of our improved lattice discretization scheme, a new calculation of the QCD equation of state and a new determination of the transition temperature in 3-flavor QCD.

Detector Development for Very Long Baseline Neutrino Experiments

LDRD Project 06-004

Milind Diwan

PURPOSE:

We are developing new concepts, originated by BNL researchers, for the design of a very large (500 kT) multipurpose Water Cherenkov detector with a broad band accelerator neutrino beam. A large mega-ton scale detector with high electron-neutrino detection efficiency, good energy resolution and background rejection is needed to reach the physics sensitivities of the next generation of very long baseline neutrino experiments and proton decay experiments. We envision placing such a detector deep underground in the proposed Deep Underground Science and Engineering Laboratory (DUSEL) facility which will be located in the former Homestake gold mine.

This research is also carried out partly in response to the charge from the US Department of Energy and National Science Foundation to the Neutrino Scientific Assessment Group (NUSAG) dated on March 3, 2006 to "address the American Physical Society's recommendation for a next-generation neutrino beam and detector configurations". To that end, the US Long Baseline Neutrino Experiment Study was launched jointly by BNL and Fermi National Lab. The co-leaders of the study are Milind V. Diwan from BNL and Gina Ramieka from FNAL. Part of the charge is to address the detector options for a very long baseline neutrino experiment. The study group was charged to address the following questions pertaining to the detector design:

"What are the associated detector options which might be needed to fully realize the envisioned physics potentials? What are the rough cost ranges for these detector options? What would be the optimal construction and operation timeline for each accelerator-detector configuration? What would be additional important physics questions that can be addressed in the same detector(s)?"

APPROACH:

Our study focuses on addressing the charge as it pertains to the design and costing of a large underground 500 kT Water Cherenkov detector. We chose a Water Cherenkov as the initial detector technology to consider due to the proven track record of such detectors in neutrino and proton decay physics. Currently, the largest such detector built is the SuperKamiokande detector which is 50 kT. Ultimately, we will need a detailed design of a large detector with mass greater than 100 kT. Our approach is in three parts:

1) Developing detailed simulations of a large Water Cherenkov detector to determine the feasibility of using this technology to achieve the required signal sensitivity and background rejection capabilities for the next generation of long baseline neutrino experiments. To that end, Brett Viren from BNL has worked with colleagues from Stony Brook University (SBU) to create a simulation program while Chiaki Yanagisawa, collaborator from SBU, has used existing simulations of Water Cherenkov detectors to understand the performance of such a detector. 2) An engineering study to determine the design requirements and cost estimate of building a 500 kT Water Cherenkov detector deep underground in the proposed DUSEL site at Homestake mine in South Dakota. We are assembling a BNL and University based engineering team to study the mechanical design of 100kT Water Cherenkov detector modules with the goal of constructing at least 5 such modules in Homestake Mine. 3) Research into new photodetection

technology and the characterization of the response of different photomultiplier tube (PMT) technologies to assess their feasibility for use to instrument 100kT Water Cherenkov detector modules. To that end we have instrumented a laboratory space for use in the automated measurement of photodetector response. This effort also includes pressure testing of PMTs. We have obtained 32 large 10.5" PMTs from Hamamatsu and 4 tubes from Photonis with diameter of 12" for destructive testing. This PMT research and development work shares testing facilities and effort with the proposed Daya Bay Reactor Neutrino Experiment of which the BNL EDG group is a leading collaborator.

TECHNICAL PROGRESS AND RESULTS:

This LDRD project has resulted in a new concept for a US national neutrino program that has been examined by national committees. This is thoroughly documented on the study website which we developed as part of this proposal.

1) It has been confirmed by two independent simulations that the background to electron events could be controlled in a Water Cherenkov detector. This background reduction work has been reported at various workshops and conferences and has been written in two technical notes and incorporated into the report on the US Long Baseline Neutrino Experiment Study.

2) The report of the US long baseline neutrino experiment study has been completed and presented to the directorates of BNL and FNAL. The report was accepted in July, 2007. The report of the NuSAG committee relies on our report and has been accepted by the DOE/HEPAP panel.

3) The concept that originated at BNL for sending a high intensity neutrino beam to a new DUSEL laboratory for neutrino CP studies has been accepted by national committees as superior to other competing approaches.

4) Our engineering effort on the mechanical design, timeline and costing of several 100 kT scale Water Cherenkov modules has been very successful and we now have a preliminary cost estimate of ~$350 M, including a 30% contingency for 3 modules (a total of 300 kT fiducial volume) and the timeline for the construction of the photomultiplier tubes. This cost estimate and timeline is included in the US Long Baseline Neutrino Experiment Study Report. We anticipate further engineering work is needed to refine the cost estimate as well as continuing the PMT R&D effort.

5) The Homestake site was chosen by a 22 member NSF panel as the site of choice for the DUSEL. The BNL contribution to this decision in terms of the science program and the facility was very important.

Detector for High Quality Imagers of Electron Microscopy

LDRD Project 06-012
P. Rehak, G. Deptuch, J. F. Pratte, and J. Fried

PURPOSE:
The technical objective is to develop an Active Pixel Imager (API) based detector for electron microscopy. The image produced by the sensor under development will be limited only by physics of the electron microscope. The detector will be capable of providing these high quality pictures at frame rates high enough to allow dynamic studies of biological objects and structures in nano-science.

APPROACH:
Detectors are a critical part of any electron microscope, since all the image, diffraction and spectroscopy information must pass through them prior to analysis. A wide range of topics, both in materials science and biology, are currently beyond reach due to limitations in detector technology. Constant progress in semiconductor (silicon) technology is responsible for the recent devices in digital imaging technology called Active Pixel Sensors APSs. These sensors were already designed, produced and tested as detectors of charged particles crossing the plane of sensors. The information being read-out is the total charge released in the active layer of silicon during the whole integration time of the sensor. The number of charged particles crossing the sensor and producing the charge is obtained from the total charge accumulated in individual pixels. These numbers of crossing particles are different from the true numbers due to imperfections of the charge measurement and because of intrinsic fluctuations of the charge produced by the passage of a single particle. Moreover, the dynamic range of the charge measurement limits the dynamic range of the particle count. The proposed detector improves all shortcomings of present APSs.

TECHNICAL PROGRESS AND RESULTS:
Most of the effort during FY 2006 was dedicated to the modeling of the device. The modeling can be divided into two main parts. i) Modeling of the process of the ionization and of the collection of the signal charge within the epitaxial part of the silicon pixel, and ii) amplification of the charge and the signal processing. The process of the ionization produced by the electron beam of the microscope and the collection of the signal charge is not part of any commercially available software. The software to simulate this part of the detection process was developed and used for the optimization of the geometry of the n- and p- wells in the pixels and for the values of voltages to be applied at individual wells. The linear part of the read-out electronics chain was designed with the help of commercial programs for the design of Integrated Circuits (IC).

In FY 2007 the design of a small scale prototype was completed, produced and partially tested. Figure 1 below shows the microphotograph of the produced chip. The large square on the right hand side is a 32 by 32 pixel matrix of independent pixels. Each pixel contains a detection volume followed by the complete chain of read–out electronics. The read-out electronics is formed by a preamplifier followed by a shaper, baseline restorer, comparator and a 15 bit scaler. The pixel architecture of this array is already an exact realization of the architecture to be included in larger arrays intended to be used in electron microscopes. A smaller rectangle on the top of left hand side is an array of 16 by 16 pixels, each pixel having the conventional three transistor read-out. This traditional read-out system was realized on pixels having a novel feature

of decreased signal charge collection time due to hole current within the epitaxial layer of the pixel. The remaining two smaller structures are single pixels where several nodes of the read-out chain are accessible to verify the functioning of the electronics.

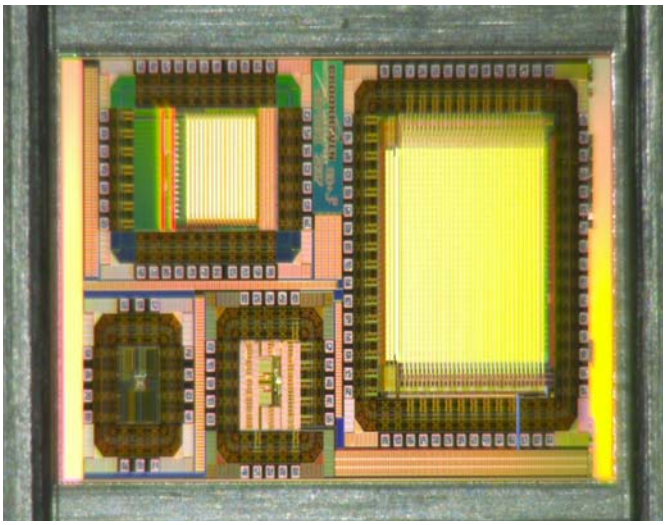

Figures 2 and 3 below show examples of test results. On the oscilloscope picture on left hand side the trace 2 is the test pulse capacitivly coupled to the preamplifier input. Trace 1 is the output of the shaper. Trace 4 is the output of the comparator. The channels of the oscilloscope are connected to the single pixel where multiple nodes are accessible. Picture at right hand side is obtained with the 16 by 16 pixels array.

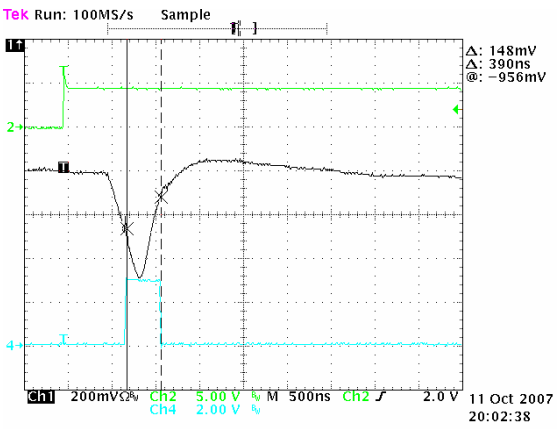

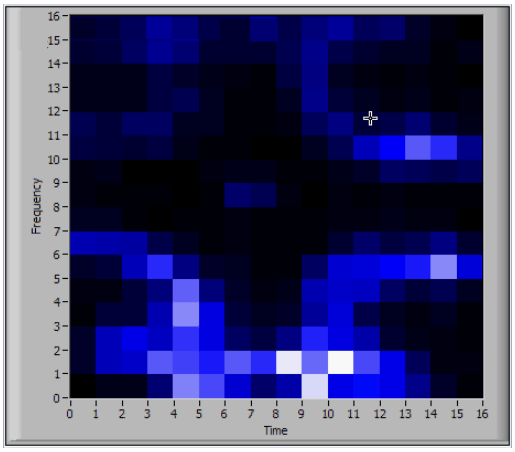

All tests performed up to now show that the prototype is functional. More tests are required before the next larger array is designed and submitted for the production. We have foreseen two more iterations of the pixel arrays design in FY 2008 before producing a sample to be used as a work horse in one of electron microscopes.

Transparent Photocathode Development

LDRD Project 06-017

John Smedley

PURPOSE:

Aim is to develop a photocathode which will provide a significant average current while being illuminated in transmission mode. Such a cathode is needed for applications where it is difficult or impossible to illuminate the cathode in reflection mode. One such application of particular importance to BNL is the diamond amplified photocathode project, which would cover the electron-emitting side of the photocathode with a thin diamond layer, forming a capsule (figure 1). This cathode is intended as the electron source for the C-AD Energy Recovery Linac project and the e-cooler upgrade that is part of RHIC II.

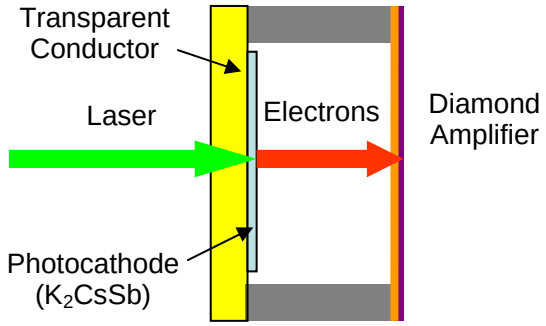

Fig. 1: Capsule with transparent cathode

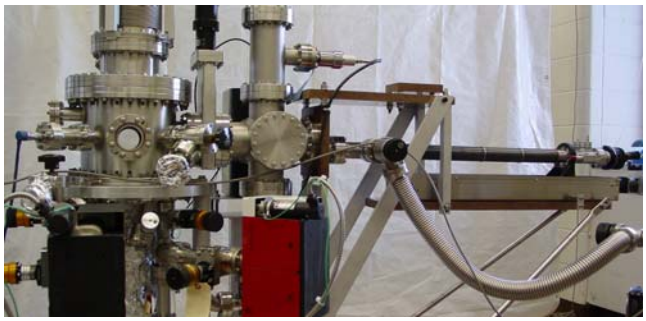

Fig. 2: Deposition system

As shown in the figure, in the transmission mode, the laser light passes through the transparent substrate and a thin conducting layer to irradiate the photocathode at the conductor-cathode interface. The electrons generated by the laser then travel through the cathode material to be emitted from the opposite surface.

Several factors will impact the performance of a transmission photocathode. The substrate must be optically transparent and a good thermal conductor. It must be coated with a layer of sufficient conductivity to provide electron resupply to the photocathode. This layer must also be optically nearly transparent and must be compatible with the photocathode material. The cathode layer should be thick enough to absorb a significant fraction of the laser photons and yet thin enough to transmit a significant fraction of the electrons generated. The resulting photocathode should be able to produce significant average current, and the lifetime at high current will need to be characterized.

APPROACH:

An existing vacuum chamber has been modified to accommodate deposition of antimony, potassium and cesium. A manipulator arm in vacuum allows the cathode substrate to be coated by each source sequentially. The deposition rate of the antimony and potassium sources is measured via a crystal monitor, while the deposition of cesium is controlled by monitoring the photocurrent during deposition. New modifications to the system permit the measurement of the thickness of the cathode after each step via optical transmission as well. After deposition, the cathode quantum efficiency can be monitored by illumination with a laser in either reflection or transmission mode. Emitted current is measured leaving the cathode, and the cathode can be biased to prevent space-charge limiting of the current. The system can use a wide variety of substrate materials for both reflection and transmission photocathodes.

We are currently studying K_2CsSb. This cathode is used in photomultiplier tubes in transmission mode, and has a high quantum efficiency (QE) for visible light. The deposition recipe will be

optimized for high QE in both reflection and transmission modes, by adjusting the thickness of cesium, potassium and antimony used, as well as the substrate temperature during deposition. Once a recipe is determined, a cathode will be tested for performance at high current and the lifetime will be measured.

TECHNICAL PROGRESS AND RESULTS:

Initial deposition was hampered by the failure of commercial alkali metal sources obtained from SAES getters to provide Cs and K. Extensive rework of our system, including a custom residual gas analyzer and construction of a smaller test chamber for source evaluation, determined that these sources were in fact defective. Subsequent tests using alkali metal sources from another vendor (Alvatec) provided acceptable deposition. **This observation had a critical impact on the design of the cathode deposition system for the CAD energy recovery linac, which can now accommodate Alvatec alkali sources.**

Several K_2CsSb cathodes have been deposited with the new sources. The best QE observed during deposition is 2.8% (@ 543 nm). The QE decays rapidly with time initially, likely due to poor cooling capability in the manipulator arm (this problem is being addressed). Figure 3 shows the QE in reflection and transmission mode 20 minutes after deposition. The transmission in both modes agrees well, considering the 74% optical loss in the copper film for the transmission mode. The position dependence of the QE is likely due to thickness variation of the cathode.

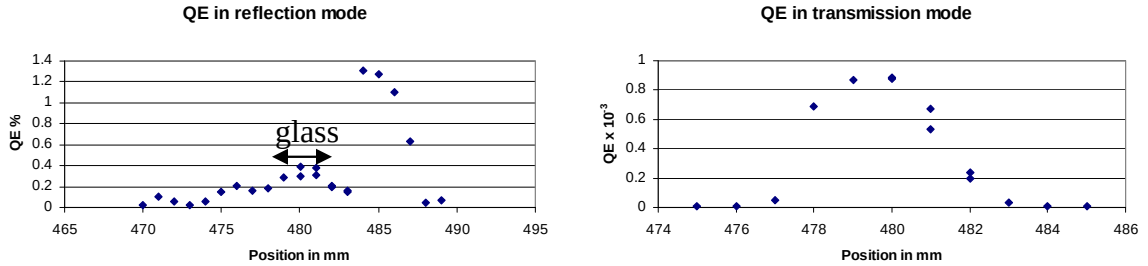

Fig. 3: QE in reflection and transmission mode, as a function of position on the cathode

To assist the optimization of the thickness of the photocathode, a Monte Carlo model has been developed based on the three step model of photoemission. This model predicts that the QE does not increase monotonically with thickness, even for reflection mode measurement. There is an optimum thickness which provides maximum QE (~30 nm). A cathode which was thicker than this optimum in some areas and thinner in others would evidence an oscillation in QE as a function of position, as observed in figure 3.

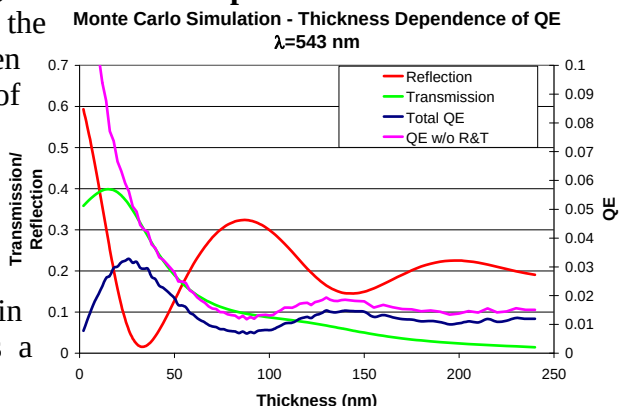

Fig. 4: Monte Carlo Model Results

Our near term plans for this experiment include: deposition of a cathode followed by rapid cooling to mitigate QE degradation; deposition of a cathode on a commercially available transparent conductor, such as Indium-Tin Oxide (ITO); deposition of a thicker cathode to test uniformity; and continued development of theoretical model to understand cathode behavior.

Synthesis and Characterization of Band-Gap-Narrowed TiO_2 Thin Films and Nanoparticles for Solar Energy Conversion

LDRD Project 06-021
Eli Sutter, Peter Sutter, Etsuko Fujita, and James Muckerman

PURPOSE:
TiO_2 is considered to be the most promising semiconductor material for solar energy conversion into chemical energy (H_2) via photo-decomposition of water because of its high stability, availability, low cost and non-toxicity. Its only disadvantage is being photoactive under ultraviolet (UV) light irradiation [wavelength (λ) < 387 nm] rather than from the main part of the solar spectrum. One promising approach to making TiO_2 highly reactive under visible light is to modify it via substitutional doping with nitrogen, carbon and boron that can lower the energy gap and shift absorption towards longer wavelengths. Under this LDRD project we are developing synthetic routes for the reliable in-situ doping of TiO_2 crystalline thin films and nanoparticles with N, C, and B. We will use the synthesized material for basic research in solar water photoelectrolysis, important aspects of which are understanding of the mechanism of doping and the interaction of H_2O with doped TiO_2.

APPROACH:
We perform epitaxy and doping in our ultrahigh vacuum (UHV) reactive magnetron sputtering deposition system combined with a scanning tunneling microscope (STM). This combination is unique as it allows us to study the synthesized doped material in-situ, without any further surface cleaning or annealing that might introduce changes, using tunneling microscopy and spectroscopy to determine the surface electronic structure and the interaction of H_2O with doped TiO_2. We use state-of-the-art analytical techniques in transmission electron microscopy (TEM) to determine dopant densities and distribution and to evaluate the stability of the doped material.

TECHNICAL PROGRESS AND RESULTS:
In this past year we made major progress in the epitaxial deposition and in-situ doping of TiO_2 thin films (both anatase and rutile) using nitrogen dioxide (NO_2) as source of nitrogen.

In-situ N-doping of TiO_2 from NO_2. Following our earlier experiments (first six months of this project) on setting-up the epitaxial growth of TiO_2 in our system we made a big step forward by establishing in-situ N-doping. Both rutile and anatase films were prepared by reactive magnetron sputtering. Both the undoped and doped rutile TiO_2 films are high quality single crystalline films The quality of the surface is excellent with large atomically flat terraces, major prerequisite for understanding the mechanism of N doping (Figure 1). The nitrogen content in the films was measured using electron energy loss spectroscopy (EELS) in the TEM in polycrystalline anatase films prepared on Si substrate (Figure 2). The nitrogen content was estimated to be ~2.5 at.%, or $TiO_{1.96}N_{0.04}$. This level of doping is similar to the levels obtained by doping after the formation of TiO_2. However, in contrast to films doped after formation, in which N-induced structural destabilization occurs, the in-situ prepared material showed excellent stability.

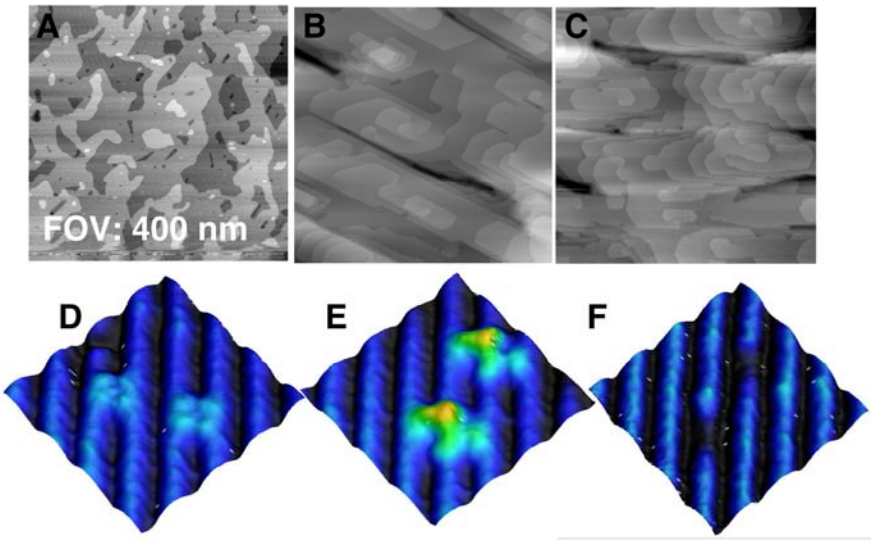

Figure 1: STM images of the surface of (A) the rutile TiO_2(110) substrate, (B) an epitaxial TiO_2 film showing large flat terraces and (C) an epitaxial $TiO_{2-x}N_x$ film doped from NO_2, deposited by reactive magnetron sputtering. (D-F) Close-ups showing surface features associated with N atoms substituting oxygen at different positions on or under the bulk terminated (1x1) surface structure (FOV 3 nm x 3 nm).

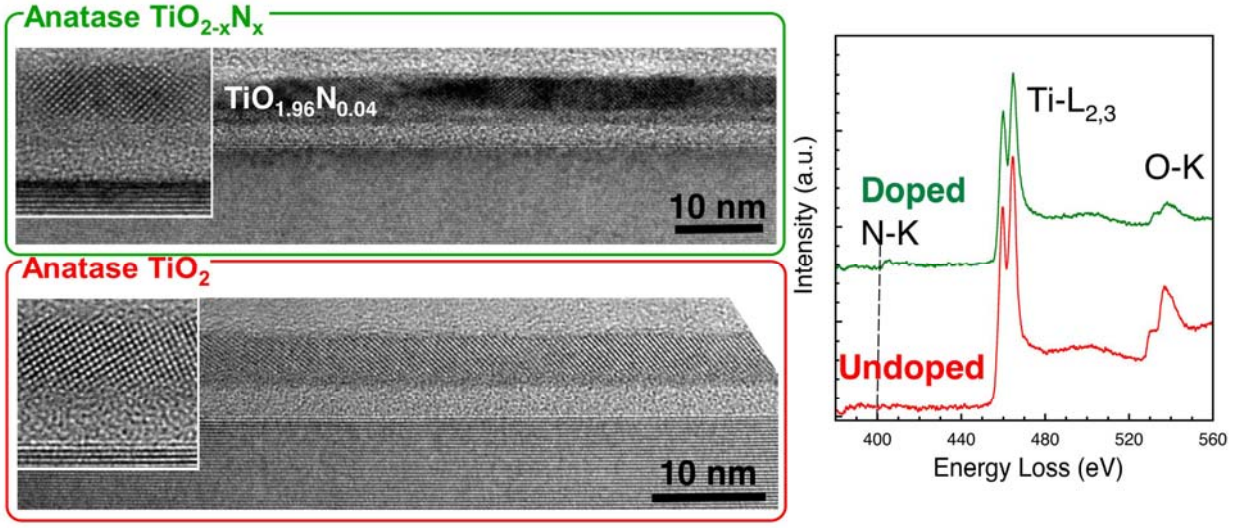

Figure 2: Left: TEM image of a $TiO_{2-x}N_x$ film doped from NO_2 and an undoped TiO_2 film. Right: EELS spectra of the two samples showing a nitrogen content of ~ 2.5 at.% in the doped sample.

The achievement of substitutional doping of TiO_2 with nitrogen at levels of a few percent provides us with unique material. We plan experiments on formation of the doped material and investigation of its properties in our exceptional deposition system combined with an in-situ STM to determine the near surface electronic structure of the doped films and elucidate the atomistic doping mechanism as well as the interaction of the doped TiO_2 with water under controlled UHV conditions.

Multiscale Analysis of *In Vivo* Nanoparticle Exposure

LDRD Project 06-026
Wynne K. Schiffer

PURPOSE:

By virtue of their unusual size, nanoparticles have greater potential to travel through a living organism than other materials or larger particles. However, there are few ways to test where these new materials disperse in living systems and whether they will be tolerated by the anticipated host. In the service of this goal, we developed a unique imaging approach to investigate nanoparticle distribution in living rodents. At the heart of this *in vivo* approach is a new family of nanoparticle probes that can be imaged using positron emission tomography (PET). By conjugating existing classes of nanoparticle materials with a positron emitting isotope such as carbon-11 or fluorine-18, we will be able to quantitatively address current questions regarding the *in vivo* distribution, clearance, metabolism and toxicity of a broad range of nanoscale materials. These studies will allow us to develop kinetic models which can be used to describe and even predict the *in vivo* behavior of a broad spectrum of nanoparticles based on fundamental differences in their physicochemical properties.

APPROACH:

PET is a highly sensitive, non-invasive medical imaging technique which is remarkably suited for *in vivo* evaluation of pharmacokinetics. We developed a strategy to synthesize positron-emitting nanoparticles for use with PET. This radiolabeling strategy is not limited to a particular type of manufactured nanoparticle, allowing us to develop models of exposure to predict the dispersion of a broad range of nanomaterials in living systems. Systematic variations in physio-chemical parameters such as elemental composition, particle number, size distribution and surface conjugation will allow us to determine how these properties influence the *in vivo* dissemination of nanoparticles. A historical goal of molecular imaging has been to develop kinetic models to predict the organ distribution and accumulation of pharmaceuticals in humans. When applied to nanoparticles, these kinetic models become a powerful tool to predict how changes in fundamental nanoparticle properties such as size, surface chemistry, charge or core material, will affect the behavior of a given particle in living systems (see Figure 1).

Because the physico-chemical properties of nanoparticles may have changed during preparation or upon exposure to the living system, the physical and chemical properties of nanoparticle preparations were evaluated at multiple points in the process, from acquisition to labeling to imaging and afterward. These evaluations were done in collaboration with Drs. Mathew Maye and Oleg Gang of the Center for Functional Nanomaterials and include Dynamic Light Scattering (DLS) and Uv-vis for concentration estimates, Transmission Electron Microscopy (TEM) to measure particle size and dispersion. Collaborations with investigators from the Department of Materials Science facilitated progress in the application of inductively coupled high density plasmas to measure nanoparticle concentrations in animal tissues. Evaporative loss experiments ensure that the carbon-11 remains with the nanoparticle in systemic circulation. PET experiments are validated using fluorescent light microscopy where appropriate (i.e. with semiconducting quantum dots) and ICP is used to quantify metals (i.e. cadmium) in tissue.

TECHNICAL PROGRESS AND RESULTS:

In the first year of this project, we successfully radiolabeled cadmium-selenide/zinc sulfur (CdSe/ZnS) semiconducting quantum dots (QDs) and tracked their distribution in living mice. DLS and UV-vis were both used to verify nanoparticle concentrations, and it was found that the

concentrations quoted by the nanoparticle vendor were overestimated by a factor of three. The integrity of radiolabeled suspensions were examined at an electron microscopic level with TEM and particles were found to be intact and unaffected by the carbon-11. Evaporative loss experiments in rodent plasma demonstrated that the isotope-nanoparticle complex is stable and that measured carbon-11 is not in the form of ^{11}C-CO2 or ^{11}C-MeOH. While Inductively Coupled Plasma (ICP) has been widely applied to analyze trace metal concentrations in environmental samples, its use in biological specimens is less established. The application of ICP to assay nanoparticle concentrations in the same animals studied with microPET has been a recent and successful endeavor, validating radioactivity measurements with trace metal analysis.

Results from PET experiments indicate that the *in vivo* distribution of radiolabeled CdSe/ZnS quantum dots is significantly impacted by core size and surface coating, and less so by core material. Smaller particles (3 nm core size) readily penetrated well-protected organs such as the brain where larger particles (10 nm) did not. Coating particles with surfactant significantly impacted particle kinetics, increasing blood circulation time.

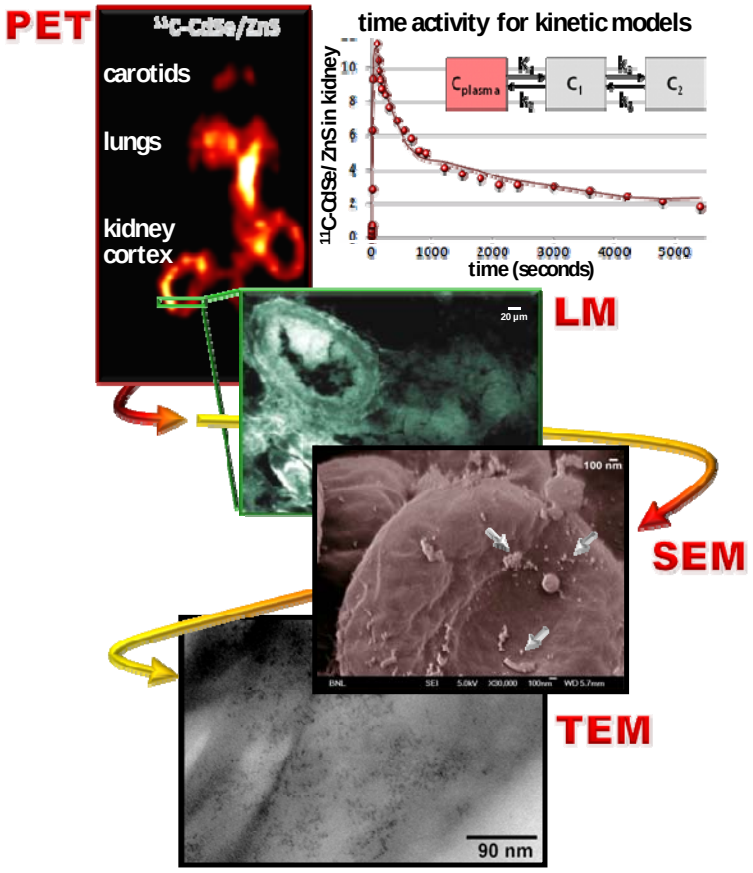

Figure 1. PET imaging with radiolabeled particles can be used to identify structural predictors of *in vivo* nanoparticle behavior (here, the cortex of the mouse kidney is highlighted). This information can used to guide later biopsy and analysis of tissue from the same animal using light microscopy (LM; scale bar = 20 µm), high resolution ultrastructural imaging by field emission Scanning Electron Microscopy (SEM; scale bar = 100 nm) and Transmission Electron Microscopy (TEM; scale bar = 90 nm). The time activity curve is also shown, where the line depicts the fit of the kinetic data to a two compartment model. According to the model fit, the K_1 of ^{11}C-CdSe/ZnS is 0.09, indicating that the nanoparticles leave plasma and enter tissue at a rate of 9% per minute. Ultrastructural microscopic analysis of tissue after the PET scan suggests that this compartment comprises the kidney tubules (TEM image).

Based on PET measurements, we can see that CdSe/ZnS nanoparticles accumulate in the liver, spleen and kidneys. Light and electron microscopic approaches successfully validated PET measurements and established the precise location of CdSe/ZnS within tissues and cells. There was a strong correlation between ICP measurements of cadmium concentrations in tissue and PET measurements of carbon-11, indicating the isotope was an excellent marker for the nanoparticle.

Development of Gadolinium-Loaded Liquid-Scintillators with Long-Term Chemical Stability for a New High-Precision Measurement of the Neutrino Mixing Angle, Theta-13

LDRD Project 06-030
Richard L. Hahn

PURPOSE:
Our R&D program in chemistry and nuclear/particle physics focuses on the development of new detector systems for neutrino oscillation experiments. In particular, we have been focusing on gadolinium-loaded liquid scintillators (Gd-LS) for the efficient detection of antineutrino interactions, with the aim of being able to measure with high precision the one remaining unknown neutrino mixing-angle, theta-13. The LS produces more light than Cherenkov radiation, and the Gd produces a coincidence tag from the neutrons that are produced in the primary antineutrino inverse beta-decay, thus substantially reducing the background from random coincidences. DOE/OHEP has been providing project support to BNL for the theta-13 experiment that is being developed at the Daya Bay nuclear power station in China. The research being done under this LDRD project is complementary to but separate from the work we are doing related to the Daya Bay project.

APPROACH:
We apply our expertise in chemistry and nuclear chemistry:
1. To develop methods to produce organic complexes of Gd with carboxylic acids that are soluble and stable in various liquid scintillating organic solvents.
2. To study chemical speciation of the trivalent Gd-carboxylate complexes to gain understanding of their chemical composition and structure, and the factors that determine their stability; e.g., $Gd^{(3+)}(RCOO)_{(3-x)}(OH)_{x.}$
3. To develop methods to assay, reduce, and/or eliminate radioactive contaminants in the Gd- and in the materials that we work with.

TECHNICAL PROGRESS AND RESULTS:
Last year we established a Gadolinium-Loaded Liquid Scintillator for High-Precision Measurements of Antineutrino Oscillations and the Mixing Angle, theta-13, and a method for Solvent Purification and Fluor Selection for Gadolinium-loaded Liquid Scintillators.

We have made substantial progress in FY-2007 in the following R&D areas:
1. We have demonstrated that Linear Alkyl Benzene (LAB) is a preferable LS compared to pseudocumene (PC), which had been the "customary" LS that was used in several previous neutrino experiments. The LAB has similar light-producing properties to PC, but it has a much higher flash point (130^{o} vs. 40^{o} C) and is environmentally more benign.
2. After doing a systematic study of the properties of several Gd carboxylates, we have decided that the nine-carbon carboxylic acid, 3,5,5-trimethylhexanoic acid (THMA), is best for Gd complexes that are prepared in LAB.
3. Our usual methods to evaluate the chemical properties of our Gd-LS have been UV-Visible spectroscopy to determine the liquid's optical attenuation length, and stability studies done over many months to ascertain that the Gd-LS does not change nor deteriorate slowly. We have added new analytical methods to our arsenal. For example, we are doing Karl-Fisher electrochemical titrations to measure the water content of our Gd-LS, and IR spectroscopy to characterize the

vibrational bands of the Gd-THMA carboxylate complexes, and to search for changes in these spectra as we change the chemical conditions under which we synthesize these Gd complexes.
4. Our customary approach has been to prepare the Gd-LS by solvent extraction. We are now evaluating an alternative synthesis method, first to prepare the solid Gd-THMA carboxylate and purify it, and then to dissolve this compound in the LAB. In doing so, we are also attempting to characterize the solid Gd-THMA complex by IR spectroscopy and possibly by x-ray diffraction at the NSLS.
5. We have begun radiochemical experiments to evaluate the effectiveness of different ion-exchange and crown-ether media, to remove uranium, thorium, and radium impurities from the Gd, down to a concentration level of 1 part per billion of impurity per Gd.
6. We have commissioned the 2-meter vertical optical system to measure attenuation lengths (of up to ~20 meters), and will begin measurements with Gd-LS and unloaded LS..

In 2008 there will be particular emphasis on points 3, 4, 5 and 6 above.

Electronic Properties of Carbon Nanotubes and Novel Multicomponent Nanomaterials

LDRD Project 06-037
John Hill

PURPOSE:
The purpose of this LDRD is to develop an interdisciplinary tool set to understand the electronic properties of organic nanomaterials. These materials are important from both a fundamental and applied perspective, with promising applications in fields such as optoelectronics and photovoltaics. Central to their application in these fields, however, will be a complete understanding of their electronic behavior – the subject of this program.

APPROACH:
The approach taken is a multidisciplinary one, bringing to bear a range of experimental and theoretical tools with a goal of understanding, and ultimately manipulating, the electronic properties of organic nanomaterials. Initial work centered on carbon nanotubes, which are the prototypical example of organic nanomaterials, and which have a wide range of potential applications, particularly photovoltaic uses. More recent work has explored CaC6, a superconducting graphite intercalation compound, and Rubrene, an organic semiconductor.

Experimentally, inelastic x-ray scattering has been used to probe the electronic response of these systems over a range of momentum and energy transfers. These data are combined with electron energy loss, optical conductivity, Raman scattering and ARPES measurements of the same system to provide a complete picture of the electronic excitation spectrum. Calculations are then used to gain an intuitive understanding of the physics of these materials. In particular, we are following a novel theoretical approach involving a real-space formalism that will allow a detailed understanding of the all-important excitons. This approach has been developed first in the context of NiO as a model strongly correlated excitonic system.

Collaborators in the nanotube project include D. Casa and T. Gog (ANL), G. Eres and D. Lowndes (ORNL) and R. F. Klie (UIC), Y. Zhu and A. Stein (BNL). Collaborators in the CaC6 project include A. C. Walters, C. A. Howard, K.C. Ranejat, M. Ellerby and D. McMorrow (UCL), A. Alatas and Bogdan Leu (ANL) and T. Valla.

TECHNICAL PROGRESS AND RESULTS:
Plans were developed to look at the exciton in Rubrene, an organic semiconductor but unfortunately, initial experiments showed that Rubrene is rapidly damaged by the incident photon beam. This photosensitivity occurs too fast to be mitigated by such strategies as moving the sample in the beam at each data collection point and we therefore don't believe this component of the project is worth pursuing further. However, we have identified another material that may have interesting excitonic properties: TiO2. This system is known to be radiation hard. Further, there are a number of interesting TiO2 nanostructures, which would allow us to probe the effects of size quantization on

the exciton. This is technologically relevant because one of the approaches to increasing the efficiency of solar cells is to increase their surface area, allowing the collection of more sunlight, nanostructures are a natural way to achieve this. Initial Raman experiments on these materials will be carried out. These experiments will search for the exciton and measure the zero momentum transfer behavior. Once successful, we will commence inelastic x-ray scattering work to explore the momentum dependence. This latter data will provide information on the spatial extent of the exciton – a question of crucial relevance to a materials efficiency as a photovoltaic.

In addition, we have continued our work on CaC6, a graphite intercalation compound which was discovered to superconduct below 11.4 K in 2005. We have measured the phonon dispersions in CaC6, and found good agreement with theoretical predictions made by Calandra and Mauri and by Kim et al. These same theoretical calculations fail to predict other experimental (phonon-derived) properties of CaC6 correctly. Thus our experimental verification of the phonon dispersion strongly suggests that it is the electron-phonon coupling that is not well understood in these systems. In order to shed direct light on the electron-phonon coupling, we have begun to look at these samples with angle resolved photoemission. Such measurements should probe the electronic structure and provide a quantitative measure of the electron phonon coupling.

Additionally, one of the unusual properties of CaC6 is the extremely high change in the superconducting transition temperature with pressure, and a discontinuity at 7.5 GPa, which suggests a phase transition. We will study the effect of pressure on the phonons in CaC6 using inelastic x-ray scattering (beamtime proposal is pending). We will also look at the possible structural transition with elastic x-ray scattering at NSLS at beamline X22C.

In addition to these efforts, we are continuing our work on large energy screening in CaC6 and other intercalates via measurements of the plasmon dispersion. Although our initial measurements were plagued with technical problems (related to the sensitivity of the samples to exposure in air), we now have largely resolved these problems. In the next nine months, we will follow-up on some of the interesting physics hinted at by the preliminary measurements.

Growth and Characterization of CdZnTe Crystals for Improved Nuclear Radiation Detectors

LDRD Project 06-038
Genda Gu and Aleksey Bolotnikov

PURPOSE:
For the detection of gamma rays, CdZnTe (CZT) is recognized as the best choice of material for room-temperature detector operation. It is quite challenging to grow crystals of CZT because of the high vapor pressures of the constituent elements. So far, no one has managed to grow adequate large and high quality single crystals for a commercial detector application. This project is to develop and demonstrate the ability to fabricate a detector with sufficient energy resolution and efficiency to satisfy the requirements of the best Nuclear Radiation Detectors in the world.

APPROACH:
Because the old single crystal growth method is not able to produce the large and high quality single crystal, we will try new crystal growth methods. The structural defects presented in new crystals have to be studied to further improve their quality.

We plan to grow single crystals by using the furnaces equipped with the infrared microscopy system. The new infrastructure and a number of optimized processes for crystal growth have been established in Condensed Matter Physics & Materials Science crystal growth laboratory. Safety requirements will be identified and implemented for this project.

The Nonproliferation & National Security Department team will carry the material cauterization experiments, including the measurements of the electrical resistivity, carrier lifetimes, structural quality, and sizes and concentrations of tellurium inclusion in as-grown crystals. In addition, the EENS team will fabricate and test the crystals as planar detectors.

TECHNICAL PROGRESS AND RESULTS:
For FY 2006, the CPM&MS team acquired the equipment and raw materials needed for crystal growth experiments. The safety experiment review approval was granted in November 2006. We started to grow the first CZT crystals on 12/20/2006.

During FY 2007, the CPM&MS team studied the crystal growth mechanisms, such as the effect of growth conditions on solid-liquid interface, crystal micro-structure, formation of Te inclusions, and *etc*. We have grown ten of 1.4 cm diameter ingots and ten of 2cm diameter ingots of $Cd_{0.9}Zn_{0.1}Te$. Fig. 1 shows one grown as a rod of 30 cm length.

For each ingot, three samples were cut out in different locations, polished and prepared for the material characterization measurements. By using IR transmission microscopy the NNSD team measured the size and concentration of Te inclusions. These investigations indicated that the very first CZT crystals have excessive concentrations of Te inclusion.

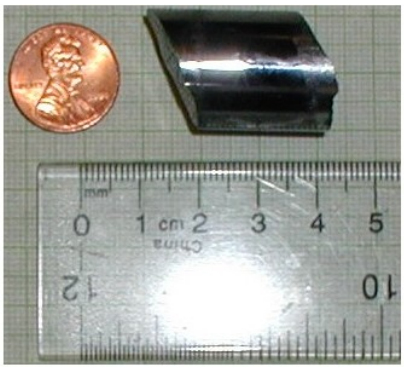

Fig. 1. one cleaved as-grown single rod with 2 cm diameter and 2 cm length.

After several iterations to adjust the crystal growth parameters the size and concentrations of Te inclusions were reduced to an acceptable level that allowed for the next step of the material investigations (Fig. 2). The gold contacts were deposited on the CZT samples to evaluate the bulk resistivity. The highest resistivity measured for the samples with low concentrations of Te inclusions was ~10^{7} ohm-cm which is still too low for detectors grade CZT material. Further improvements in the growth process are needed to improve this value by 2-3 orders-of-magnitude.

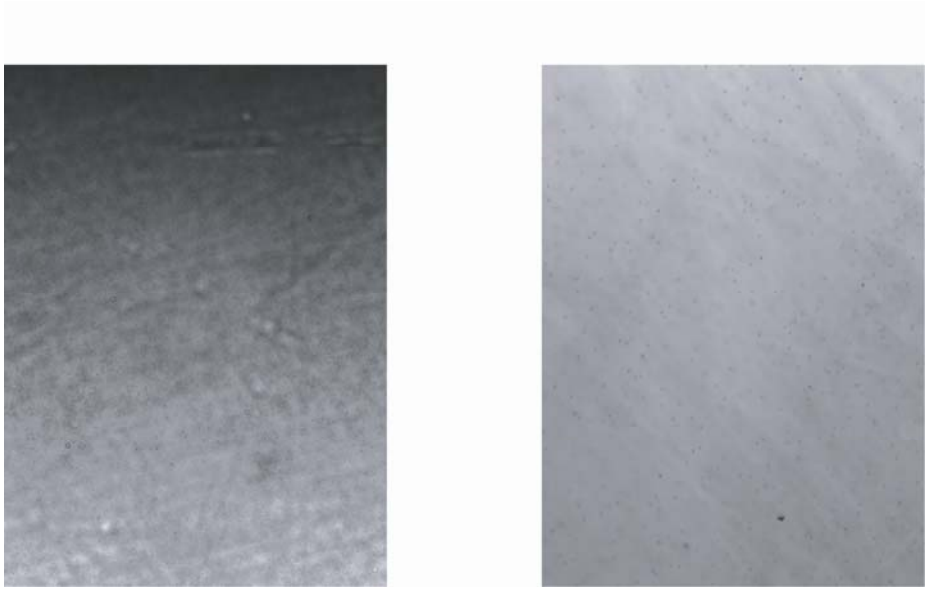

Fig. 2. Drastic reduction in concentration of Te inclusions measured for the samples from latest (right) ingots in comparison to the sample (left) form the fist ingot.

For FY 2008, we will try to study the effect of doping, with substances such as In and Al, on the resistivity and physical properties of single crystals. We want to grow the high resistivity (~10^{10} ohm-cm) and high electron mobility-lifetime products (~$10^{-3}$$cm^2$/V) and hole mobility-lifetime products (~10^{-5} cm^2/V) of large single crystals of CZT materials. The goal is to grow the best single crystal of $Cd_{0.9}Zn_{0.1}Te$ so that we can make the best detector in the world.

Design, Synthesis and Characterization of a New Class of Hydrocarbon Polymers Containing Zwitter Ions and Nano-structured Composites for High Temperature Membrane In PEM Fuel Cells

LDRD Project 06-039
Xiao-Qing Yang

PURPOSE:
Membranes are a critical component of the fuel cell stack; Novel membranes with higher ionic conductivity, better mechanical strength, lower cost, and longer life are critical to the success of fuel cell technologies and other technologies that depend on ionic transport. Polymeric membranes that conduct protons and remain hydrated up to high temperatures are needed. Unfortunately, no breakthrough has been accomplished in designing and synthesizing these new polymeric membranes with satisfactory proton conductivity and mechanical strength at high temperature in recent years. Therefore, the innovative approach of synthesizing new Zwitterion containing polymer membranes with aromatic backbones is of high risk and could be highly rewarding.

APPROACH:
The Key is to balance the water uptake and mechanical properties of the membrane
Our approach is therefore a molecular design of Zwittion containing polymers to enhance the water uptaking and water holding function. The molecular design involves a balanced aromatic backbone and sulfonic acid containing side chains

TECHNICAL PROGRESS AND RESULTS:
The enormous challenge we encountered in 2006 was the difficulty in finding a proper procedure to synthesize the polymer with a sulfonic group containing Zwitterions. The polymerization was prohibited by the Zwitterion groups which had been attached to the monomers we synthesized. If we first polymerize the monomer without the Zwitterion, then the Zwitterion grafting after polymerization failed. Our great progress in 2006 was the development of a new synthesis procedure combining a functionalized aromatic co-polymer backbone with a post-polymerization Zwitterion attachment using sulton. Using this new procedure, several new polymer membranes were synthesized.

In FY2007: a new family of sulfonic acid and side-chain Zwitterion containing co-polymers for both the fundamental studies and practical applications for fuel cells have been designed and synthesized.

Using molecular designs, new monomers and polymers have been synthesized to solve the solubility problem of bibenzimidazole type of polymers the sulfonated polybenzimidazole (PBl) can be considered as a good example of using Zwitterion for the proton conducting membranes. This material has received much attention, both as a proton exchange membrane candidate and also as a host for phosphoric acid. Unfortunately, the sulfonated PBI's are insoluble and brittle, making them unusable for polymer electrolyte membrane (PEM) fuel cells.

In FY2007, a new dibenzimidazole monomer with two extra benzen rings and OH end groups were designed and synthesized and polymerizations using this monomer were also successfully carried out. The polymer membrane has good solubility in organic solvents and water-uptake

properties. New monomers and copolymers (two-unit and three unit polymers as shown in Schemes I and II respectively) were designed and synthesized to gain the tunability of water binding sites of the copolymer in order to balance the conductivity and the mechanical properties. Six new polymer membrane samples were distributed to Los Alamos National Lab. for testing in polymer electrolyte membrane fuel cells. Five other samples were distributed to University of Massachusetts at Boston for water uptake, ionic conductivity, gas permeability, mechanical properties and other physical property test.

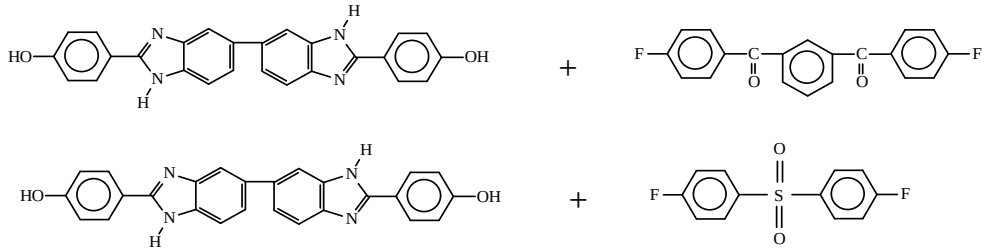

Scheme I Synthesis of polymer membranes with two functional units

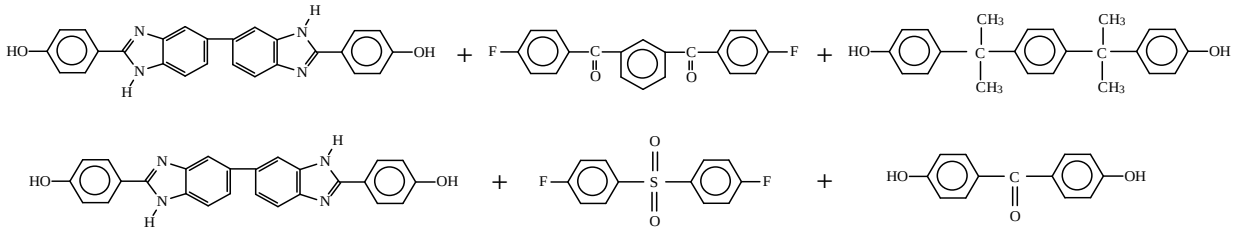

Scheme II Synthesis of polymer membranes with three functional units

Novel Materials for Hard X-Ray Optics

LDRD Project 06-46
K.Evans-Lutterodt

PURPOSE:
In order to take full advantage of existing and future medium energy synchrotron high brightness x-ray sources, we will need high quality hard x-ray optics with sub-10nm resolution and with high efficiency, to enable the full range of hard x-ray microscopy and spectroscopy techniques that will benefit nano-science. Thus we plan to fabricate high quality kinoform lenses out of silicon and diamond.

APPROACH:
The limiting resolution for an optic is proportional to the $\lambda/(N.A.)$, where N.A. is the numerical aperture of the optic, which is the angular range subtended by the optic as viewed from the focal point. For refractive optics, the numerical aperture of a single lens is limited by the small value of the real part of the refractive index δ, leading to resolutions of order $\lambda/\sqrt{(2\delta)}$.

We plan to get around this limit by fabricating compound lenses, i.e. an array of single lenses. In order not to lose too much intensity as we add lenses to the compound lens, we need to investigate suitable choices of lens materials. One excellent choice might be diamond, in addition to the material currently used which is silicon.
A further obstacle for high resolution hard x-ray optics, is that conventional diffractive optics need to be fabricated with feature sizes that are of the order of the desired optic resolution. We plan to take advantage of one of the features of the kinoform type of optic, which allows one to fabricate optics with feature sizes that can be many multiples of the desired optic resolution, i.e. using a kinoform in higher order. For all choices of materials the major obstacle is the quality of the reactive ion etching, because any deviations from vertical sidewall position result in phase errors in the optics and imperfect lens behavior. Thus we plan to try to obtain deep reactive ion etching of silicon and diamond wafers, with sidewalls as smooth and as vertical as possible.

TECHNICAL PROGRESS AND RESULTS:
We have hired a Post-doctoral fellow, Abdel Isakovic to develop improved etching processes for silicon, and to begin investigate diamond etching, and he started Nov 20, 2006.

1. Improved Silicon Etching

A new reactive ion etcher was delivered to BNL CFN in October 2006. Abdel's first job was to

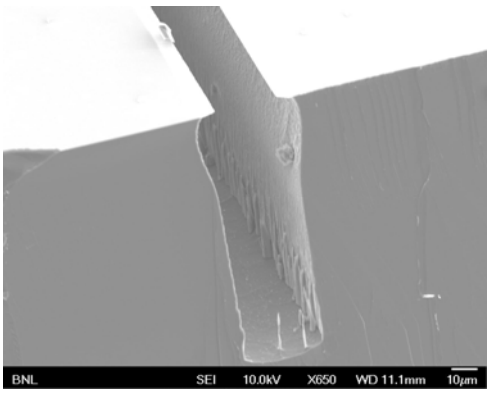

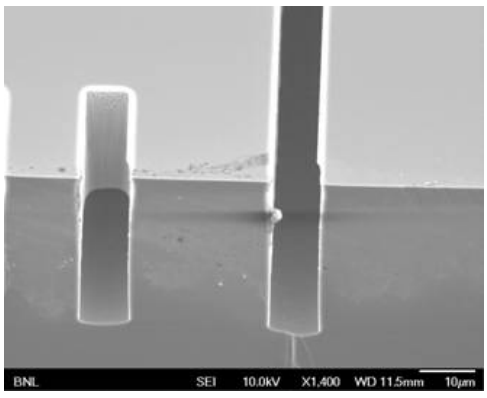

commission the etcher which was done. Then he worked on developing a silicon cryo-etch. On the left is the best etch for silicon that the manufacturer provided for their machine. On the right is an etch developed by Abdel that is substantially better. The sidewalls are vertical, and they are clearly smoother.

2. Diamond Etching
   An etch for diamond has also been developed. Using the cryo-etcher mentioned above, a recipe was developed which was a cyclical oxygen, argon gas process. This has an added benefit of being environmentally friendly. This etch impacted not only our work but also assisted a different group that is developing high brightness diamond based electron beam sources.
3. Diamond Lens Fabrication
   Using the newly developed diamond etch, a diamond lens has been fabricated, as is shown in the Figure below. Here we take advantage of the reduced absorption of the diamond material by fabricating in higher order. This means that the segments are larger than we would usually use for a silicon lens, motivated by the difficulty of diamond fabrication. This lens was tested at the Advanced Photon Source at Beamline 8-ID, and it demonstrated focusing behavior. Unfortunately this first lens was etched 4microns deep, which is not deep enough to minimize diffraction effects, and so it is difficult to be quantitative about the measurement. Nevertheless armed with this encouraging result further diamond lens fabrication is in progress.

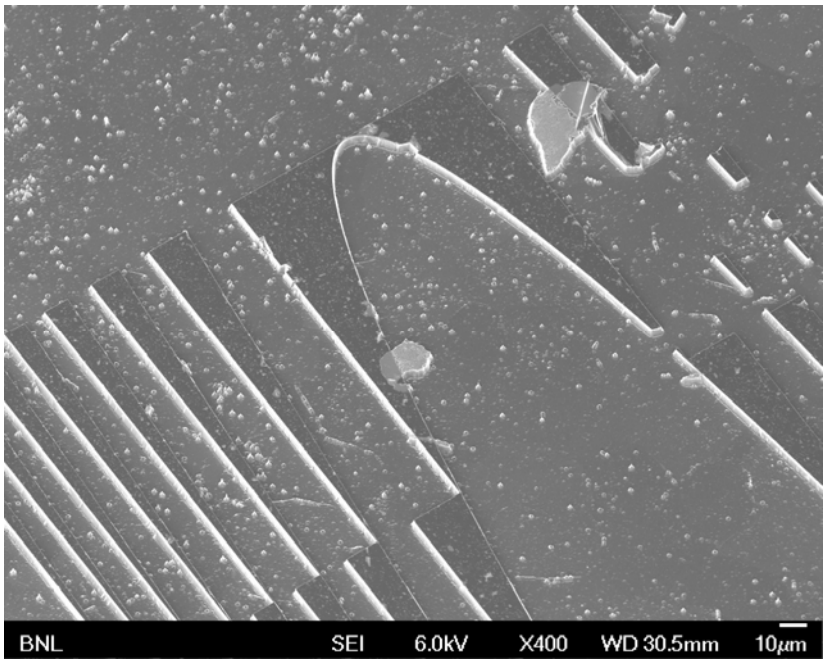

Summary New etching capabilities have been introduced to the BNL campus, and more specifically, competitive etching strategies for etching deep vertical sidewalls in silicon and diamond have been developed. A preliminary version of a diamond lens has been fabricated, and indications are that future, deeper etched versions of these lenses will behave as expected theoretically, which will be a good advance for hard x-ray optics at high brightness light sources.

Nano-Crystallography of Individual Nanotubes and Nanoparticles

LDRD Project 06-047
Christie Nelson

PURPOSE:

The goal of this project is to develop techniques for carrying out x-ray nano-crystallography of individual nanotubes and nanoparticles. X-ray nano-crystallography promises to provide extremely high resolution— on the sub-Angstrom level— for the precise structural characterization of nanomaterials. Since the functional properties of many nanomaterials are determined by their structural properties, this characterization is extremely important. The work on this project is also motivated by the new capabilities that the proposed National Synchrotron Light Source II (NSLS-II) will provide, with focusing down to the nanometer scale. In order to fully take advantage of some of the anticipated NSLS-II capabilities, exploratory work on the feasibility and potential of x-ray nano-crystallography is required.

APPROACH:

In the absence of an existing synchrotron radiation source with the anticipated NSLS-II brightness, the focus of the project to date has been on studies of the radiation damage to nanotubes and nanoparticles. Specifically, the goal is to answer the question of whether or not individual nanotubes and nanoparticles will be able to survive the radiation dose required to result in useful images. To pursue this, the team that includes co-investigators Chi-chang Kao (NSLS), Natasha Bozovic (SJSU), Ivan Bozovic (CMPMS), and James Misewich (CMPMS), and collaborators Haiding Mo (NSLS), Matt Sfeir (CMPMS), Tony Bollinger (CMPMS), Aaron Stein (CFN), Song Jin (UW Madison), Wenjun Liu (APS), Paul Zschack (APS), and Ken Evans-Lutterodt (NSLS), have studied the radiation damage of carbon nanotubes and metallic nanowires at both the Advanced Photon Source (APS) and the NSLS. Beam time for these studies has been provided through the General User Programs at each facility on beamline 34-ID at the APS, and on beamline X13B at the NSLS.

TECHNICAL PROGRESS AND RESULTS:

During FY06, radiation damage studies of carbon nanotubes at the APS were carried out. Scanning electron microscope (SEM) images taken before and after the x-ray exposure indicated that these nanomaterials were unable to withstand even a short exposure. These studies also suggested the need for a real-time monitor of sample integrity during future radiation damage studies. Therefore in FY07, real-time studies of nanowire transport during x-ray exposure were planned.

The first material that was investigated using real-time techniques was copper. The copper nanowires were prepared by evaporating copper onto a SiO_2-coated silicon wafer. The wafer was placed in a chip carrier that was wire bonded to gold contact pads (see Figure 1), and the current flowing through the array of nanowires was monitored. These real-time studies were carried out on APS beamline 34-ID, with the monochromatic x-ray beam focused to a ~0.5 x 0.5 μm^2 spot. Intriguingly, as can be seen in Figure 1, a gradual decrease in the resistance was observed over a total exposure of about two days, after which the resistance continued to decrease and then stabilized at a value of 4 ohms. No sign of damage was observed through a comparison of SEM images taken before and after the beam time.

The second material that was investigated using real-time techniques was Ni_2Si, which is of interest for potential use in microelectronics applications because it can carry a large current

density (~10^8 A/cm^2). Single-crystal Ni_2Si nanowires with a diameter of ~20 nm were grown using a chemical vapor transport method, and titanium/gold contacts that were wire bonded to a chip carrier were fabricated using standard e-beam lithography (see Figure 2). The current flowing through the Ni_2Si nanowire was monitored during real-time studies carried out on NSLS beamline X13B. On this beamline, the monochromatic x-ray beam was focused to a ~1 x 2 μm^2 spot, and the current was monitored for nearly seven days. Once again, the resistance was observed to decrease during the x-ray exposure; however, unlike with the copper nanowires, the resistance recovered its initial value approximately two days after the end of the beam time.

Taken together, the real-time studies of copper and Ni_2Si nanowires indicate that these metallic nanomaterials can withstand significant x-ray exposure, and therefore may be suitable for x-ray nano-crystallography experiments. Following up on this, future studies are planned for FY08, and we hope to make use of a newly-commissioned beamline at the APS: nanoprobe beamline 26-ID, which focuses to a ~30 x 30 nm^2 spot. The factor of ~100 increase in flux density over that delivered at APS beamline 34-ID may enable simultaneous real-time studies of radiation damage as well as x-ray nano-crystallography of the single-crystal Ni_2Si nanowires. This work will likely require the fabrication of a small vacuum chamber in order to control the sample environment, which may also be useful for future studies of other individual nanotubes or nanoparticles. An example of another nanomaterial of interest for these future studies is high-T_c nanowires, and an SEM image of nanowire patterning that was recently carried out at BNL is shown in Figure 3.

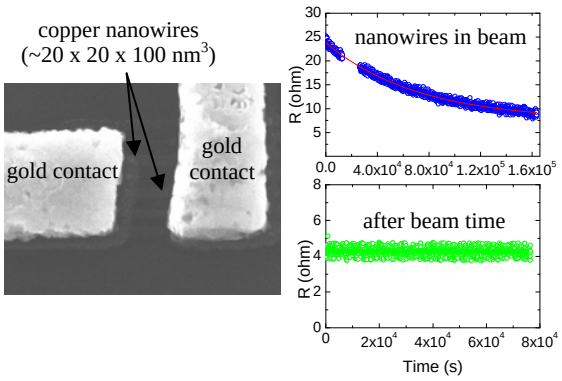

Figure 1: On the left, an SEM image of copper nanowires in parallel between gold contacts. On the right, the resistance of the nanowires is displayed as a function of x-ray beam exposure (top) and after the beam time (bottom).

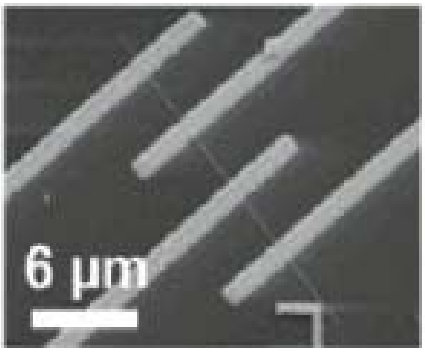

Figure 2: An SEM image of a single-crystal Ni_2Si nanowire, with titanium/gold contacts for four-terminal transport measurements.

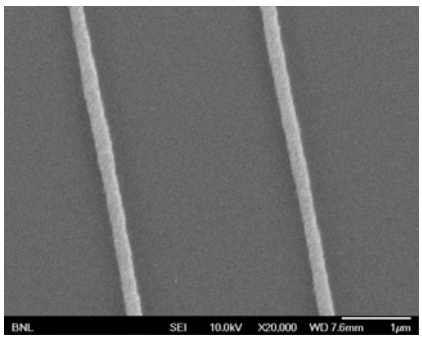

Figure 3: An SEM image of a high-T_c film grown on a nanowire patterned substrate.

High-Temperature Superconducting Magnet Development

LDRD Project 06-052
Toshiya Tanabe

PURPOSE:

High-Temperature Superconducting (HTS) accelerator magnets that could replace conventional synchrotron light source lattice magnets have been proposed. They are expected to reduce operating cost and to facilitate upgrades in machine performance. Present accelerator systems employ one of two magnet technologies: (a) Conventional, employing room-temperature iron yokes with water-cooled copper coils; (b) Low-temperature superconducting (LTS), using NbTi or Nb3Sn superconductors cooled to around 4K by liquid helium. HTS magnet technology now offers a third option for synchrotron light sources and accelerators with moderate magnetic field requirements. In this project we seek to demonstrate technologies that are viable and provide a basis for design of future light source lattice magnets.

APPROACH:

1. We will develop cost-effective designs for form/fit/functional HTS coil/cryostat ("cryopack") replacements for copper coils in conventional sextupole magnets. We plan to use commercial first-generation HTS (BISSCO) conductor initially, but we may try 2nd generation (YBCO) or even MgB2 conductor if these become available in practical lengths. As a case study, we will address replacing the coils in an existing NSLS sextupole magnet with HTS coil/cryostat packages. The sextupole is inherently more complex than a dipole or quadrupole, so design concepts developed here could be applicable to the other types of lattice magnets such as dipole and quadrupole.
2. We will develop integrated HTS magnet, yoke and cryostat designs, without the restriction of retrofitting existing iron yokes if possible, but maintaining a footprint and envelope comparable to the conventional magnet it is to replace. We will strive to attain higher fields than in the original magnet, to provide operating headroom and perhaps allow future performance upgrades. Several optional cooling methods will be explored, including cold gas systems and cryocoolers.
3. We will then construct and test HTS coils and "cryo-coilpacks" individually, and finally on a one-pole, magnetic equivalent to a sextupole magnet.
4. We will connect it to the cold He gas refrigerator and characterize the field quality.
5. We will generate preliminary life-cycle cost estimates for an HTS-based magnet system for a facility such as the NSLS, for example.

The work will be performed jointly by NSLS and Superconducting Magnet Division staffs.

TECHNICAL PROGRESS AND RESULTS:

1. Preliminary 3D magnetic simulations using Radia were conducted to estimate the effect of smaller coil dimensions to the resulting multipole fields.
2. Thermal transfer simulations using ANSYS were carried out to ensure the sufficiently uniform temperature distribution on the coils.
3. BISSCO tape from SUMITOMO Electric were purchased.
4. New winding machine was made by modifying the existing one for another NSLS project.
5. Cryostat design completed.

1. More elaborate 3D magnetic simulations using Opera3D/Tosca were carried out.
2. Two BISCCO sets of coils were wound, quench tested and encapsulated in cryopacks.
3. Crystats were vacuum leak tested.
4. One YBCO coil was quench tested.
5. Multichannel quench detection circuit was developed.
6. Field measurement system was developed.

(a) (b)

Fig. 1: (a) A photograph of one set of coils. 13 coils are stacked. (b) A photograph of quench test using liquid nitrogen. Average quench current was 70A.

(a) (b)

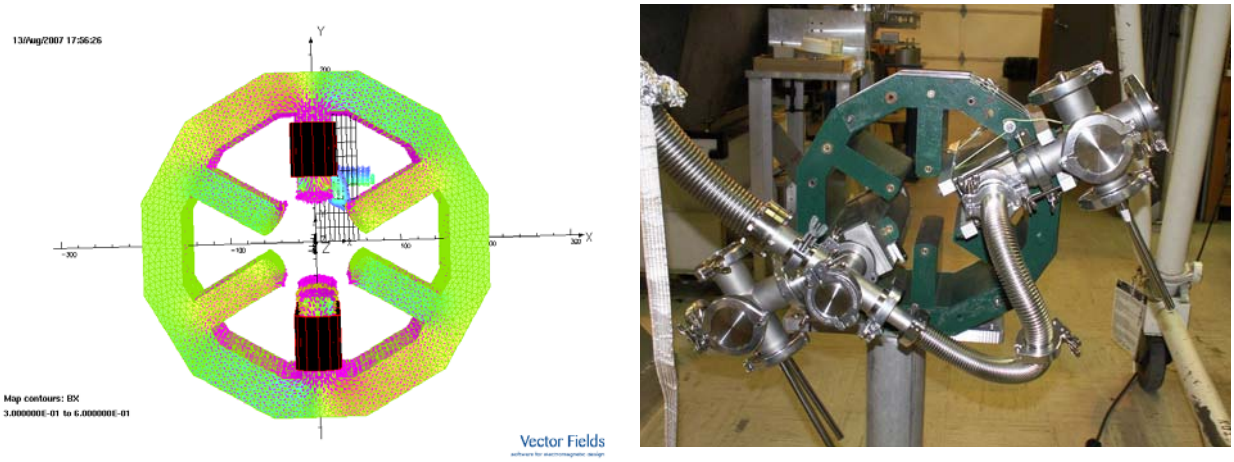

Fig. 2: (a) Opera 3D / Tosca simulation results. Vector plot of magnetic flux. (b) A photograph of completed system.

Epigenetics: Methamphetamine (MAP)-Induced Brain Dysfunction and Methylation of DNA

LDRD Project 06-056
John J. Dunn and Panayotis K. Thanos

PURPOSE:

Vertebrate DNA contains about 3.3 billion bases and is heavily methylated at cytosine residues in CpG dinucleotide sequences to form 5mCpG except for short stretches of CpG-rich DNA, CpG islands, about 0.5 to 2 kb long which are normally free of cytosine methylation. Methylation within CpG islands is a common way to regulate nearby gene activity without altering the DNA code. Recent studies have suggested that aberrant methylation within CpG islands which is referred to as an epigenetic modification may play an important role in mediating stable changes in nervous system function including the behavioral changes seen in psychiatric disorders such as schizophrenia. Our hypothesis is that similar changes are probably associated with methamphetamine (MA) associated drug-induced dependence and psychosis. Our goal is to develop methods to detect methylated CpG dinucleotides near genes with clinical relevance following MA treatment of rodents using DNA samples isolated from the nucleus accumbens and other brain tissues. The technology is relevant to developing systems to understand drug addiction, cancer and aging as well as the cellular responses of human cells to low doses of ionizing radiation for DOE's Low Dose Radiation Program. The methodology also is applicable to understanding how cytosine methylation regulates gene expression in plants and is therefore potentially important for future research as part of BNL's initiative to develop sustainable biofuels.

APPROACH:

The major principle behind our work is that largely intact CpG islands with methylated residues can be isolated by exploiting the differential affinity of these DNA fragments for recombinant proteins containing methyl-CpG binding domains. The fragments can then be identified by hybridization or by cloning and sequencing. Both approaches are being used in our present studies. One disadvantage of current methods is the large (microgram) amounts of template which are required and the need for samples from control tissue. Both would be severe obstacles for follow up studies with precious human samples or with the much smaller brains from genetically engineered mice. To overcome some of these limitations we are developing (1) new improved methods for methylated-CpG island recovery assay (MIRA) followed by analysis on commercially available Nimblegen microarrays and (2) a novel method for genome-wide amplification and profiling of methylation status that is independent of control tissue. A schematic diagram of the latter approach is given in Figure 1. Its underlying principle is the observation that DNA circles can be efficiently amplified *in vitro* by a process referred to as multiple displacement amplification or MDA. Briefly, genomic DNA is digested with MseI, an enzyme that leaves CpG islands largely intact, and self-ligated to form circles. Subsequently, one-half of the sample is digested with the methylation-sensitive restriction enzymes HpaII and BstUI to cut unmethylated CpG islands, and the remaining half is digested with the methylation-specific enzyme McrBC to cut methylated CpG islands. The probability of a McrBC recognition sequence (Purine-mC[$N_{40–3000}$]Purine-mC) being present within a methylated CpG island is close to 100%; similarly and the probability for either a methylated HpaII or BstUI site being present in a methylated CpG island is also high (~90%). The digests are then treated with a mixture of enzymes that will destroy any linear DNAs in either sample regardless of their

methylations status. The restricted samples are then subjected to MDA, differentially labeled with Cy3 and Cy5 fluorescent dyes and hybridized to the 385,000 probe set RN34 Nimblegen rat CpG island/promoter microarrays. The resulting data will be used to correlate occurrence of mCpGs with specific gene expression differences using quantitative polymerase chain reaction on cDNAs from different brain cell types and layers with the methylation status of cognate promoters or cis-acting regulatory elements. As part of this project, we have also cloned, expressed and purified the *Escherichia coli* McrA protein which is known to restrict DNA containing mCpG dinucleotides. Current efforts are aimed at determining whether McrA is a nuclease or if it exerts its biological effect by binding to mC containing DNA.

Figure 1. Flow diagram for the Reference-independent procedure for differential amplification and labeling of methylated and unmethylated CpG islands.

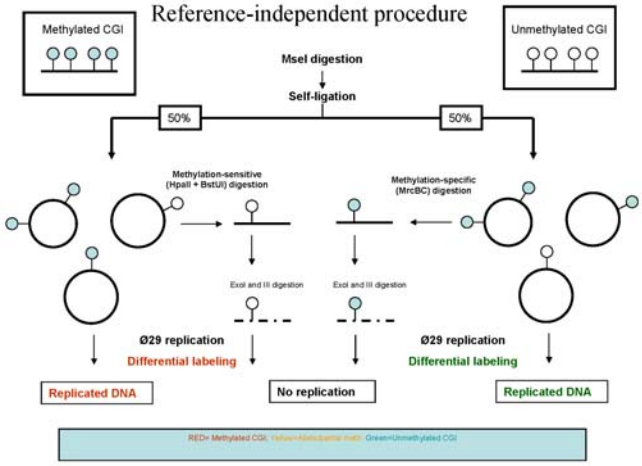

TECHNICAL PROGRESS AND RESULTS:

One approach has been to reengineer the MBD2b expression clone used for production of a main component of the MIRA assay. In brief, this involved replacing one affinity tag (GST) used in protein purification with another (His_6-Strep) designed in our lab thereby making purification of large amounts of the recombinant protein more straightforward. The purified protein has been used to obtain samples from brain tissues of control and chronically MA administered rats for hybridization to the Nimblegen arrays. Data analysis is currently in progress. These results will be extended and included, if warranted, as preliminary data in a grant proposal to NIH/NIDA.

Molecular Mechanism of Chromosomal Replication Initiation in Eukaryotic System

LDRD Project 06-060
Huilin Li

PURPOSE:

In 1992, Dr. Bruce Stillman discovered the Original Recognition Complex (ORC) in yeast. This achievement was hailed as one of the most important discoveries since the DNA structure. The structure is required to understand the operation mechanism of ORC. However, ORC proves to be very difficult for traditional structure biology such as x-ray crystallography, because of its multi-component nature and its property of binding to a long stretch of DNA (~ 50 base pairs). Our goal is to determine the molecular architecture of ORC by the emerging method of cryo-electron microscopy (cryo-EM) and image processing. Structures of ORC and ORC in complex with initiation factor Cdc6 at medium resolution will provide important insight into the mechanism of DNA replication initiation. This collaborative project with the Stillman group promotes the scientific exchange and strengthens the tie between BNL and Cold Spring Harbor Laboratory. Continued support to this project will facilitate establishing the cryo-EM program in the Biology Department as an important complement to the core strength of NSLS and NSLS-II in structural biology.

APPROACH:

Eukaryotic chromosomal replication is an intricate process that requires the coordinated and tightly regulated action of numerous molecular machines. Failure to ensure once only replication initiation per cell cycle can result in uncontrolled proliferation and genomic instability, two hallmarks of tumorigenesis. The yeast ORC constitutively binds to and marks the replication origin throughout the cell cycle. Licensing of the DNA replication origin starts when the critical cell division cycle protein Cdc6p binds to ORC. Cdc6p binding activates an ATPase switch in ORC. This activation causes an extended pre-replication complex (pre-RC)-like nuclease protection footprint on origin DNA. Our preliminary EM work reveals a ring-like structural feature in the ORC-Cdc6p complex that is similar in size to the replicative hexameric mini-chromosome maintenance helicase. This result supports the emerging concept that the helicase is loaded by replication initiators in a mechanism similar to the loading of the DNA polymerase clamp proliferating cell nuclear antigen by the replication factor C clamp loader complex. The formation of the extended pre-RC-like footprint by ORC and Cdc6p, a crucial event in replication origin licensing, is adenosine triphosphate-binding and -hydrolysis dependent.

Building upon our previous study on this system, our goals are to (1) further define the molecular organization of the ORC, and (2) investigate the conformational changes of ORC-Cdc6 upon ATP binding and hydrolysis events that underlie the DNA melting and helicase loading process.

This work is in collaboration with Dr. Bruce Stillman, the president and CEO of Cold Spring Harbor Laboratory. The Stillman lab performs the molecular biology and biochemical portion of the work, and my lab carries out the cryo-EM and image processing and structural reconstruction.

TECHNICAL PROGRESS AND RESULTS:

During the past year, we focused on and have completed our goal of defining the ORC organization. We utilized a maltose binding protein (MBP) fusion approach and designed a unique EM image classification procedure for this purpose. The MBP fusion approach eliminated the uncertain occupancy and unspecific binding problems associated with the traditional immuno-labeling and the functionalized nanogold-labeling methods. The MBP fusion constructs were found to be active in origin DNA binding and competent for Cdc6 interaction. The unique image classification procedure we developed anticipated and dealt with the flexibility problem of the fusion protein. With this approach, we successfully mapped all six subunits of the ORC complex, thus providing unambiguous determination of the overall organization of the ORC. The detailed ORC architecture suggested potential modes of interaction with DNA origins.

To complement our structural studies, the Stillman lab conducted the molecular biology and biochemical studies to verify the binary protein interactions identified in our EM work. The *in vitro* translation approach has now been completed. We are very satisfied that both methods produced consistent results.

A manuscript combining our EM study with our collaborator's biochemical data has been submitted to the Proceedings of the National Academy of Sciences USA. This work significantly advances our understanding of molecular event occurring at the chromosome origin at the onset of replication.

For the next year, we plan to improve the resolution of the ORC structure by extensive electron microscopy and by using the New York Blue to computationally process the large data set.

Diversification of Isoflavonoid Biosynthesis

LDRD Project 06-061
Chang-Jun Liu

PURPOSE:

Plant phenolics play vital roles in plant structure construction and plant defense responses. Isoflavonoids, as a large family of polyphenolics, are major anti-microbial phytoalexins in plant-pathogen interactions, and signaling molecules mediating plant-microbial symbioses for N_2 fixation or Pi absorption. Moreover, isoflavonoids constitute the most potent group of phytoestrogens with potential dietary utility in chemoprevention of several lines of human diseases. Diverse biological activities of isoflavonoids lie on their characteristic chemical structures. The biosynthesis leading to a variety of isoflavonoid structures remains to be elucidated and the catalytic mechanisms of the key enzymes that govern the formation of the characteristic isoflavonoids are elusive. In addition, the structural diversification of isoflavonoid chemicals are required for exploring their biological values. The goal of this project is to characterize the key biosynthetic enzymes responsible for isoflavonoid formation and modification; and to explore the structure and function of the key enzymes, thus further to apply the means of structure-based protein evolution to diversify isoflavonoid biosynthesis.

APPROACH:

We are applying biochemical genomics, X-ray crystallographic structural biology and protein mutagenesis/engineering approaches to functionally characterize isoflavonoid biosynthetic enzymes responsible for *O*-methyl- and *O*-acylation; to explore the structure-function relationship of those key enzymes; and to systemically engineer novel enzyme variants.

TECHNICAL PROGRESS AND RESULTS:

During FY 2006 we determined several sets of crystal structures of a *Medicago truncatula* *O*-methyltransferase in complex with different substrates and created sets of enzyme variants in order to probe their regio-specific methylation. We also identified 77 putative acyltransferase genes by analyzing model legume *Medicago truncatula* Expression Sequence Tag database. Subsequently, we functionally determined 5 acyl (acetyl and malonyl)transferases responsible for (iso)flavonoid modification.

During FY 2007, we continued analyzing the unique structural features of the crystallized isoflavone *O*-methyltransferase. Of particular interest, we revealed two substrate/product binding sites on the enzyme surface, in addition to the active site catalytic pocket of protein. Depending on the binding of isoflavones on the surface or catalytic pocket functional sites, isoflavone *O*-methyltransferase displayed distinct crystalline packing. The amino acid residues observed in the surface binding sites are largely conserved in the sequences of a number of (iso)flavonoid *O*-methyltransferases. Structure-guided mutagenesis demonstrated that retaining such surface binding sites is critical for isoflavone substrate turnover. The observation of isoflavone-enzyme surface interactions suggests a biochemical and structural mechanism adopted by natural product biosynthetic enzymes for trapping low concentrations of substrate *in vivo*.

Meanwhile, we detected the identified 5 acyltransferase genes' expression in different tissues and under different treatments. We demonstrated that those identified acetyl and malonyltransferase genes displayed distinct tissue-specific expression patterns and differentially responded to biotic and abiotic stresses. Consistent with the gene expression of malonyltransferase, the level of the accumulated malonyl isoflavone glucoside natural product in *M. truncatula* roots under the normal growth condition or drought stress was drastically changed. Subsequently, we over-expressed one malonyltransferase gene in a previously engineered *Arabidopsis* line that accumulates genistein glycosides, and the transgenic lines produced malonylated product. These results unambiguously demonstrated that the identified acyltransferase is biologically responsible for the malonylation of isoflavone metabolites in planta; and the transgenic results also show the potential applications in metabolic engineering of more stable and chemically diverse isoflavones in non-legume plants. Furthermore, confocal microscopy of the transiently expressed isoflavone malonytransferase-Green Fluorescence Protein (GFP) fusion showed the strong fluorescence distribution in both the cytoplasm and nucleus of *M. truncatula* and tobacco leaf cells. Deletion of a short C-terminal polypeptide or deletion of one motif that conserved in acyltransferase superfamily members caused improper folding of the transiently expressed GFP fusion protein in living cells and impaired the observed nuclear localization of the enzyme.

We also determined a few structural complexes on a novel phenolic methyltransferase responsible for sulfhydryl methylation, built the initial structural model on a acyltransferase and re-evaluated the substrate specificity of a group of O-methyltransferases for polyphenolic (isoflavonoids) and phenolic (monolignols) and initiated the directed-protein evolution in order to create novel biosynthetic enzymes.

In the following fiscal year, we will continue the structure-function studies on several sets of acyltransferases and methyltransferases, and will adopt additional mutagenesis, biochemical and biophysical techniques to further probe the enzyme catalytic properties and mechanisms and create novel enzyme catalysts. We will further systemically characterize the remaining two (iso)flavonoid acetyltransferase function as we did for isoflavone malonyltransferases during FY 2007.

Metabolic Flux Analysis in *Arabidopsis thaliana*

LDRD Project 06-065
Jörg Schwender

PURPOSE:

Limited arable farm land and increasing demand of plant biomass for fuel production make the detailed understanding of the formation of different storage compounds in plants a topic of high importance. The objective of this LDRD project is to study the formation of seed storage compounds. Flux analysis applied to *Arabidopsis thaliana*, a well characterized plant model organism, will help to understand how plants allocate carbon resources into different storage compounds and how this process is controlled and regulated. A large number of mutant lines and other genomic resources are available in *A. thaliana* that can be used to study the impact of genetic modifications in central metabolism by means of detailed flux maps. In addition, ^{13}C-tracer methods will be adapted to enable medium throughput "fluxome" profiling, allowing fingerprinting of metabolic phenotypes prior to detailed, more time consuming flux analysis studies.

APPROACH:

Systems biology approaches employing genomics, metabolomics, and similar techniques provide plentiful information that identifies and describes parts of cellular infrastructure like genes, enzymes and metabolites. So far the *in vivo* function of the cellular metabolic infrastructure cannot be predicted from this kind of information but has instead to be measured. Metabolic Flux Analysis (MFA) allows measuring cellular biochemical conversions *in vivo*, i.e. to quantify the interaction of enzymes and metabolites within the living cell.

Metabolic flux analysis can help to understand the complex effects of changes in genotype on the metabolic phenotype. By applying methods of *in vivo* ^{13}C-steady state metabolic flux analysis, two principal types of insights can be expected: First, for transgenics which have a severe phenotype of altered seed composition, flux maps may identify critical metabolic branch-points where carbon flux is redirected to other end products. Second, for transgenics altered in functions of central metabolism but without metabolic phenotype, the flux maps may reveal how redundant metabolic functions (like bypass routes) compensate for the loss of a metabolic connection.

Culture conditions developed by the Principal Investigator for *Brassica napus* embryos have to be carefully adapted to *Arabidopsis* embryo cultures. Critical for analytical procedures is the small size of *Arabidopsis* embryos (50 µg). Developing seeds of *A. thaliana* at an early stage of development are dissected out of the siliques under aseptic conditions and put into a liquid culture medium containing ^{13}C-labeled sugars and amino acids as principal carbon and nitrogen sources. After culture, the ^{13}C-enrichment in different carbon positions of the labeled metabolites is analyzed by gas chromatography / mass spectrometry methods. Comparison of the labeling signatures (mass isotopomer fractions) between wild type and mutant reveals whether metabolites have a different metabolic history, i.e. if the formation of the carbon structure differs between wild type and mutant. For mutants that differ in their flux profile, detailed analysis of flux distribution can be performed. For this purpose, physiological parameters (content of oil, protein, starch) have to be measured.

TECHNICAL PROGRESS AND RESULTS:

In FY 2006, microscopic dissection and culture of growing embryos from *A. thaliana* was established and existing analytical procedures were adapted to analyze very small amounts of embryo tissue. Labeling profiles for different *Arabidopsis* wild types (ecotypes) were compared to each other which established that transgenics generated in different ecotype backgrounds can be compared to each other to reveal differences specific to the transgenic event. Different mutants were compared based on a flux fingerprinting approach. This allows us to find out quickly if any change in metabolic flux can be detected. In general, the mutants did not reveal differences in metabolic phenotype as expected.

In FY 2007, it appeared as a limitation of the project that the transgenics obtained from outside sources, such as strain collections, require detailed and time consuming verification of genotype. In order to be more independent from receiving transgenics, *in vitro* gene silencing was tested by using antisense oligo-deoxynucleotides in embryo cultures of *B. napus* and *A. thaliana* wild type. However, with different gene targets we could not successfully demonstrate an *in vitro* inhibition of gene expression. A further constraint to the approach turned out to be the production of sufficient amounts of cultured embryo tissue, since for detailed flux studies physiological parameters (content of oil, protein, starch) have to be measured. The analysis of tissue composition on a microscopic scale by use of Fourier transform infrared microscopy is currently still under progress.

For several wild types and about 15 transgenics, statistical analysis of the metabolite labeling signatures was performed. Significant genotypic effects were found for the *wrinkled* mutant, a mutant with regulatory defect in oil synthesis. The multivariate statistics methods that were applied capture experimental variability as distinct components apart from components that refer to true metabolic differences.

Transformation and Fate of Nanoparticles in the Environment

LDRD Project 06-066
Jeffrey Fitts and Oleg Gang

PURPOSE:
The objective of this work is to determine how the molecular-level chemical characteristics of the organic shell and inorganic core components of water-soluble nanoparticles govern their transformation and fate in the natural environment. Our results will demonstrate that ongoing studies of this type are required in order to produce accurate toxicity and environmental risk assessments of nanoparticles. The potential and scale of follow-on funding will benefit from our efforts to integrate this work with BNL investigators with expertise in synthesis, molecular scale characterization, toxicological studies, and risk assessment modeling.

APPROACH:
This work focuses on the behavior of water-soluble nanoparticles because they pose the greatest risk to the environment and humans. This type of particle is typically composed of an inorganic often crystalline core and an organic outer shell which is necessary to prevent particle aggregation and modify nanoparticle surface charge. Based on our knowledge of contaminant behavior, once these nanoparticles are released into the environment they will interact with microbiota, which are ubiquitous in soils and water resources, and this will result in 1) modification of the molecular chemical nature of the particle, specifically the crystalline core and/or 2) profound changes in the surface chemistry of a particle's organic shell.

This work seeks to develop an understanding of the interactions between naturally-occurring soil and groundwater microorganisms with functionalized nanoparticles, specifically organic-coated gold (Au) nanoparticles. This work is done in collaboration with Post Doc Garry Crosson (BNL EE). In order to study processes specific to the inorganic core, we use nickel hydroxide nanoparticles, given that the breakdown products are known toxins and both the nanocrystalline core and reaction products are ideally suited to synchrotron-based studies at the NSLS. In contrast, Oleg Gang and Matthew Maye (CFN) synthesize Au nanoparticles with a variety of organic functionalizations. By contrasting different functionalities we investigate mechanisms of nanoparticle reactivity and transport that depend on the organic coating and particle charge.

We study nanoparticle chemistry in pure cultures and cultures containing important soil minerals. In addition, batch sorption studies are used to study the interactions of nanoparticles with aquifer materials and microbiota. The pure cultures of bacteria used include an aerobic (O2-respiring) strain Pseudomonas fluorescens and an anaerobic (fermentative) strain Clostridium sp. and soil minerals include quartz sand, clays and iron oxides. Abiotic and biotic processes are examined to understand the role of microbiota and soil minerals in modifying transport behavior.

The fate of the nanoparticles in the soil matrix of the batch studies is characterized on a macroscopic scale by determining a distribution coefficient (Kd) for each type of nanoparticle and on the molecular scale in terms of their physical chemical state (e.g., dispersed in solution, mineral or cell-surface associated, embedded in an extracellular matrix, or localized intracellularly). A suite of methods are used to determine the molecular scale interactions including transmission electron microscopy (TEM) at the CFN with Dr. Eli Sutter, scanning electron microscopy (SEM) at Stony Brook University (SBU) with Dr. James Quinn, and scanning transmission x-ray microscopy (STXM) at the NSLS with Prof. Chris Jacobson (SBU).

The chemical modification of the nanoparticle crystal core and organic surface is interrogated by spectroscopic methods at the NSLS with Dr. James Ablett.

The molecular scale studies are used to identify the predominant mechanisms of biotransformation in order to understand how such transformations affect nanoparticle fate and transport. Ultimately this information is included in risk assessment models of nanoparticles by collaborating with Dr. Vasilis Fthenakis (BNL NE).

TECHNICAL PROGRESS AND RESULTS:

In FY 2007, the most significant accomplishment came about through collaboration with Prof. Chris Jacobsen's (Stony Brook University Physics) group using their scanning transmission x-ray microscope (STXM) at beamline X1A at the NSLS. Our work combined oxygen and carbon K-edge spectroscopy imaging with simultaneous darkfield imaging of nickel hydroxide nanoparticles in bacterial biomass. The x-ray microscope operates at a 30 nanometer spatial resolution. Using a new segmented detector we were able to simultaneously measure scattering from nanoparticles in the detector's exterior ring (darkfield) and oxygen x-ray absorption spectra in the detector's inner ring (brightfield). This work establishes this method as a unique and powerful approach to studying the chemistry of nanoparticles in soft-matter – including soil bacteria, human cells and polymer-nanoparticle composite materials. The new method should have significant appeal within the soft-matter research area at BNL's Center for Functional Nanomaterials and the prospect of improved spatial resolution at NSLS II down to 1nm will enable the interrogation of single nanoparticles within soft-matter systems.

A second important aspect of this work involved studies of citrate-capped Au nanoparticles. We studied these nanoparticles over a range of particle diameters in pure bacterial cultures and mineral batches. SEM and TEM studies suggest that the Au nanoparticles interact with aerobic bacteria (Pseudomonas fluorescens) but do not penetrate the cell wall. Most significantly this type of nanoparticle preferentially interacts with and aggregates in the extracellular organic matrix of an anaerobic bacterium versus the bacterial cell wall. This organic matrix is only produced by certain bacterial species. In addition, synchrotron-based x-ray microprobe studies of these same nanoparticles in batches containing bacteria and quartz sand indicate that nanoparticle attenuation only occurs when soil bacteria are present. These results provide a powerful example of the importance of understanding the charge, reactivity and stability of the organic shell of water soluble nanoparticles when predicting their fate and transport.

Development of a Cloud Condensation Nucleus Separator

LDRD Project 06-071

Jian Wang

PURPOSE:

The technical objective of this project is to develop a novel Cloud Condensation Nucleus Separator (CCN separator) that is capable of separating CCN and non-CCN at climatically important supersaturations. Once the CCN and non-CCN are separated, their microphysical, chemical, and optical properties can be further analyzed using a variety of aerosol instruments. Detailed studies can be carried out on what type of aerosols and how those aerosols affect the properties of clouds, which will lead to an improved understanding of the aerosol indirect effect on global climate. The development of the CCN separator supports the laboratory strategic research initiative of Aerosol Research, and is closely related to the Atmospheric Science Program of DOE. Given its unique capability, the CCN separator would likely be deployed in field studies with aerosol instruments from other research institutions, and be able to attract follow on research support from agencies besides DOE.

APPROACH:

Atmospheric aerosols could strongly influence the climate by scattering and absorbing sunlight (direct effect) and by changing the microphysical structure, lifetime, and amount of clouds (indirect effect). Among the effects of aerosol on climate, the indirect effects of aerosol are the most uncertain components in climate systems. Successful prediction of aerosol effects on climate requires a detailed understanding of the aerosol indirect effects, i.e. what type of aerosols and how those aerosols affect cloud properties. Among aerosol particles, only those that can grow into cloud droplets at certain supersaturations, which are also called cloud condensation nucleus (CCN), affect the cloud properties. Whether a particle can serve as a CCN under particular supersaturations depends on its physical size, chemical composition, water solubility, and surface property, etc. Detailed understanding of aerosol indirect effects necessities characterizing the physical and chemical properties of CCN in different air masses and under a variety of meteorological conditions. Such studies are very rare, mainly due to the lack of a method for separating the CCN from the rest of aerosol particles (Non-CCN).

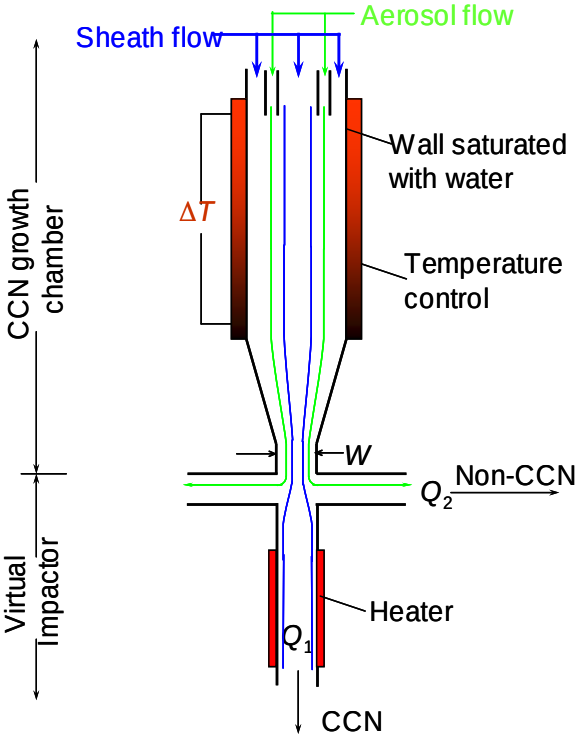

Figure 1. Schematic of the CCN separator.

The proposed CCN separator is capable of separating CCN and non-CCN under climatically important supersaturations. The schematic of the CCN separator is given in Figure 1. The CCN separator consists of two major components. The first component is a CCN growth chamber that grows CCN into supermicron droplets under a prescribed supersaturation. The growth chamber is a cylindrical column, and its inner wall is made of porous ceramic that is maintained wet with water. Precise temperature controls are applied to generate a linear temperature gradient along the axial direction of the column. Due to the differences in water vapor diffusivity and air thermal diffusivity, a constant supersaturation is achieved near the centerline of the column. A wide range of supersaturations can be achieved by varying the flow rate, and the temperature gradient. The aerosol sample is introduced from the top of the column, and is confined in an annulus region sandwiched by particle-free sheath flows. Exposed to the supersaturation environment, CCN will grow into supermicron droplets at the end of the growth chamber. The grown droplets, along with non-CCN that remain unactivated, are then accelerated out of the chamber in a jet flow through a focusing nozzle. The second component, a Virtual Impactor (VI), separates the grown droplets and non-CCN by taking advantage of the substantial differences in their inertia. Non-CCNs, which are small and have little inertia, follows the gas flow streamline and exit from the sides (Q_2 Fig. 1). In contrast, supermicron droplets that are activated from CCN have enough inertia to cross the flow streamlines and be collected by the flow Q_1 (Fig.1). After separation, the CCN and non-CCN can be subsequently characterized using a suite of aerosol instruments.

TECHNICAL PROGRESS AND RESULTS:

We have carried out detailed simulations of the CCN separator and finalized its design. Detailed simulations revealed that the original proposed design, which employs a Counter-Flow Virtual Impactor, is not capable of separating grown CCN from non-CCN at low but climatically important supersaturations. The current design uses a Virtual Impactor, which significantly improves the performance of separation. Simulation showed the current design is capable of separating grown CCN from non-CCN at supersaturations as low as 0.1%. The physical dimensions and operation parameters have been determined. The operating flow rate of the CCN separator will increase accordingly with increasing supersaturation. At lower supersaturations, a lower flow rate will be used to increase the residence time of the particles within the growth chamber, which allows CCNs to grow into sufficient large sizes and be separated. At high supersaturations, droplets grow faster, and operating at higher flow rate increases the sample rate and statistics of further characterizations. The CCN growth chamber is now ready and the temperature and flow controls have been thoroughly tested and perform well. The mechanical designs of the virtual impactor and its interface to the growth chamber have been completed.

In FY 2008, we will complete the construction of the virtual impactor and its interface to the growth chamber. The performance of the CCN separator will be tested using particles of known CCN activities.

Aluminum Hydride – An Ideal Hydrogen Source for Small Fuel Cells

LDRD Project 06-074
Jason Graetz

PURPOSE:

Aluminum hydride (AlH_3) is an attractive hydrogen storage material for low temperature fuel cell applications. AlH_3 can be prepared in seven different crystallographic phases or polymorphs. Each phase has a unique structure and atomic arrangement and therefore exhibits different thermodynamic and kinetic properties. The purpose of this project is to synthesize and characterize the three primary crystalline polymorphs of AlH_3: α, β and γ. The crystallographic structures, thermodynamic and kinetic properties of each of the phases will be determined. This data will be used to establish the relative stabilities of the different AlH_3 polymorph structures and H_2 evolution rates as a function of temperature. Finally, the development of a more convenient synthesis route and the possibility of using AlH_3 as a hydrogen source for small fuel cells will also be explored.

APPROACH:

AlH_3 is a covalent binary hydride prepared as non-solvated AlH_3 through a reaction between lithium alanate ($LiAlH_4$) and aluminum chloride ($AlCl_3$) in an ether solution. Although the existence of at least 6 non-solvated polymorphs other than α-AlH_3 has been known for some time (~30 years), little is known about these other phases. Structural, kinetic and thermodynamic studies of α-AlH_3 were performed in the sixties and seventies, but the structures and properties of the remaining polymorphs are still unknown. The focus is thus to perform a fundamental materials characterization of the non-solvated, crystalline, AlH_3 polymorphs.

The approach is to prepare different polymorphs of AlH_3 (α, β and γ) using an organometallic synthesis route. Low temperature H_2 evolution rates will be measured by isothermal decomposition in a Sievert's type apparatus for all three polymorphs. Structural characterizations of γ and β AlH_3 and AlD_3 will be performed using synchrotron x-ray powder diffraction at the NSLS and neutron powder diffraction at IFE (Norway), respectively. Thermodynamic values will be measured using differential scanning calorimetry. The possibility of hydrogenating Al metal (to form AlH_3) under high pressure will also be investigated.

TECHNICAL PROGRESS AND RESULTS:

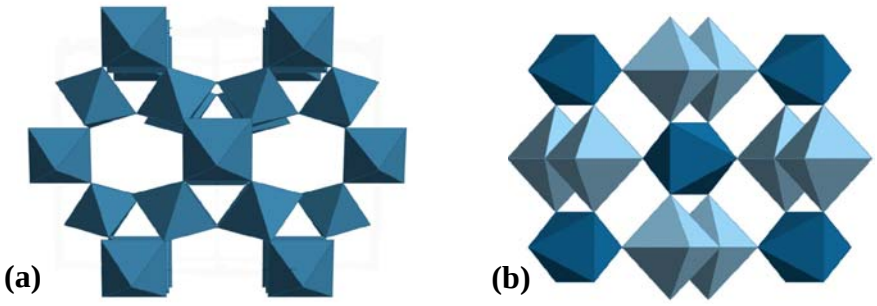

Figure 1. Crystal structure of (a) β-AlH_3 [101] and (b) γ-AlH_3 [010] determined from synchrotron x-ray and neutron diffraction.

In FY06 we found that the H_2 evolution rates for freshly prepared of α, β and γ-AlH_3 met the DOE full flow target for a 50 kW fuel cell (1 gH_2/s) at 114°C (based on 100 kg AlH_3). This year we have measured the low temperature isothermal decomposition curves for the α and γ phases. Significant low temperature decomposition was observed in γ-AlH_3, which released H_2 at a steady rate of 6.0 gH_2/h at 27°C. This is equivalent to complete decomposition in less than 2.5 months at room temperature (not including a short induction period). At the same temperature α-AlH_3 undergoes a one-month induction period (Figure 2a) where no H_2 is evolved and then decomposes at a rate of 1.0 gH_2/h. This is equivalent to a total capacity loss over a 14-month period. This type of slow, low temperature H_2 release may be useful for many applications (remote sensors, data transmission, etc.) particularly those involving portable or remote power systems with a small hydrogen powered fuel cell. However, other applications, such as a fuel cell vehicle, will demand a material with greater low temperature stability. Therefore, we have explored a number of methods of stabilizing AlH_3 by controlling crystallite size and introducing surface coatings. An example of a stabilized form of AlH_3 (Fig. 2b) prepared by Dow Chem. Co. exhibited decomposition rates more than 1000x slower at 140°C. More recently we have been using transition metals (e.g. Ti) to catalyze the decomposition reaction. Surprisingly, we found that even at the low dopant levels (~10 ppm) Ti significantly increases H_2 rates and reduces the temperature necessary to meet the DOE rate target to 100°C (Figure 2b). In summary, we demonstrated that the stability of AlH_3 can be adjusted to accommodate both high temperature and low temperature applications.

Last year we reported on the structure of β-AlH_3 (and β-AlD_3), which crystallizes in the *Fd-3m* space group (Figure 1a). Similar to α-AlH_3 (R-3c), the structure of the β phase is composed of corner connected AlH_6 octahedra with each H atom forming a bridging bond between octahedra. This year we determined the structure of γ-AlH_3 (and γ-AlD_3) using x-ray and neutron powder diffraction. The structure of the γ phase is tetragonal (Pnnm space group) and consists of both corner and edge-shared octahedral as shown in Figure 1b. The β and the γ phases are both less stable than the α phase. Differential scanning calorimetry revealed a free energy difference of 1.9 kJ.mol H_2 between γ and α and 1.0 kJ/mol H_2 between the β and α phases.

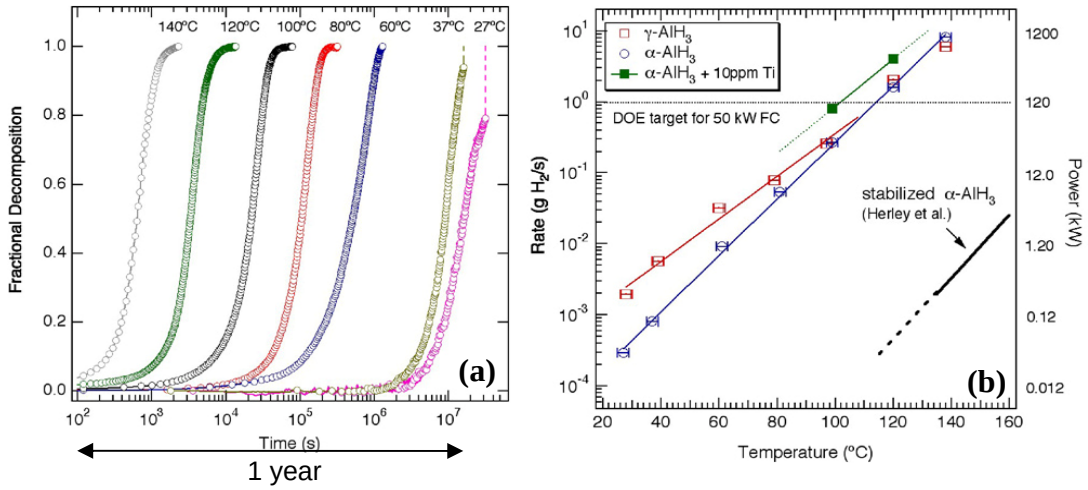

Figure 2. (a) Isothermal fractional decomposition curves from α-AlH_3 at temperatures from 140°C to 27°C and (b) hydrogen evolution rate (or power) as a function of temperature for γ-AlH_3, α-AlH_3, Ti-catalyzed α-AlH_3, and a stabilized form of α-AlH_3.

Gamma Ray Imager for National Security Applications

LDRD Project 06-087
Peter Vanier and Paul Vaska

PURPOSE:
Our goal is to develop a compact and robust, room-temperature gamma-ray imager which can be used to detect, localize, and identify illicit nuclear materials. We are examining the performance of a scintillator-based coded aperture prototype for this application, which is readily expandable to larger areas and hence larger sensitivities. This will potentially culminate in a practical system that fulfills a critical need in the nation's security infrastructure.

APPROACH:
Our approach is to combine BNL's expertise in homeland security (NNSD), medical imaging (Medical Dept.), and electronics (Instrumentation Div.) to deliver a unique and practical device for this application. We have chosen the coded aperture approach because it is the most efficient to image the localized radiation sources expected in this application.

Proven scintillator/photosensor technology provides very high counting efficiency with some ability for isotope identification. Specifically, the bright and efficient scintillator, gadolinium oxyorthosilicate (GSO), was selected and coupled to solid-state avalanche photodiode (APD) photosensors. This combination is fully compatible with a highly integrated, low-power readout microchip in development by the Instrumentation Division. This chip was designed for detectors based on a similar scintillator containing lutetium (LSO), but LSO has a high intrinsic background radioactivity from lutetium. GSO is similar in many respects, such as the required shaping time, but has essentially no activity.

The microchip couples directly to a data acquisition system which has been developed and validated for the RatCAP project, providing a very compact, robust and practical data acquisition backbone. An overview of the system is shown in Fig. 1.

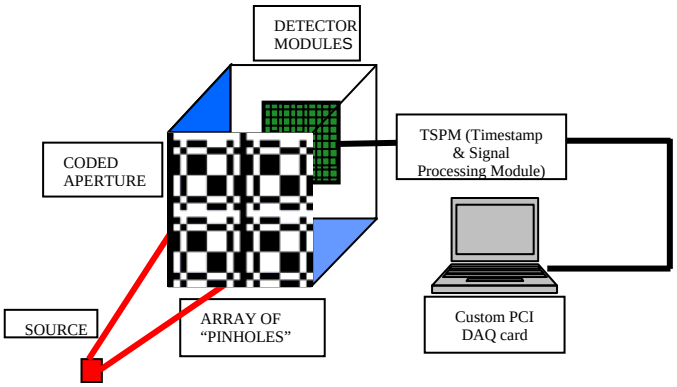

Figure 1. System overview.

Sachin Junnarkar and Paul O'Connor of the Instrumentation Division have provided critical electronics development, and Sean Stoll of the Physics Department and Srilalan Krishnamoorthy, a graduate student from Stony Brook University, have constructed and tested the components and prototype system.

TECHNICAL PROGRESS AND RESULTS:

In FY06, we studied the fundamental detector properties and developed a design for a prototype imager. In FY07, we acquired all the necessary components (225 GSO crystals, matching APDs, and 7 electronic readout ASICs). We were fortunate to obtain the photodetectors (APDs) at substantially reduced cost which allowed construction of a larger and more practical prototype with 15 x 15 detectors covering a 15 cm x 15 cm area. The printed circuit board to mount the detectors and electronics was developed in the Instrumentation Division and the imaging plane, shown in Fig. 2, was assembled, debugged, and tested. The data acquisition required some adaptation of the firmware Preliminary imaging results were obtained using a simple direction finder tungsten mask (shown in Fig. 3, manufactured through NNSD) and a Ge-68 gamma source (monoenergetic 511 keV gamma rays). Sensitivity and energy resolution were sufficient to see lines as high as the 2.6 MeV gamma from Th-232 as shown in Fig. 3 (right).

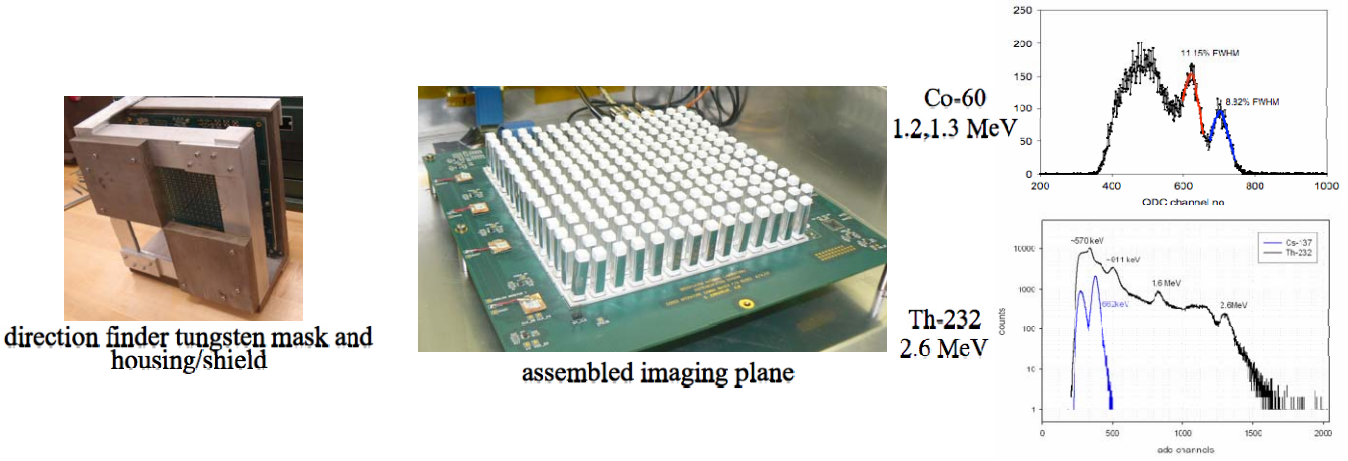

Figure 2. Mask, imager, and energy spectra from GSO-APD detectors.

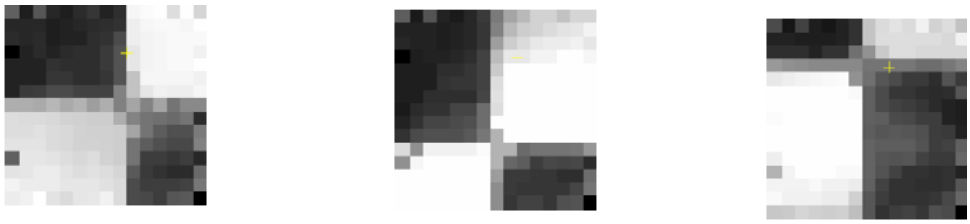

Figure 3. Images using Ge-68 source at ~1 m distance.

Although funding is no longer available under this LDRD, the system electronics is being optimized to obtain imaging results for the next phase of funding through NA-22, DHS, or DOD.

Neurogenomics: Collaboration Between the Biology Department and the Brookhaven Center for Translational Neuroimaging to Investigate Complex Disease States

LDRD Project 06-088
Nelly Alia-Klein

PURPOSE:
This neurogenomics project links genetic data from human subjects with the neuroimaging data obtained from our protocols with the aim:

- To streamline human DNA collection and storage to study the relationship between variations in a certain gene and the explicit expression of the gene product in the brain;
- To advance in understanding how genomic data compiled with brain imaging data could be used as a tool to predict behavior.

APPROACH:
Next to nothing is known about how the distributions of neurotransmitters in the brain vary as a function of polymorphisms that encode the activity of those same neurotransmitters. The reason for this is that there are very few laboratories in the world that have mastered the integration of molecular genetics and neuroimaging, which represents a fledgling field called *neurogenomics*. The thinking behind neurogenomics is that differences in polymorphisms, accounting for transcript abundance, reflect a mechanistic link between genes and behavior. In fact, basic studies show that genetic transcription is not always predictive of protein expression and it has been noted that some differences in gene expression are a consequence, not a cause, of a behavioral change. By having the blood sample of each subject enrolled in neuroimaging studies at BNL, we will be in a position to link the genomic data with the neuroimaging findings and behavioral analysis. Together, this provides a unique opportunity to develop a modern integrative science of neurogenomics in BNL. As a novel approach to study gene-brain-behavior correlations we plan to implement epigenetic analysis.

TECHNICAL PROGRESS AND RESULTS:
Aim 1 - *Streamline DNA collection from every human subject participating in brain imaging study*. We currently have 3 protocols for DNA collection, storage and analysis from human research protocols that are CORIHS approved. A separate protocol specifically designed for the genomic studies has been approved and is currently implemented. In this new protocol, we specify methods for analysis of brain function-relevant genetic polymorphisms in human subjects. Elena Shumay was hired as Research Associate to run the genetic research. She received training in genetics (Mammalian Genetics (Jackson Lab.); bioinformatics (in Bioinformatics, Cold Spring Harbor Lab); and Translational Research (Course in Translational Research, Rutgers University). We had set up and equipped the neurogenetics laboratory. Blood samples were collected from **70 human subjects** (substance abusers and healthy controls); 54 of the subjects were genotyped for polymorphism in monoamine oxidase A (MAO A) polymorphism.

Aim 2 - *To advance in understanding how genomic data compiled with brain imaging data could be used as a tool to predict behavior*. Due to this laboratory's expertise on MAO A imaging with PET technology, we used this data to investigate relationships with aggressive traits. The

absence of MAO A enzyme due to genetic deletion produces aggressive phenotypes in mammals. However, nothing is known about brain MAO A activity (the gene product) and trait aggression. As an abstract to the Society for Nuclear Medicine, we reported the first in vivo human study to document an association between MAO A enzymatic activity in the brain and trait aggression. Using Positron Emission Tomography with [^{11}C]clorgyline and the Multidimensional Personality Questionnaire in healthy men, we found that lower levels of brain MAO A activity correlated with higher trait aggression and not with other personality traits and there were no differences as a function of MAO A genotype. These results show brain MAO A activity and not genotype predicts trait aggression underscoring the relevance of MAO A as a neurobiological marker contributing to antisocial behavior.

In the figure below: Trait aggression and brain MAO A activity. (A) top panel: aggressive subjects who endorsed 9 or more aggression questions, and bottom, subjects who endorsed 2 or less aggression questions (Based on 1 standard deviation above or below the aggression mean). (B) Correlation between MAO A activity in temporal cortex and the MPQ aggression scale. The regression line represents the total correlation (r= -0.63, 0 = 0.0004, Rsq=0.40). The circles denote high (n=17) the squares low (n=10) MAO A genotype.

A. B.

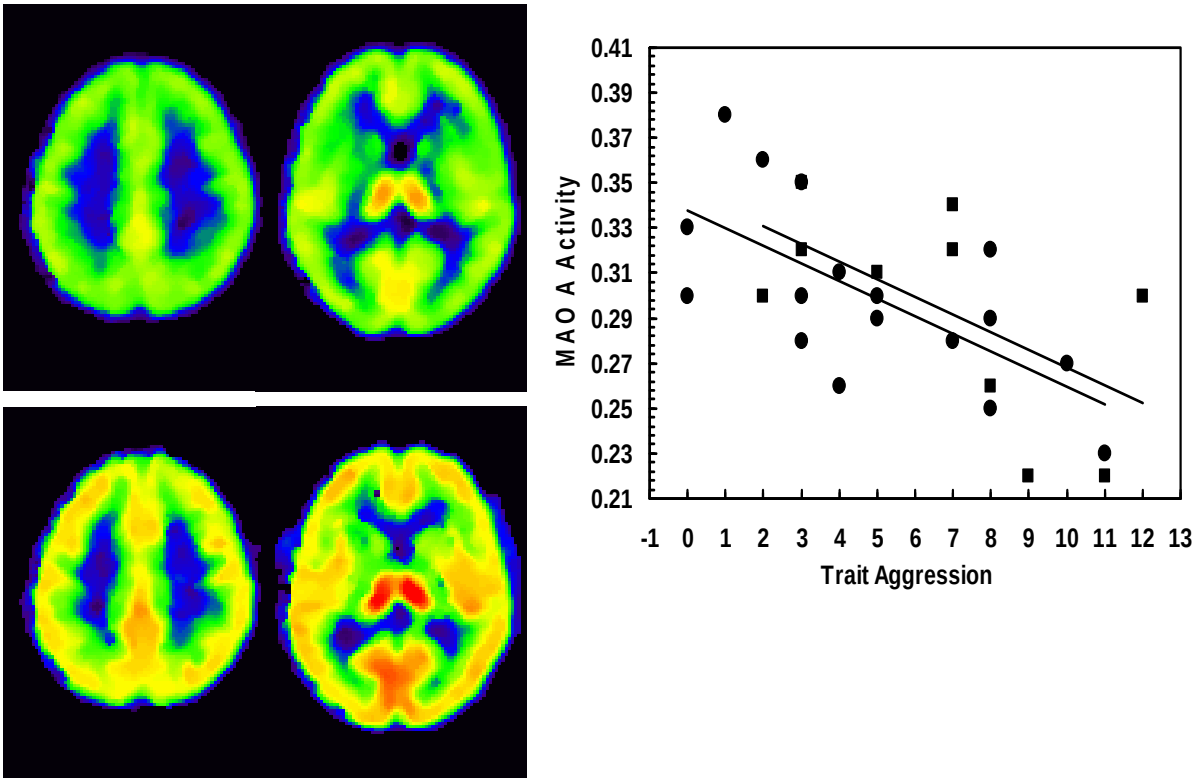

Nanoparticles Labeled Neural Stem Cells Tracking *In Vivo* by Magnetic Resonance Microscopy (MRM)

LDRD Project 06-092
H. Benveniste, M. Maletic-Savati, and Stan Wong

PURPOSE:
The objective is to develop and implement new technology to track the fate of neuronal (progenitor) stem cells (NSC) on a bio-systems level *in vivo* using (a) stem cells and nanoparticles coated with organic moieties (for tracking of exogenous stem cells) in combination with MR imaging and (b) non-invasive MR spectroscopy and metabolomics for tracking of endogenous stem cells.

APPROACH:
Over the past several years, attempts have been made to generate nanoparticles, such as superparamagnetic iron oxide (SPIO), that, when internalized by NSC *in vitro*, can be used for NSC tracking in the live brain using MR microscopy. NSC internalization of SPIO typically requires that the particles are pre-coated with poly-lysine which is a time consuming step. In collaboration with the BNL CFN (Dr. Stan Wong) we have therefore investigated new particle approaches to label NSC using an alternative coating materials. Another approach for tracking of NSC which we have investigated in collaboration with Dr. Maletic-Savatic and her team at SBU is to use proton nuclear magnetic resonance (1H-MRS) and metabolomic profiling of NSC as a means of tracking them in the live brain.

TECHNICAL PROGRESS AND RESULTS:
In FY 2006 ^{1}H-MRS of NSC in the live brain was accomplished successfully and the data has been published recently in Science (Manganas et al., Science, Nov 9; 2007). We were able to obtain reliable MRS spectra in the live rodent brain of the pre-identified NSC-specific MRS peak at 1.28ppm. The extracted MRS data collected in two brain regions (hippocampus and cortex) were correlated with histological evidence of the presence and lack of NSC in the hippocampus and cortex, respectively. We used many different experimental approaches to prove our hypotheses which included injection of NSC into brain regions devoid of stem cells and the demonstration of an increased 1.28ppm peak area in rats exposed to electroconvulsive shock which is known to also increase NSC in the hippocampus (in collaboration with Dr. Fritz Henn). The data analysis approach developed by Dr. Petar Djuric at SBU was pivotal for the project. This MATLAB based algorithm enables extraction of the 1.28ppm spectra using single value decomposition (SVD) analysis.

We have now embarked on refining our MRS methodology to be able to acquire stem cell spectra in the much smaller mouse brain at an improved time resolution (which will be essential for a wide variety of future projects). Previously the MRS spectra were acquired over 50 min using a voxel size of 20mm^3; Figure 1 shows the new mouse cradle system which we designed in collaboration with Dr. Smith from the Medical Department and Tom Lambertson from Central Shops and MRS spectra that we collect from the mouse hippocampus in ~10 minutes.

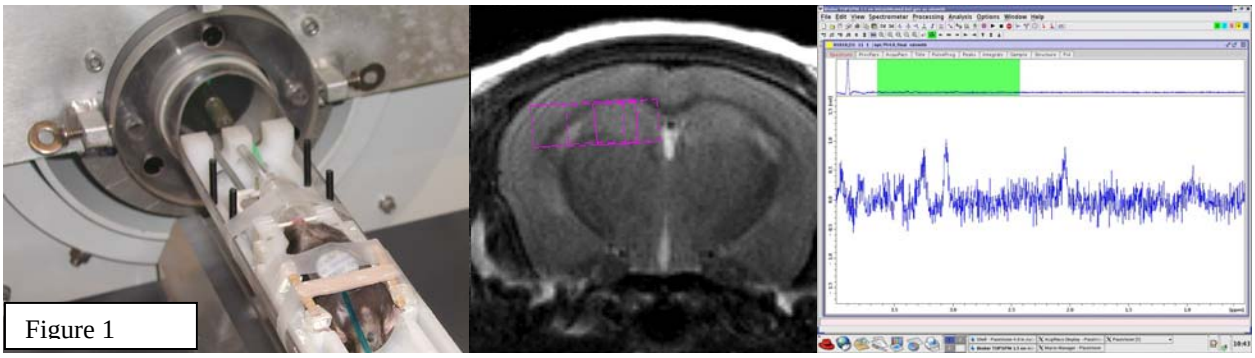

Figure 1

SVD analysis performed in collaboration with Dr. Peter Djuric demonstrates that we can identify and track stem cells in the small mouse brain. Several steps are needed including water peak removal, filtering, elimination of nuisance peaks and repeated fitting. Figure 2 shows the last two steps of the SVD analysis performed in MATLAB and identification of the 1.28 ppm peak.

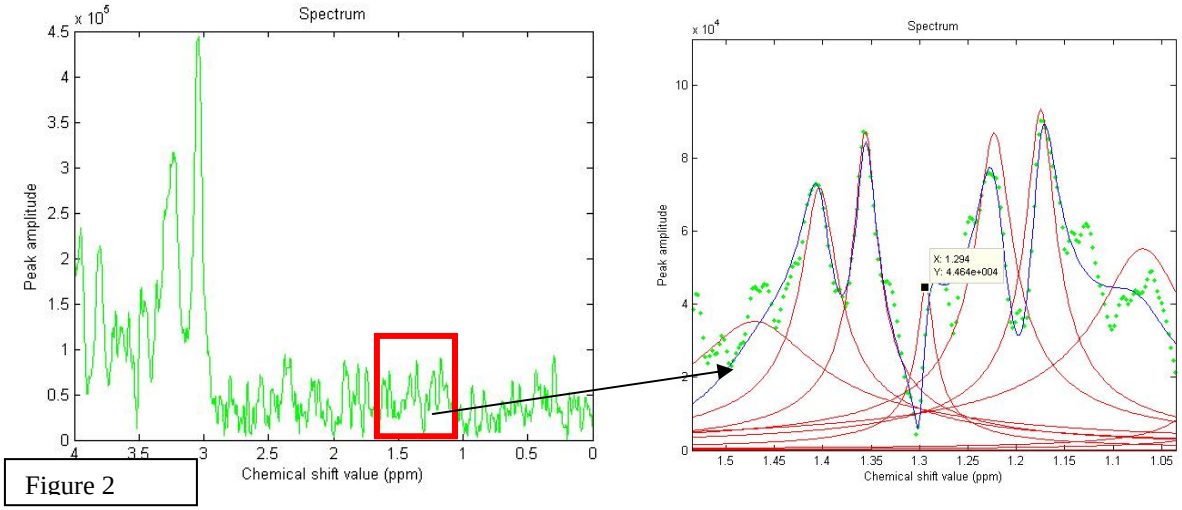

Figure 2

In collaboration with Dr. Stan Wong we are also underway in investigating an iron oxide nanoparticle coated with surfactant. The size of these particles has been verified with TEM and is approximately 12nm. We have exposed NSC to these particles with and without using the polylysine (poly-Lys) coating step. Our preliminary data shows that the nanoparticles after incubation with the neurospheres do not attach when plated for further differentiation. Importantly, we have performed parallel experiments with control neurospheres and verified that under these conditions the neurospheres do attach and differentiate normally. Interestingly, histological staining with trypan-blue shows that the neurospheres loaded with the new particles are healthy looking and alive so the new iron oxide particle is not toxic to the cells. Finally, when we triturated the neurospheres loaded with the nanoprobes and plated (almost) single cells, only the cells that did not endocytose the new particles differentiated, and none of the loaded cells attached/differentiated. We do not yet have an explanation as to why the iron oxide nanoparticle coated with surfactant interferes with neural stem cell differentiation. We are planning experiments to investigate this intriguing finding.

MicroCT Methods of Quantitative Adipose Imaging: Development of a Long-Term Assessment Technique for Studying Obesity in a Rodent Model

LDRD Project 06-094
Gene-Jack Wang

PURPOSE:

A reproducible and accurate method of quantifying regional- and total-body fat is needed for studying obesity in rodents. MicroCT is an ideal technique for this purpose. First, when used at low beam-energies it offers a large differential image contrast between fat and lean tissue that helps to distinguish them. As a result it produces total body fat with fine reproducibility. Depending on the subject's size, the optimal spectral beam energy for imaging the obese mice is 20-25 keV. Second, the exquisite spatial resolution of microCT in the three-dimensional CT-reconstructed images minimizes partial volume effects that otherwise limit the method's precision. Our microCT system, SkyScan Model 1076, is very suitable for assessing fat in small rodents because of the wide range of beam energies available, namely 20- to 70-keV mean spectral energies, and also because of its fine spatial resolution, with pixel sizes of 9-, 18-, and 35-μm. We evaluated the energy-selective methods of single- and dual-energy quantitative CT (SEQCT and DEQCT, respectively), and used SEQCT to measure total body fat in mice. We also obtained a 0.4% precision in measurements in repeated chicken-fat phantom studies. Our findings also demonstrate the importance of tailoring the beam's energy to the subject's size. The work, an integral part of Drs. Wang and Thanos' Obesity Research, could attract external funding for it further development and its implementation with clinical CT.

APPROACH:

We used a low- and a high-energy beam. For the former, the x-ray tube was operated at 41 kVp and beam was filtered with 0.5 mm, producing 24-keV mean energy; the latter was produced at 100 kVp with 0.25 mm Cu beam filtration, and had 70 keV mean energy. The low-energy beam produced a large differential contrast between the fat and lean tissue (0.58:1.0), while the high-energy beam was used to better differentiate between lung tissue and fat. The images were acquired at 35 μm pixel size, which means a spatial resolution of about 60 μm full-width-half-max (FWHM) in the CT reconstructed images. This spatial resolution adequately minimizes partial volume inaccuracies in body regions where the fat and lean tissue are intertwined at fine dimensions. SEQCT was used to measure the total body fat in mice (Fig. 1) and phantoms. To analyze the images we adopted the following steps. First, the projection data were reconstructed to produce a whole-body CT data set. Second, we employed the values of the voxels in the CT data set, i.e., the attenuation coefficients of the tissues, to generate histograms of the voxel values (Fig. 2). These histograms clearly separated the fat voxels from the lean ones everywhere in the body of the mouse except for the lung region where the spectra of the attenuation coefficients for fat and lung tissues partially overlapped. Following this, we counted the fat voxels over the entire body of the mouse by setting the integration window on the histogram spectrum in such a way to exclude lean tissue (and bone) but to include both fat and lung tissue. Then, the total number of lung voxels was counted over the chest region by setting the histogram window to excluding both fat and lean tissue; the resulting lung voxel counts subsequently were subtracted from the total body fat counts. Finally, the resulting net fat voxel count was converted to grams of fat using the reference gram/voxel ratio we obtained from a study of mouse fat phantom containing a known amount of fat. The measurements typically took about 40 min and the absorbed dose to the animal was 0.3 Gy. Finally, we used three mice to compare the absolute

value of the total body fat measured with our technique to that measured by the Bruker's minispec Lean/Fat Analyzer at Columbia University.

TECHNICAL PROGRESS AND RESULTS:

The precision (reproducibility) of the total body fat measurement (standard deviation divided by the mean value) obtained from repeated studies with the chicken-fat phantom was 0.36%, which we consider excellent. The pieces of the fat in the saline solution were moved around between measurements, and the bottle was repositioned in the system, to produce an independent CT image each time. This degree of precision would be invaluable for applying the method to longitudinal studies. Our studies with the obese mice produced a reproducibility of 1.9% for total body fat normalized to the animal's weight. This reproducibility also is remarkably good. Finally, the average value of the total body fat in three mice measured with the above method was only 65% of that measured with the minispec at Columbia University 3 days earlier. This discrepancy seems to stem from two factors. First, the mice experienced weight loss (1.7 g in average; which was 5.8 % of their body weight) between the two measurements. Although a 5.8% correction was introduced in the minispec fat results to correct for this loss, the percent fat loss could have been larger than the percent weight loss. Second, the two methods do not measure the same quantity; SEQCT measures only solid fat while minispec measures fat in all its forms.

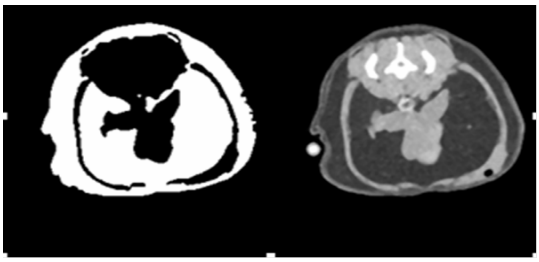

Figure 1. SEQCT image of an obese mouse abdomen with its fat regions highlighted.

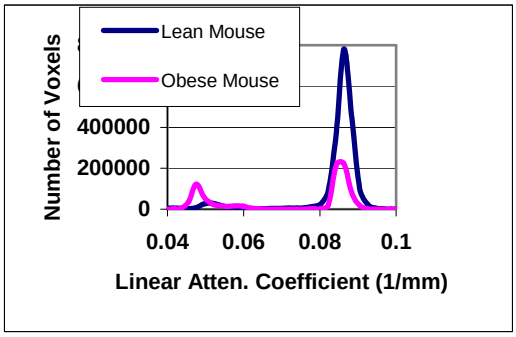

Figure 2. Whole body histograms of the CT voxel values.

The 0.36% reproducibility of the total body fat in chicken-fat phantoms obtained with the microCT-based SEQCT method suggests that it may be ideal for measuring total body fat in mice, particularly for using in longitudinal studies. The mice should tolerate the radiation dose of ~0.3 without ill effects. Finally, the histogram method provides the regional attenuation coefficient profiles of fat at high signal-to-noise ratio, which is very valuable. The method is rich in information on the quality of the fat, and can be applied to small body regions with an adequate signal-to-noise ratio. In particular, we observed that the fat peak in the obese mice histogram shifts towards lower attenuation coefficients compared to lean mice (left peaks in Fig. 2). Because in fat cells the cytoplasm's attenuation coefficient is smaller than that of the cell nucleus, and because growth of the fat cell is only in its cytoplasm and not in its nucleus, the method allows us to calculate the relative fat cell size in different stages of obesity, which could be another useful piece of information.

Photocatalytic Reduction of CO_2 in Supercritical CO_2

LDRD Project 06-097
David C. Grills

PURPOSE:

The goal of this project is to determine if the photocatalytic reduction of CO_2 into useful chemicals and fuels can be achieved more efficiently than current state-of-the-art methods. We propose to employ supercritical CO_2 ($scCO_2$) as both the reaction medium and primary reactant. This is an innovative approach since it eliminates the need for toxic organic solvents and will hopefully lead to many potential advantages, such as significantly higher reaction rates and catalyst turnover frequencies. With the ever-increasing costs of energy and the rapid depletion of the world's fossil fuel supplies, there is an urgent need for new technologies that will make use of renewable energy sources such as solar energy. The conversion of the abundant molecule, CO_2 into useful fuels and chemicals with solar-driven photocatalysts is thus an attractive possibility. This project seeks to explore a novel approach to this problem, with the ultimate aim of developing new, efficient photocatalysts tailor-made for use in $scCO_2$.

APPROACH:

Supercritical fluids are a curious hybrid of gases and liquids. The use of $scCO_2$ (CO_2 at pressures and temperatures exceeding 1070 psi and 31 °C, respectively) as a replacement for conventional solvents in chemical processes has become increasingly common in the last two decades. However, its combined use as a solvent/reactant has received much less attention. The tunable physical properties of $scCO_2$ (*e.g.* density, viscosity *etc.*) and the fact that extremely high concentrations of CO_2 can be achieved (~20 M @ 3000 psi/35 °C) offers the possibility of dramatic enhancements in catalyst efficiency for the photoreduction of CO_2.

Various different transition-metal complexes have been investigated as potential photocatalysts for the reduction of CO_2 due to their long-lived charge-separated photoexcited states. A major setback however, has been that solvent molecules tend to coordinate to vacant sites at the metal center in the active catalytic species, and thus compete with CO_2 reactant molecules, substantially reducing the catalytic activity. Our approach therefore, is to completely eliminate the use of conventional solvents by replacing them with $scCO_2$, leaving CO_2 as the only available reactant to bind with the catalyst's metal center.

The project involves chemical synthesis to structurally modify a family of previously studied CO_2 photoreduction catalysts in order to render them soluble in $scCO_2$. This is necessary because $scCO_2$ is a relatively poor solvent, similar in solvating power to hydrocarbons such as hexane. The photochemical and photophysical properties of these new catalysts are then studied in conventional solvents and subsequently in $scCO_2$. This involves the use of fast time-resolved spectroscopic techniques (UV-vis and IR) on the nanosecond timescale to probe and characterize the intermediate species generated during photocatalysis. Catalyst efficiencies are determined by steady-state irradiation studies.

TECHNICAL PROGRESS AND RESULTS:

Experiments in $scCO_2$ solution require a specialized apparatus capable of operating at relatively high pressures (up to *ca.* 5000 psi). However, photo-initiated catalysis in $scCO_2$ adds another dimension of difficulty since optically transparent windows that can withstand the high pressures must also form part of the sample cell. An apparatus has therefore been constructed for preparing

and mixing solutions of photocatalysts in $scCO_2$. This consists of a network of high-pressure valves and stainless steel tubing connected to a CO_2–filled syringe pump. At the heart of the system is a custom-made temperature-controlled high-pressure spectroscopic cell (see below) that contains 10 mm thick CaF_2 windows, which are transparent throughout the UV, visible and IR regions.

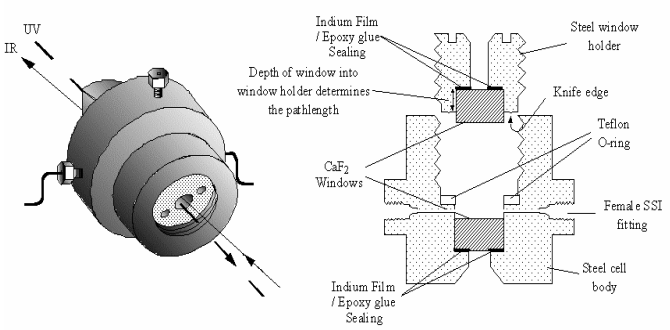

So far we have synthesized two new potential CO_2 photoreduction catalysts that are soluble in $scCO_2$. These are the dinuclear compound, $[Re(CO)_3(dnb)]_2$ (dnb = 4,4'-dinonyl-2,2'-bipyridyl), and the mononuclear $Re(CO)_3(dnb)Cl$. Both of these molecules possess long nonyl alkyl chains attached to the bipyridyl rings, which have rendered the catalysts soluble in both *n*-hexane and $scCO_2$. In order for the new compounds to behave as efficient CO_2 reduction photocatalysts they must initially produce a metal-to-ligand charge transfer (MLCT) excited state upon absorption of light. Such MLCT states are typically short-lived, on the order of nano- to microseconds. Thus, it is important to first probe the photophysics of these complexes in $scCO_2$ using time-resolved spectroscopic methods in order to identify the spectroscopic signature of a MLCT excited state upon photoexcitation. This has been performed for $Re(CO)_3(dnb)Cl$, both to demonstrate that we can successfully couple the high-pressure optical cell with our existing time-resolved spectroscopy apparatus, and also to identify and characterize the MLCT excited state. The figure to the left shows typical data obtained for $Re(CO)_3(dnb)Cl$ dissolved in $scCO_2$ (2500 psi, 35 °C) following 355 nm pulsed laser excitation. The transient absorption spectrum shows two bands at 370 and 480 nm, which are highly characteristic of an MLCT excited state for this family of complexes. The corresponding emission spectrum from this excited state exhibits a broad, featureless band at 609 nm, which is also typical for an MLCT state. The lifetime of the excited state was measured to be 34 ns at 35 °C, which is sufficiently long enough to allow quenching by sacrificial electron donors and the initiation of a CO_2 reduction cycle.

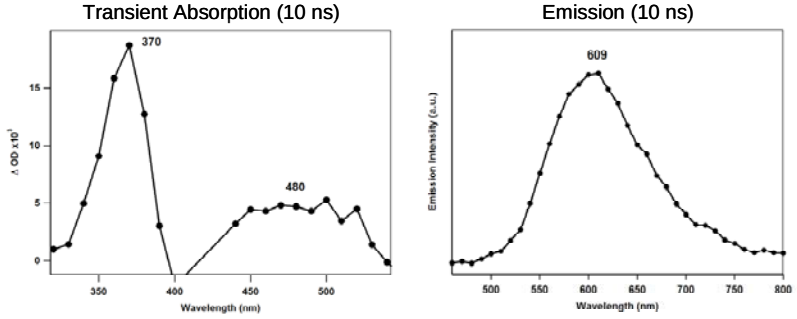

Following the successful identification of an MLCT excited state upon photoexcitation, the CO_2 reduction efficiencies of the new catalysts will now be investigated in $scCO_2$ in the presence of sacrificial electron donors such as triethylamine. These results will be compared with analogous experiments in conventional solvents. In addition, we have designed and are currently synthesizing a new family of CO_2 reduction catalysts bearing perfluoroalkyl substituents. These substituents are specifically tailored to enhance the solubility of the catalysts in $scCO_2$, which will hopefully lead to enhanced reactivity.

QCD Thermodynamics at Non-Zero Temperature and Density

LDRD Project 07-001
Frithjof Karsch

PURPOSE:
The objective of the project is to improve our understanding of the QCD phase diagram through a systematic study of phase transitions in an extended parameter space defined by the quark mass, the temperature and the baryon chemical potential. The aim is to reach better control over the baryon density or chemical potential dependence of the QCD transition and improve current studies of the chiral critical point in the QCD phase diagram. The project provides important input to the preparation of experimental programs (low energy runs at RHIC and the CBM experiment at FAIR) that aim at a study of QCD at high baryon number density.

APPROACH:
It is expected that the QCD phase diagram changes qualitatively when going from vanishing baryon chemical potential to values of the order of a few hundred MeV. Model calculations suggest that a line of first order phase transitions emerges at non-zero baryon chemical potential starting at a critical point (2^{nd} order phase transition point). Similarly the transition changes from a continuous crossover to a first order phase transition when the quark mass is reduced to sufficiently small values. We will use Taylor expansion techniques to analyze the phase diagram of QCD and study the connection between transitions that exist at small quark masses and those conjectured to exist at non-zero quark chemical potential. For this purpose we developed a program that automatizes the calculation of higher order Taylor expansion coefficients. This will allow us to extent the Taylor series for thermodynamic observables at least to 8^{th} order order in the baryon chemical potential. This will considerably improve over earlier studies performed with heavier quarks and will result in an estimate of the radius of convergence of the Taylor series that allows to locate the critical point in the QCD phase diagram.

The numerical calculations are performed in the context of studies of QCD Thermodynamics performed by the RIKEN/BNL-Bielefeld-Columbia Collaboration on the QCDOC and BG/L computers at BNL as well as on a supercomputer, apeNEXT, at Bielefeld University, Germany. The collaboration involves about 15 members from Bielefeld University (Prof. E. Laermann et al.), Columbia University (Prof. N.H. Christ, Prof. R.D. Mahinney et al.) and members of our BNL based Lattice Group (S. Ejiri, P. Petreczky, K. Huebner, C. Pica, C. Schmidt, W. Soeldner and myself).

TECHNICAL PROGRESS AND RESULTS:
During most of FY2007 we have developed the programs necessary to perform Taylor expansions at high order. These techniques have also been used in a collaboration with colleagues in Japan to perform first studies of QCD at non-vanishing baryon chemical potential using Wilson fermions. We furthermore showed that a study of effective potentials for the QCD partition function, performed at non-zero chemical potential in the Taylor expansion approach, allows to give criteria for the existence of a critical point at non-zero chemical potential and allows to estimate its location in the temperature-chemical potential phase diagram. We performed first calculations of Taylor expansion coefficients up to 8^{th} order on data sets generated for the study of the QCD equation of state with almost physical light and strange

quarks. These results are still preliminary. We also worked on an alternative approach to study the QCD phase diagram – the so-called density of state method.

Lattice QCD Simulations on BlueGene/L

LDRD Project 07-002
Frithjof Karsch

PURPOSE:
The objective of the project is to build up a computational environment with highly optimized programs and libraries that allows to perform efficient QCD thermodynamics simulations on BG/L computers. This requires to port the Columbia Physics System (CPS) software package, which forms the basis for the comfortable computing environment used on the RIKEN/BNL and DOE owned QCDOC computers, also to BlueGene/L. CPS will be used to run efficiently QCD thermodynamics projects on BlueGene/L.

APPROACH:
The BlueGene/L architecture has many features in common with the QCDOC computers installed at BNL. The basic parallel computing paradigm thus can easily be mapped onto the BlueGene/L machines. However, on QCDOC central parts of the computing programs have been coded in Assembler to reach satisfactory efficiency. These parts of lattice QCD programs require an individual treatment on different computer architectures and need to be ported to BlueGene/L. Moreover, recent advances in lattice simulation and integration schemes (RHMC algorithm, Omelyan integration, quotient force terms) as well as the development of refined fermion discretization schemes with improved flavor symmetry (stout action, domain wall fermions) require the development of new programs. These have to be optimized for new computers such as BlueGene/L and have to be integrated into a common library environment, the CPS software package used by our BNL based Lattice Group (S. Ejiri, P. Petreczky, K. Huebner, C. Pica, C. Schmidt, W. Soeldner and myself) in the joint research projects with the lattice group at Columbia University as well as research groups at LLNL and LANL.

TECHNICAL PROGRESS AND RESULTS:
Early in FY2007 we installed and tested CPS on BlueGene/L machines at Argonne, Livermore as well as the John von Neumann Center (NIC) in Juelich, Germany. We could successfully port our QCD thermodynamics package to and started to tune the RHMC algorithm used for our simulations. With the arrival of a BlueGene/L at the New York Center for Computational Science, which is hosted by BNL, the CPS has been installed and further developed on this machine. To compensate for the reduction in sustained performance on BlueGene/L compared to the QCDOC machine we started to change parts of the code to single precision calculations in those parts of the program where the use of double precision is not essential.

The QCD thermodynamics project on BlueGene/L computers is now part of the so-called hotQCD Collaboration, a consortium of lattice gauge theory groups in the US. The goal of this collaboration is to extend existing studies of QCD thermodynamics by performing simulations with parameters that are even closer to the continuum limit. This will improve control over systematic errors in the continuum extrapolation and will improve results obtained for the QCD equation of state and transition temperature. With the arrival of the BlueGene/L at BNL early user time on this machine could be used efficiently to complete the studies of the equation of state started by the RIKEN/BNL-Bielefeld-Columbia Collaboration on the QCDOC machines.

Proof-of-Principle Laser System for ILC Positron Source

LDRD Project 07-004

Igor Pogorelsky

PURPOSE:

Development of an intense, high-repetition polarized positron source is one of the most critical issues to realize in the International Linear Collider (ILC) project. Positrons will be produced by stopping gamma-rays (γ-rays) on a target. Accordingly, this calls for an intense polarized γ-source. Compton back-scattering between a CO_2 laser and 4-GeV electron beam is one of leading ideas for such a γ-source that is an alternative to a more conventional wiggler approach that requires 150 GeV electrons.

Matching a high-repetition bunch format of the ILC requires a ~10-kHz, picosecond laser of a ~10-kW average power that widely exceeds industry capability. We propose to circumvent this constraint by "recycling" each laser pulse for multiple electron/laser interactions thus lowering the required laser parameters ~100 times. The goal of this project is to demonstrate the feasibility of this approach thereby leading the way to its practical application for ILC and similar e^-e^+ collider projects.

APPROACH:

Capitalizing on the 5-ps, 1-TW peak power CO_2 laser available at the Accelerator Test Facility (ATF), a record-high quantum efficiency of Compton scattering in a single-pulse laser/e-beam interaction has been demonstrated. The demonstrated Compton photon yield satisfies and even exceeds the ILC requirements for a single laser/e-beam interaction. Up-scaling this effect to multiple (up to 100) similar interactions over the duration of one laser shot requires placing the laser/e-beam interaction point (IP) inside a high-Q regenerative laser ring cavity as shown in Fig.1, and actually constitutes the proposed laser pulse "recycling" method.

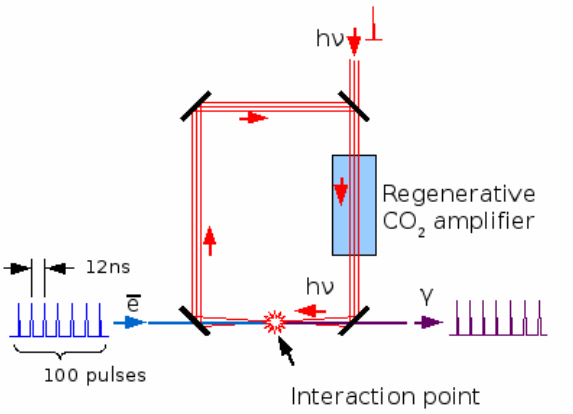

According to this scheme, an infrared CO_2 laser pulse (hν) circulates inside the ring cavity and, at each pass, interacts with a counter-propagating electron bunch (ē) to create a γ-pulse. Optical losses of the laser pulse after each round-trip are compensated by an amplifier located within the cavity. Development, simulation and experimental testing of such a regenerative CO_2 laser amplifier constitute the major part of this project. Along with I. Pogorelsky (PI, Scientist), the main contributors to this project are Vitaly Yakimenko (Scientist, Head of the ATF) and Mikhail Polyanskyi (Post-Doctoral Research Associate).

TECHNICAL PROGRESS AND RESULTS:

Proof-of-Principle Experiment.

In order to demonstrate the viability of the proposed compact polarized γ-source concept, a proof-of-principle experiment has been completed at the ATF. In this experiment, a pair of confocal parabolic mirrors has been set inside a ring cavity that includes a 3 atm. CO_2 laser amplifier as well. This mirror assembly was exactly the same as has been used previously in the

ATF Compton scattering experiment except that no electron beam was present at this time. The objective of this experiment was to demonstrate the feasibility of maintaining a laser pulse train through the Compton IP. A representative result obtained in these experiments is shown in Fig.2. A seed laser pulse has been injected through an axial hole in a parabolic mirror that is normally intended for e-beam and γ-ray transmission. By adjustment of the set-up parameters (injected pulse energy, amplification factor, optical configuration, round-trip loses etc.) and matching the optical losses to the amplifier gain we were able to achieve trains up to 1-μs-long with ±3% pulse-to-pulse stability. Although the laser pulse used in these tests was notably less powerful than our ultimate target (200 ps, ~30 mJ instead of 5 ps, 1J) we consider this result as a strong indication of viability of the proposed concept.

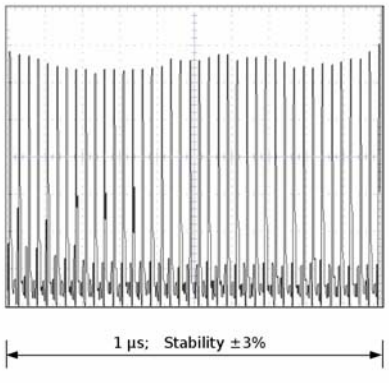

This result marks an important milestone on the path from the initial conceptual proposal to its realization. Our further efforts are aimed towards testing this approach for more powerful 5-ps CO_2 laser pulses using the big-aperture, 10-atm CO_2 amplifier available at the ATF.

Computer Simulations

Another important part of this project is the development of a computer model of a regenerative picosecond CO_2 laser amplifier. This development is carried out in collaboration with Prof. V. T. Platonenko (Moscow State Univ.), a world-recognized expert in theory and simulations of ultra-fast gas lasers. This model shall serve as a guide for choosing the right parameters for the amplifier and ring cavity in order to achieve the ILC requirements. Simultaneously, the program should provide a deeper insight into the dynamics of the laser pulse (duration, satellite time-structure, phase shift, radial profile, etc.) as it evolves in the regenerative amplifier. By now, the core computer program is written and tested. Preliminary results have been presented at a collaboration meeting at ANL.

Ongoing improvement and expansion of the program includes the use of amplifiers with different isotopic CO_2 mixtures. Using such isotopes may open the way to implementing laser amplifiers of a moderate pressure that contributes to reducing the ILC project cost and technical complexity. After finalizing the software and it's verification on the aforementioned experimental result, the model will be used for parametric optimization and choosing optimal configuration on a larger-scale.

Future Prospects and Milestones

Our initial proof-of-principle experiment and an operational computer model provide a solid platform for further progress of this LDRD project towards achieving its goals. The main efforts will be directed towards simulation and practical demonstration of extending the single-shot laser operation into a train of pulses close to the ILC requirements, which is the second milestone of the project. Towards this end, we work with international manufacturers of high-pressure CO_2 lasers over a business proposal for high-repetition-rate lasers that match the ILC beam format.

Sensitive Searches for CP-Violation in Hadronic Systems

LDRD Project 07-005
Yannis K. Semertzidis

PURPOSE:
The goal of this investigation is to develop a proposal for a sensitive electric dipole moment experiment of the deuteron. The sensitivity scale of the method will allow it to be the best experiment over current and future experiments in hadronic electric dipole moments (EDMs). If a deuteron EDM is found it will point to a new, large CP-violation source that could help explain the matter-antimatter asymmetry of our universe.

APPROACH:
The Storage Ring EDM Collaboration is working on a new concept of studying CP-violation in hadronic systems. This new concept includes the development of a special storage ring where polarized deuteron and probably proton beams can be stored so that their EDM can be probed in a very sensitive way.

The systematic errors regard beam and spin dynamics resonances, as well as polarimeter associated systematic errors. Waldo MacKay, Vadim Ptitsyn, Mike Blaskiewicz, Alfredo Luccio, Alexei Fedotov, Ilan Ben-Zvi, Mei Bai and others of CAD are helping with their expertise in the proposal writing and systematic error study. In the Physics dept., William Morse and William Marciano are the other collaborators. We have also hired Fanglei Lin (supported with this LDRD) a recent Ph.D. of S.Y. Lee of IUCF, a world expert on spin dynamics systematic errors. Dr. Fanglei Lin did her Ph.D. thesis on the spin resonances of AGS working closely with Mei Bai of CAD. Yuri Orlov of Cornell University, a word expert on spin and beam dynamics in accelerator physics, is working on spin resonances, and spin coherence time.

TECHNICAL PROGRESS AND RESULTS:
We have hired a post doc. She has managed to implement the ring lattice (lattice is the set of the storage ring elements) proposed by Yuri Orlov into a special tracking program and has computed the beam parameters. She can now run the various checks on spin coherence time, beam and spin resonances.

Waldo MacKay, Vadim Ptitsyn, William Morse and I are working closely together on developing new techniques to eliminate a whole class of systematic errors and improve the statistical sensitivity of the experiment. We made very good conceptual progress but the work is still in progress.

Alfredo Luccio is working on ring lattice optimization using his self developed program that describes the spin and beam dynamics in a very efficient way. Only with his program can we study the various aspects of the stored beam for 100s -1000s.

The goals for the next fiscal year regards the study of spin dynamics resonances, the development of a lattice with long spin coherence time and understanding whether or not our new ideas can improve even further the statistical accuracy of the technique.

Feasibility and Design Study for a Detector for e+p, e+A, p+p, p+A, and A+A Collisions at BNL

LDRD Project 07-006
Thomas Ullrich

PURPOSE:
The aim of this project is to work on the design of a detector for the future Electron Ion Collider (EIC). This can only be achieved if accompanied by detailed physics simulations that allow the design to be optimized. This is done by iteratively testing of all the relevant observables for the various physics studies in e+p and e+A can be extracted with sufficient quality for a given layout. The e+A case is especially challenging in a collider environment. To allow the exploration of all aspects of QCD we also intend to investigate if a multi-purpose detector can be designed that would also allow the measurement of p+p and p+A collision.

The outcome is expected to provide a solid detector design that can serve as a baseline detector for the EIC. The design should allow the systematic study of e+p and e+A collision over a broad kinematic range. Results of these studies are expected to provide first input to the 2012 NSAC Long Range Plan, which will be essential for the future of the EIC project.

APPROACH:
A future Electron-Ion Collider embodies the vision of the field of High Energy Nuclear Physics for reaching the next QCD frontier: the study of gluons which bind all atomic nuclei. A high luminosity EIC, with center-of-mass energy in the range from 30 to 100 GeV with polarized electron and nucleon beams and the full mass range of nuclear beams could be sited either at BNL (eRHIC) or at JLAB (ELIC). The new EIC facility will require the design and construction of an optimized detector profiting from the experience gained from those operated at DESY. A central collider detector providing momentum and energy measurements plus particle identification for both leptons and hadrons will be essential.

The aim of this project is to design a suitable detector for the new EIC facility. The techniques used to study the physics at the EIC is sufficiently different to that at RHIC (using electron-hadron collisions as opposed to hadron-hadron collisions) that new detectors are required. The design approach being used is to generate simulated e+A collisions and then examine them in conjunction with various preliminary designs for detectors based on those at DESY (lower energy e+p collisions) in order to optimize the design of a new detector.

TECHNICAL PROGRESS AND RESULTS:
The first major hurdle, which has been overcome, was the lack of Monte Carlo programs/generators to simulate e+A collisions. There is, however, a rich set of generators for deep inelastic and diffractive e+p collisions available. Therefore, we adopted a staged approach making use of the existing generators for elementary collisions (such as Pythia and RAPGAP) and use their output as input to a newly developed generator that takes care of the nuclear geometry (“Glauber” wrapper) and the subsequent interactions in the nuclei. For this purpose an existing HIJET program, originally developed to simulate nuclear collisions (A+A) was used as a baseline and severely modified. The HIJET e+A program serves basically as a kind of “afterburner” that handles correctly the distributions of the nucleons in the nuclei (Wood-Saxon density profile) and propagates the partons created in the e+p collisions allowing for further interactions in the nucleons of the nuclei.

The problem with this approach is that there are no nuclear effects such as shadowing, or the EMC effect included within HIJET. However, these effects are important for subsequent studies and hence need to be added into our scheme. One approach is to generate the events with different parton distribution functions (PDFs) depending on the impact parameter of the incoming electron. It is currently being investigated if these different PDFs have any effect on the final state particle distributions and whether it is possible to identify which PDFs were used based upon final-state distributions alone. Another approach is to use a novel generator developed at Lund University that is based on the Mueller Dipole Model that allows one to "dial" in nuclear effects such as shadowing by modifying the dipole size.

In parallel a detector simulation environment based on the GEANT simulation package has been establish. This already includes existing approximate descriptions of proposed EIC detector concepts (see Fig. 1 and 2) and will serve as a basis for further development based on their physics performance. We are in contact with the RHIC Computing Facility and will soon receive some moderate, but sufficient in the short term, computing resources for our simulations. We also intend to create a web site for EIC software distribution to share the current design concepts as they are adapted with collaborators in, and outside of, BNL.

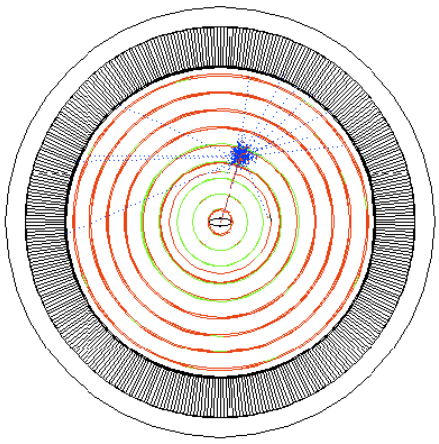

Figure 1: *Front view of an e+p collision in a large scale EIC detector generated using the GEANT simulation package.*

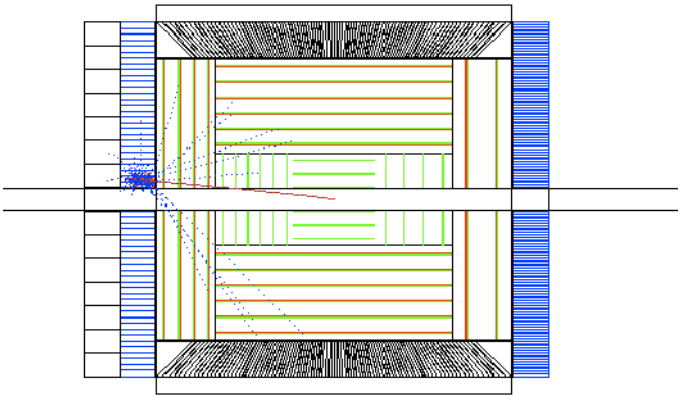

Figure 2: *Side view of the same e+p event as shown in left figure.*

A Novel and Compact Muon Telescope Detector for QCD Lab

LDRD Project 07-007
Zhangbu Xu

PURPOSE:

We propose an R&D study of a large-area and cost-effective muon telescope detector (MTD) for RHIC, and for next generation detectors at future QCD Labs, which employs state-of-art multi-gap resistive plate chamber (MRPC) with large module and long strips. Conventional muon detectors rely heavily on tracking stations while this new R&D project proposes to use good timing and coarse spatial resolutions to identify muons with momentum of a few GeV/c. This R&D project will focus on studying the capability of muon identification based on timing resolution from the MRPC detector with large module, long strips and fast electronics for online trigger. We have carried out a timing resolution study at the FermiLab test beam facility (T963), operated a prototype in a real environment at STAR in Au+Au collisions, and plan to install a prototype for p+p and d+Au collisions at RHIC in run 2007-2008. This has allowed us to assess the detector's time resolution, its triggering efficiency, and its particle identification capability. A large-area muon detector around center of mass at RHIC will be crucial for advancing our knowledge of Quark-Gluon Plasma (QGP). It directly addresses many of the open questions and long-term goals proposed in four RHIC white papers published in Nuclear Physics A **757** (2005). Since muons do not participate in strong interactions, they constitute penetrating probes to the strongly interacting Quark-Gluon Plasma.

APPROACH:

A compact detector identifying muons of momentum at a few GeV/c should achieve hadron rejection of a few orders of magnitude and allow us to investigate dimuon pair from virtual (heavy) photon decays, QGP thermal radiation, possible correlations of quarks and gluons as resonances in QGP, initial lepton production, and heavy flavor (charm and bottom) quark production. In addition to an effective trigger and cleaner signal-to-background ratio, electron-muon correlation can be used to distinguish lepton pair production and heavy quark decays.

The same Basic technology but with small pads has been proposed in STAR and PHENIX at RHIC and ALICE at Large Hadron Collider (LHC) as Time-of-Flight Detectors. This R&D project will focus on studying timing and spatial resolution from the MRPC detector with large module, long strips and fast electronics for online trigger to achieve necessary muon identification and hadron background rejection.

Components for the prototype and contributions from other collaborators:

1. *Long MRPC modules: Prof. Cheng Li, and Dr. Yongjie Sun (USTC/China), Prof. Yi Wang and Dr. Xiaobin Wang (Tsinghua Univeristy/China)*
2. *Front-end electronics and gas box: Drs. Bill Llope and Geary Eppley (Rice)*
3. *Trigger electronics and logics: Dr. Jack Engelage (UC Berkeley, Space Lab)*
4. *Simulations: Guoji Lin (Yale University)*

5. *T963 test beam: Dick Majka, Nikolai Simernov, Guoji Lin (Yale University), Yi Wang and Xiaobin Wang (Tsinghua Univeristy/China), Zhangbu Xu (BNL)*
6. *Prototype in STAR for 2007—2008 and data analysis: Lijuan Ruan and Patricia Fachini (BNL)*
7. *Test setup at BNL physics building: L.J. Ruan, X.B. Wang, and Z.B. Xu*

TECHNICAL PROGRESS AND RESULTS:

1. We have successfully produced four (4) Long MRPC modules in China
2. Cosmic ray tests at USTC and BNL physics department show timing resolutions <70ps, better than our original goal of 100ps.
3. Test beam results show good space resolution (<1cm), and good timing resolution (70ps) with prototype front-end electronics
4. Modules installed outside the STAR magnet iron have been used to successfully trigger the data acquisition system, and offline tracking of particles from Time-Projection Chamber ~~is~~ was able to match with hits from Long MRPC.
5. Magnetic field mapping in STAR and tracking of particles through high-density material have been performed in STAR from this project. Preliminary data from Au+Au collisions at RHIC in 2007-2008 are being analyzed.

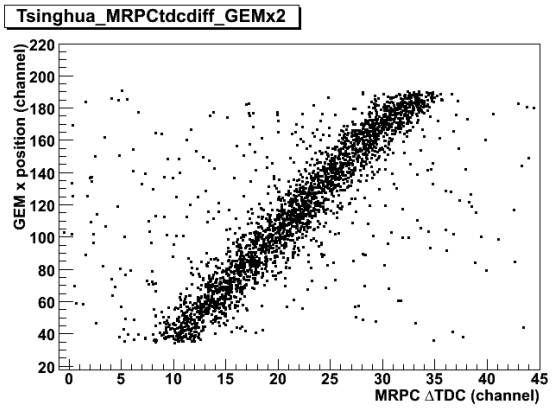

Fig.1 Position of the incident beam particles measured by GEM detector vs position calculated from the timing difference of the two-end long MRPC strip. Data are from T963

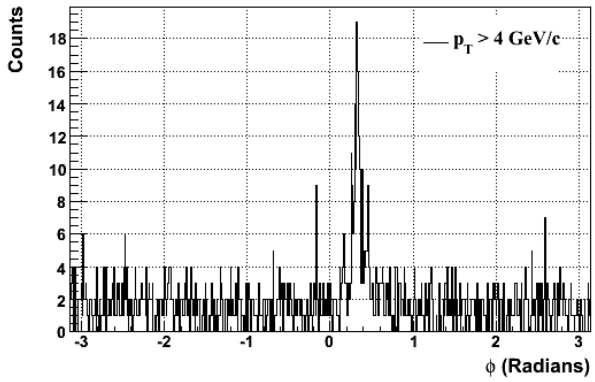

Fig.2 Azimuthal angle distribution of particles from STAR Time-Projection Chamber in Au+Au collisions at transverse momentum p_T>4 GeV/c. The peak shows an enhancement of particles yields at the angle where MTD is positioned

Future work and milestones:

1. Analyze the test beam(T963) data and data taken in Au+Au collisions at STAR
2. Obtain data in d+Au and p+p collisions at STAR in 2007—2008 run
3. Assess time resolution, hadron rejection, and muon identification efficiency
4. Optimize the detector configuration and electronics
5. Proposal for full-coverage muon telescope detector for STAR

Design Optimization of a Reactor Neutrino Experiment

LDRD Project 07-010

David Jaffe

Purpose:

Use of Geant4-based simulation to evaluate and optimize proposed elements of the Daya Bay Reactor Neutrino Experiment including options for the muon veto system and tracker. A portion of the funding is to be used for simulation and software workshops (one per year).

Approach:

The Daya Bay experiment offered the opportunity for Brookhaven to become a leader in the reactor neutrino effort that strives to measure the currently unknown neutrino mixing parameter $\sin^2 2\theta_{13}$. The muon veto system is essential in order for the Daya Bay experiment to reach its design sensitivity. Careful evaluation and optimization is needed to ensure that the cosmogenic background can be sufficiently well-suppressed and that the remaining background can be reliably estimated. Extensive use of Geant4-based simulation, validated by comparison with relevant data, is employed to evaluate muon veto system designs and background estimations. Many of the studies have been done in collaboration with Hongshang (Kevin) Zhang, a postdoc has been hired

Technical progress and results:

Design of the muon veto system is being finalized for a January 2008 Technical Design Review (CD2/3a) by the DOE Office of Science utilizing results drawn from simulation studies carried out by Kevin. Software was written to create an event display permitting validation of the simulated geometry. Additional software, aided by the event display, was written to implement an algorithm for the reconstruction of the cosmic muon trajectories in the innermost portion of the Cerenkov water pool. Extensive tests indicate that a precision of <50 cm on the distance of closest approach of the muon to the antineutrino detector (AD) is achievable; this precision should be sufficient to reliably estimate muon-induced background. Additional software was written to implement a model of water absorption to aid in setting the design specification for water purity for the Cerenkov water pool. A suite of software has been developed to evaluate the effect of changes in water purity, the reflectivity of the pool liner and AD cover, and the PMT coverage and deployment on the muon detection efficiency. These evaluations have confirmed the feasibility of tyvek as pool liner and AD cover, set the specification of water purity and determined the PMT deployment pattern that achieves the desired efficiency with a reasonable number of PMTs. A brief two-day simulation workshop in June was largely successful in initiating research using simulation by new graduate students in the US.

Future work includes development and implementation of muon reconstruction algorithms using the outer water shield, the RPC detector and the ADs, both individually and in combination. The use of the muon reconstruction for background estimation and inter-detector alignment will also be evaluated with simulation. A more extensive, week-

long software workshop is tentatively planned for Spring 2008 and will involve all Daya Bay collaborators.

Development of Laser Beam Shaper for Low Emittance Electron Beams

LDRD Project 07-019
Triveni Rao and Thomas Tsang

PURPOSE:

We propose to design, build and test a laser beam shaping module that can convert the conventional Gaussian shaped output of a laser to a rectangular shape and explore the possibility of delivering teardrop profile and ultimately any arbitrary shape required by the RHIC II and e cooler. In photoinjectors, the electron beam characteristics are dictated by the driving laser beam, which can in principle, be tailored to any arbitrary shape. Detailed simulation of electron transport processes in the photoinjector gun suggested that laser beam profile with a teardrop shape (modified ellipsoid) is ideal for generating a low emittance electron beam. In order to validate the electron beam transport simulations, it is desirable to measure the emittance for different electron beam/laser beam profiles. The ability to switch between Gaussian, rectangular, ellipsoidal beams in one drive laser system is thus highly desirable to achieve low emittance electron beam and to understand their transport characteristic. Hence the precise shaping, control and manipulation of the laser beam are critical to delivering reproducible, low emittance electron beam.

APPROACH:

The beam shaper is the key element of the research program. Although a number of techniques can be used to shape the laser beam, after evaluating various techniques theoretically and experimentally, a Gaussian-to-flat-top refractive spatial beam shaping device Newport ZB-128X is selected. This passive device is identified to be the most suitable in terms of technical feasibility, simplicity, and reliability for use in high average power laser system. The initial beam shaping is aimed to generate a rectangular spatial beam profile. A passively mode-locked Nd-vanadate laser oscillator, Time-Bandwidth Cheetah-X, is presently used for testing the refractive beam shaper module. The parameters of this laser are close to the one planed to be use for the ERL experiments. A CCD camera, DataRay USB TaperCamD20-15, is used to measure the spatial beam shape. This camera has a tapered pixel array size of 15.8x15.8 mm, sufficiently larger for the examination of uniquely larger spatial beam shapes. A home-built repetitively scanning autocorrelator is used to measure the laser pulse width before and after the beam shaper.

TECHNICAL PROGRESS AND RESULTS:

The laser output power is improved after servicing the laser oscillator and replacing the second-harmonic crystal. An average output power of 2.4 Watts is achieved at 532 nm in 10 picosecond duration with a repetition rate of 82 MHz in s-polarization output. The divergence of the laser is determined to be ~0.16 mrad by measuring the $1/e^2$ laser spot size right at the exit of the laser beam shutter and at 1-meter away, see Figure 1(a). The laser spot is first expanded by a pair of telescope lenses, plano-concave f=-10 cm followed by plano-convex f=40 cm, to match the input spot size required for the bam shaper. This expanded beam is passed through the beam shaper with more than 2 Watts of flat-top-beam output and a measured through-put of 88%. To fine-tune the input beam size and divergence, the refractive shaper is strategically positioned at 75-inch from the exit aperture of the laser oscillator. Figure 2(a) shows the near Gaussian shape of the input beam with $1/e^2$ spoet sizes of 4.61 and 4.76 mm in horizontal and vertical dimensions,

while Figure 2(b) shows the corresponding flat-top-beam output of 7.26 and 7.03 mm, respectively.

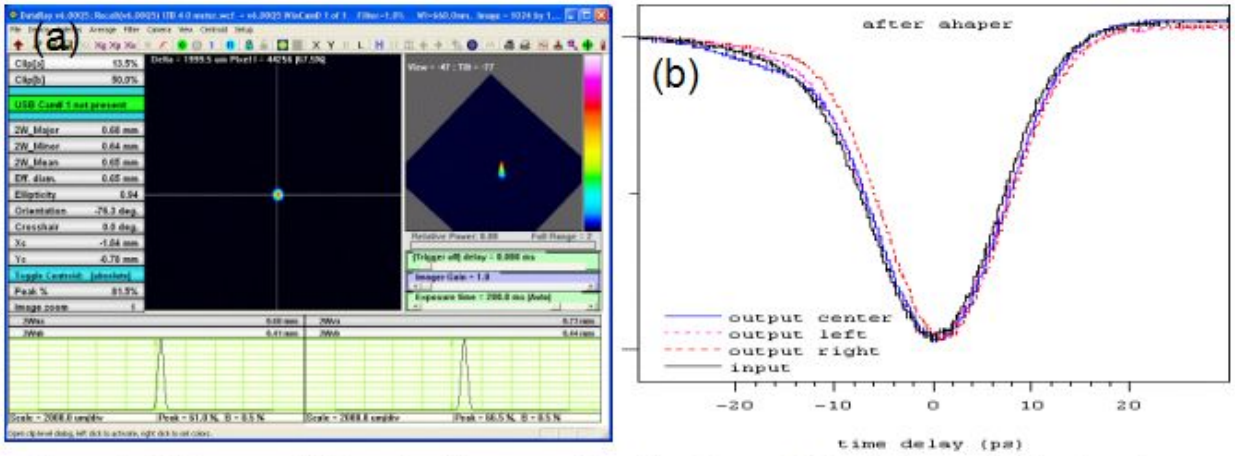

Figure 1 (a) laser oscillator output beam profile, (b) autocorrelation before and after the shaper

It is apparent that the refractive beam shaper has transformed the spatial shape from vertical to horizontal. Since the cylindrical symmetry of the input Gaussian beam profile is imperfect, i.e., the profile is slightly elliptical instead of circular, only a near perfect flat-top-beam is obtained. It is speculated that the imperfect Gaussian beam input is a result of the limited temperature tuning capability on the phase matching of the LBO second-harmonic crystal. As a result, the SHG crystal was slightly tilted to provide additional angle tuning, generating a slightly tilted wavefront, thus a slight elliptical beam shape. Therefore a good symmetry and uniformity of the input Gaussian beam is essential for generating a high quality flat-top-beam output profile. The laser pulse width measured before and after the shaper as well as at different portion of the flat-top-beam region did not show any change, see Figure 1(c), suggesting that the dispersion of the refractive shaper is negligible at this relatively long pulse width of ~10 ps .

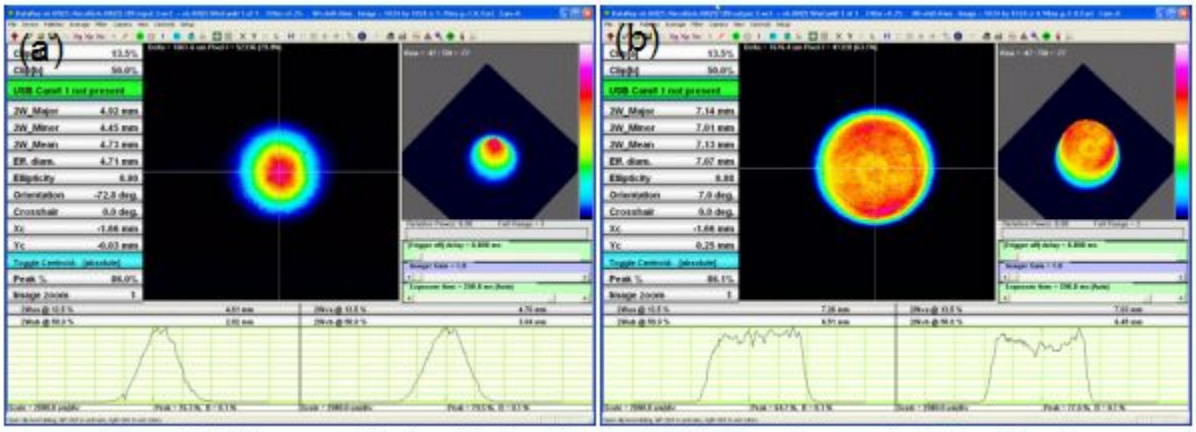

Figure 2 (a) beam profile input to the shaper , (b) flat-top-beam output from the shaper

Continued effort is made to temporally shape the laser pulse width from a Gaussian to flat-top providing a true temporal and spatial flat-top-beam profile. The laser beam shaping is an enabling technology that is needed for any high current low emittance electron beam source, especially RHIC II, eRHIC, ILC and future light sources.

Surface Engineered and Core-Shell Nanowires: Nanoscale Building Blocks for Third Generation Photovoltaics

LDRD Project 07-023
Peter Sutter, Eli Sutter, and Nicholas Camillone III

PURPOSE:
Nanostructures, in which reduced spatial dimensionality and quantum confinement modify the intrinsic electronic and optoelectronic properties of a given material, have a significant but as yet unrealized potential for performance improvements in photovoltaic (PV) devices. Semiconductor nanowires (NWs) are an important example of a self-assembled nanoscale material with potentially large impact on future PV device technologies. This project focuses on exploring, at a fundamental level, the synthesis, electronic, and optoelectronic properties of semiconductor nanowires with controlled surface termination, and of nanowire-based core-shell structures. The results will help establish a fundamental scientific basis for evaluating possible NW-based third-generation PV device structures.

APPROACH:
We use in-situ transmission electron microscopy (TEM) to establish the formation of nanowire heterostructures. We further combine the synthesis of novel NW-based architectures, such as surface-passivated and core-shell NWs, with measurements of the single NW electrical (transport, photo-transport, rectification) properties under well-controlled ultrahigh vacuum (UHV) conditions in our unique UHV Nanoprobe system with in-situ sample preparation capabilities.

TECHNICAL PROGRESS AND RESULTS:
In the first year of the project we made significant progress in the formation of high-quality semiconductor-carbon core-shell nanostructures using real-time in-situ TEM at variable temperature.

Metal-induced assembly of ordered carbon shells on semiconductor nanowires: Using in-situ TEM experiments at variable temperature, we established the controlled assembly of multilayer graphene carbon (C) shells on group III-nitride NWs. While the semiconductor surface itself is inert, C-shells form spontaneously around NWs whose surface is decorated with small catalytic metal particles (Fig. 1). Importantly, the encapsulation of III-nitride (GaN) NWs was achieved by decoration with group III (In) metal clusters, avoiding the usual transition metal catalysts whose incorporation as trace impurities degrades the electronic and optoelectronic properties of GaN. The findings on group III-nitride NWs, together with earlier work on group IV semiconductors, demonstrate that encapsulation in graphene C-shell can be achieved on any semiconductor NW material whose surface is decorated with small metal clusters.

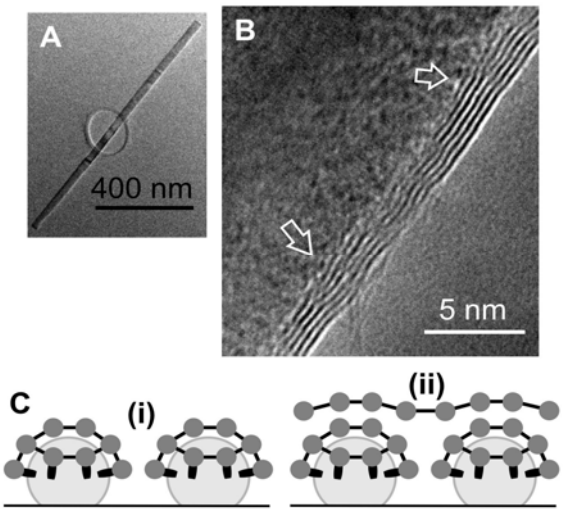

Figure 1: A – Overview TEM image showing a typical In-terminated GaN NW completely embedded in a C-shell. **B –** Detail of the core/shell interface. Arrows mark the position of some of the In clusters at the NW surface. **C -** Schematic representation of the initial stages of the assembly of the carbon shell – envelope of curved graphene flakes around In clusters (i), serving as a template for extended graphene layers (ii).

A Carbon-shell actuated "Zeptoliter Pipette": The successful assembly of C-shells on semiconductor NWs have inspired in-situ experiments on the controlled delivery of zeptoliter liquid volumes and phase transformations of free-standing nanodroplets. We demonstrated the operation of a pipette, made of a Ge NW encapsulated in a C-shell, which, observed by TEM, delivers a metal alloy melt with zeptoliter (10^{-21} L) resolution. We used the exquisite control to produce nearly free-standing $Au_{72}Ge_{28}$ drops suspended by an atomic-scale meniscus at the pipette tip, and to image their phase transformations with near-atomic resolution, and make breakthrough advances in understanding phase transformations of small objects. Our observations challenge the long-accepted theory of crystallization – classical nucleation theory – by providing experimental evidence for an intrinsic crystallization pathway of nanometer-sized fluid drops that avoids nucleation in the interior, but instead proceeds via liquid-state surface faceting as a precursor to surface-induced crystallization.

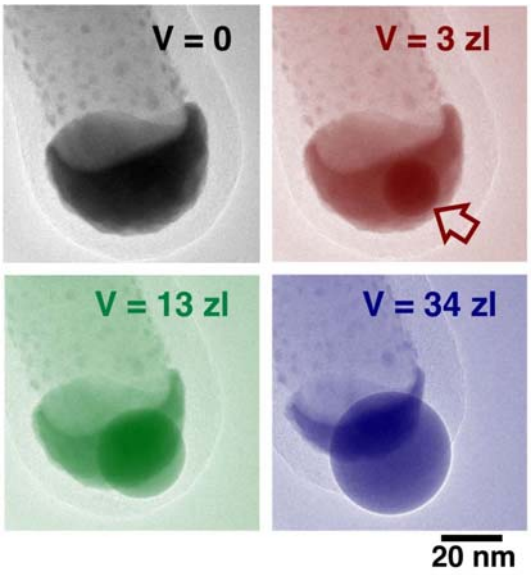

Fig. 2: Operation of the Zeptoliter Pipette in a TEM: Driven by a multilayer carbon shell, pressure is built around a Au-Ge alloy particle at the tip of a Ge nanowire. Following the melting of the Au-Ge alloy, the opening of an atomic-scale channel in the shell triggers the controlled expulsion of a Au-Ge alloy drop with zeptoliter (zl) resolution.

The successful formation of ordered C-shells on different semiconductor NWs is a major achievement and a prerequisite for the investigations of the electronic structure and (photo-) electrical properties of single NWs and core-shell structures. Single NW electrical measurements using a new Nanoprobe system have been initiated and are in progress. In these experiments, electrical contacts are positioned on selected individual NWs to evaluate key photovoltaic properties: electrical conduction, light absorption and photo-resistance in NWs; rectification and carrier separation across the radial heterojunction of core-shell structures.

Precision Assembly of Nano-Objects – Approaching Artificial Photosynthesis

LDRD Project 07-025

William Sherman and Oleg Gang

PURPOSE:

This project aims to develop techniques for positioning and manipulating nano-objects, such as gold nano-particles, in DNA scaffolds with sub-nanometer precision. Numerous earlier experiments developed extensive methods for constructing complex nanoscale structures and mechanical devices out of DNA. However, attempts to attach nanoparticles to these structures have met with only limited success, generally failing to convert the high level of positional control inherent in the DNA structures to the attached guests. We are using novel attachment methods and construction techniques to help overcome these limitations. Nature constructs photosynthetic devices with sub-nanometer precision, but attempts at constructing artificial photosynthetic systems have been hindered by their inability to reach that level of control. The methods we are developing will provide tools for solving that problem, as well as techniques for systematically studying the electrical and optical interactions of nano-objects at various distances and orientations.

APPROACH:

In recent decades, biological research has driven intense exploration of DNA and other nucleic acids. Chemists have learned to routinely synthesize strands of DNA with any desired sequence of bases up to about 150 nucleotides in length. This has opened the possibility of using DNA for non-biological applications. With careful planning of the base sequences, a set of DNA strands that are simply mixed together, heated, and slowly cooled will organize themselves into structures that maximize the amount of classic Watson/Crick base pairing. This simple and well understood interaction has been used to direct strands of DNA to fold themselves into a broad variety of structures: triangles, parallelograms, cubes, tetrahedra, octahedra, knots, etc. and these structures can be organized further into 1-, 2- and 3-dimensional arrays. Techniques have also been developed for selectively removing strands of a given sequence from a construct, which has allowed the development of DNA based mechanical devices that can move rotationally or linearly via depending on their construction. Since a DNA double helix is about 2 nm in diameter, and the distance between stacked bases is about 0.34 nm, DNA has moved to the forefront of techniques for engineering on the nanometer scale.

Interest has naturally focused on leveraging the positional control of DNA to organize other materials with desirable properties (e.g. photo-voltaic materials). Several methods have been used to attach gold nanoparticles to DNA nanostructures. Most attempts have used nanoparticles covered with many strands of DNA docking on scaffolds with multiple binding sites packed close together. In these systems, the nanoparticles can bind in many configurations and form disordered patterns over well-ordered substrates. The primary goal of our experiments has been to overcome this difficulty by building DNA cages with multiple interior binding sites that form redundant connections to exactly one nanoparticle and hold it precisely in a fixed position. This strategy transfers the strengths of structural DNA nanotechnology to the bound nanoparticle: it can be organized into regular arrays, or be decorated with other nano-objects at a variety of different angular orientations. Finally, the nanoparticles can be manipulated via DNA machinery to different spacings and orientations.

TECHNICAL PROGRESS AND RESULTS:

The funding for this project was delayed by several months. Fortunately, once the funding was approved and we were allowed to advertise for a research associate, we found an excellent researcher in Dr. Mudalige, who started work in August.

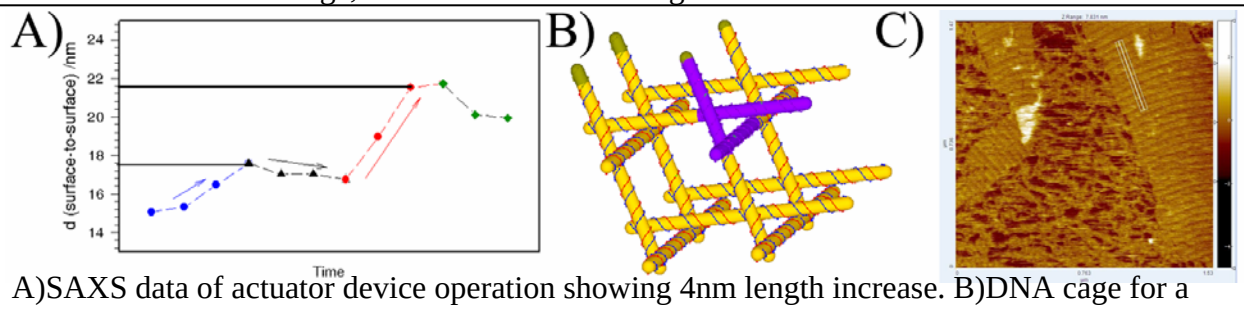

A)SAXS data of actuator device operation showing 4nm length increase. B)DNA cage for a single nanoparticle with one of the 8 component triangles in purple. C)1.5x1.5µm Atomic Force Micrograph Dr. Mudalige took of an array similar to the scaffolds we are planning to build.

The preliminary experiments have focused on constructing an actuator device, capable of changing lengths from 18 nm to 25 nm, and using it to change the spacing between gold nanoparticles. The sequences for the strands were designed, and the strands were synthesized and purified. Polyacrylamide Gel Electrophoresis (PAGE) was used to evaluate the operation of the actuator without nanoparticles attached. It was determined that the system assembled cleanly, without multimer formation, that it remained clean throughout operation, and that the electophoretic migration speed varied with the size of the system as expected. The next experiments involved attaching nanoparticles in solution via the actuator device and observing the distance between nanoparticles via Small Angle X-ray Scattering (SAXS) as the actuator was operated. In this experiment the particles formed an aggregate, with multiple actuators connecting multiple nanoparticles in a disorganized agglomeration. The distance was observed to vary from 21.6 nm to 17.6 nm between configurations (A above), however, the disordered system could confound the proper operation of the actuator, so more careful experiments followed. Individual pairs of nanoparticles joined by DNA actuators were prepared via a novel solid-support assembly technique. The size of the assemblies was then monitored via Dynamic Light Scattering (DLS) while the actuator shifted between its two states. The length of the actuator was observed to change by 2.6 nm in this experiment.

The caged nano-particle project has been at the modeling and design stage. The original plan, involved 7-base triangles with two attachment ports each. That system would have required refrigeration to stabilize, so we adjusted to 14 base triangles (B above). Further, we determined that the system would maximize ordering if the attachment ports are only on one of the four constituent triangles, instead of all of them. Physical modeling and distance calculations were used to find the optimal placements for the ports. With the positions selected, the distance between the three ports that are supposed to bind a given nanoparticle is 10.6 nm. The next nearest binding port is about 11.9 nm away (from one of the three target sites). However, there is a double helix blocking the direct line between these two ports, so the effective length of a DNA binder is a few nanometers longer than the target strands. The base sequences for the DNA segments that connect the subcomponents have been designed, and the computer model of the strand topology has been built to facilitate design of the rest of the base sequences.

Photocatalytic Carbon Dioxide Reduction to Methanol using Metal Complexes with an NADH Model Ligand

LDRD Project 07-027
Etsuko Fujita and James T. Muckerman

PURPOSE:

The aim of this project is to explore CO_2 reduction to methanol employing a new methodology to photochemically produce hydride donors using fuctionalized metal complexes with a reduced nicotinamide adenine dinucleotide (NADH) model ligand. This new bioinspired approach seeks artificial photosynthetic systems for catalytic hydrogenation/reduction of CO_2 beyond CO and $HCOO^-$ (which have been produced as the only products of photoreduction of CO_2 in homogeneous systems). This is high-risk research, but it is a very important area to investigate to secure future energy needs. This research, if successful, would not only produce a valuable chemical fuel from solar energy, it would recycle the carbon dioxide released when it is burned.

APPROACH:

A combination of experimental and theoretical approaches is pursued to investigate the mechanism and kinetics of several promising transition-metal complexes with NADH-model ligands for the photocatalytic reduction of CO_2 to methanol. In particular, rhenium and ruthenium complexes containing the pbn (*i.e.*, 2-(2-pyridyl)-benzo[*b*]-1,5-naphthyridine) ligand offer promise as photocatalysts for the hydride-transfer reactions required to reduce CO_2 beyond CO, all the way to methanol. This approach will create new directions for the solar energy conversion of CO_2 into energy-rich fuels through *low energy paths* using functionalized transition-metal complexes as hydride ion donors. The basic knowledge obtained through this study – *e.g.*, the energetics of coupled proton and electron transfer for redox leveling and proton addition and removal, and catalysis *via* hydride transfer, and bond forming/cleavage – will be essential for designing more effective proton-coupled multi-electron-transfer reactions for fuel production.

TECHNICAL PROGRESS AND RESULTS:

We prepared a polypyridylruthenium complex with an NAD^+/NADH model ligand, $[Ru(bpy)_2(pbn)]^{2+}$ (bpy = 2,2´-bipyridine, pbn = 2-(2-pyridyl)-benzo[*b*]-1,5-naphthyridine), which acts as a catalyst in the electrochemical reduction of acetone to 2-propanol similar to the enzymatic NAD^+/NADH. While the mechanism remains unclear, this is the first example that an NADH model complex such as $[Ru(bpy)_2(pbnHH)]^{2+}$ (or other intermediates in this system) works as a catalytic hydride donor for the formation of 2-propanol. We have recently reported clear evidence of photochemical and radiolytic formation of $[Ru(bpy)_2(pbnHH)]^{2+}$ with H^+. These results open a new door for photocatalytic hydride (or proton-coupled-electron) transfer reactions originating from metal-to-ligand charge-transfer (MLCT) excited states of metal complexes with a bio-inspired NADH-like ligand, and for the utilization of photogenerated hydride donors for CO_2 reduction.

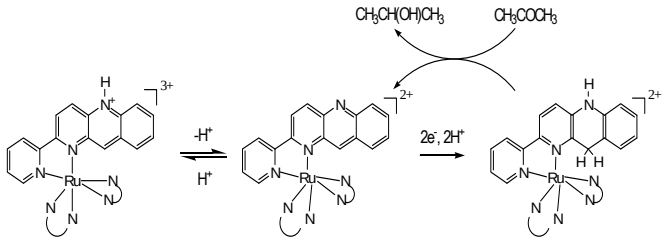

Scheme 1 Protonation and acetone reduction by $[Ru(bpy)_2(pbn)]^{2+}$

Thermodynamic hydricity, the ability to donate a hydride ion (H^-), for metal hydrides and dihydrobenzonicotinamides in acetonitrile has been determined through systematic studies of electrochemistry and acidity by DuBois and his coworkers. Hydricity is defined as the free-energy change for dissociation of H^-, in contrast with acidity and homolytic cleavage. Experimental estimates of hydricity of substrate DH are obtained from cycles based on combinations of the processes from the free-energy changes as $\Delta G^o_{H^-} = \Delta G^o_{H^+}(D–H) - 2\ E^o(D^+/D^-) + \Delta G^o_{H^+}(H_2) + E^o(NHE)$, where $\Delta G^o_{H^-}$, $\Delta G^o_{H^+}(D–H)$, $E^o(D^+/D^-)$, $\Delta G^o_{H^+}(H_2)$, and $E^o(NHE)$ are hydricity of DH, acidity of DH, reduction potential of DH, H_2 acidity, and reduction potential of H^+, respectively. Hydricities obtained in our preliminary calculations in acetonitrile solution are compared to experimental values in Table 1. The computed electronic energy hydricity differs somewhat from the hydricity free energy (comparable to that derived from experimental data) in that it does not include the contribution of zero-point and thermal energy or entropic effects, but these effects are generally small and trends can be compared. The strongest hydride donor, CHO^-, will transfer a hydride to any acceptor listed below it. Several metal complexes seem capable of hydride transfer to CO_2 in acetonitrile: Cp(bpy)Mo(CO)(H) from the metal and Re(bpy)$(CO)_3$(CHO) and Re$(CO)_3$(dcb)(CHO) from the C–H of the formyl ligand.

Table 1. Computed Electronic Energy Hydricities in Acetonitrile (B3LYP/LANL2DZ level of theory)

Hydride Donor	Product	El. Energy Hydricity (kcal/mol)
CHO^-	CO	–61
CH_3CHN^-	CH_3CN	0
isopropoxide$^-$	acetone	24
Cp(bpy)(CO)MoH (+ CH_3CN)	Cp(bpy)(CO)Mo$(NCCH_3)^+$	39[a]
$[Re^I(bpy)(CO)_3(CHO)]^0$	$[Re^I(bpy)(CO)_4]^+$	45
$[Re^I(CO)_3(dcb)(CHO)]^0$	$[Re^I(CO)_4(dcb)]^+$	49[b]
$HCOO^-$	CO_2	51 (43)
N-Me-nicH	N-Me-nic$^+$	60
N-Bz-nicH	N-Bz-nic$^+$	61 (59)
Cp(bpy)(CO)MoH	Cp(bpy)(CO)Mo$^+$	65[a]
para-monohydroquinone$^-$	para-benzoquinone	69
$[CpRe^I(NO)(CO)(CHO)]^0$	$[CpRe^I(NO)(CO)_2]^+$	70 (55)[c]
H_2 (+ CH_3CN)	CH_3CNH^+	80 (76)
$[Ru^{II}(bpy)_2(pbnHH)]^{2+}$	$[Ru^{II}(bpy)_2(pbnH^+)]^{3+}$	92
isopropanol	$CH_3C(OH)CH_3^+$	94
$[Ir^{III}(bpy)_2(pbnHH)]^{3+}$	$[Ir^{III}(bpy)_2(pbnH^+)]^{4+}$	104
para-hydroquinone	para-monohydroquinone$^+$	128

[a] LANL2DZ/6-31G(d,p) 6D basis; [b] dcb=(4,4')-dichloro-(2,2')-bipyridine; [c] Experimental value corresponds to Cp*, not Cp as calculated; N-Me-nicH =N-methylnicotinamide, N-Bz-nicH=N-benzylnicotinamide; calculations compared to DuBois ΔG^o values (in parentheses) are in blue.

The computed electronic energy hydricity differs somewhat from the hydricity free energy (comparable to that derived from experimental data) in that it does not include the contribution of zero-point and thermal energy or entropic effects, but these effects are generally small and trends can be compared. The strongest hydride donor, CHO^-, will transfer a hydride to any acceptor listed below it. Several metal complexes seem capable of hydride transfer to CO_2 in acetonitrile: Cp(bpy)Mo(CO)(H) from the metal and Re(bpy)$(CO)_3$(CHO) and Re$(CO)_3$(dcb)(CHO) from the C–H of the formyl ligand.

Our preliminary calculations predict that the reduction of acetone to 2-propanol can take place in acetonitrile by the sequential transfer of a proton from solution followed by a hydride from $[Ru(bpy)_2(pbnHH)]^{2+}$ in two slightly exoergic steps. The calculations also predict that neither $[Ru(bpy)_2(pbnHH)]^{2+}$ nor $[Ru(bpy)_2(pbn)]^{2+}$ can reduce CO_2. We are therefore exploring the development of a stronger hydride donor than $[Ru(bpy)_2(pbnHH)]^{2+}$ with the guidance of calculations of hydricities to screen the possibilities.

In order to test if this type of scenario will work, we have prepared several new complexes including $[Ru(bpy)_2(pbnHH)]^{2+}$, Re(pbn)$(CO)_3$Cl and $[Re(pbn)(CO)_3(PCy_3)]^+$. We have started examining the acid-base and electrochemical properties of the ground and excited states of Re(pbn)$(CO)_3$Cl and $[Re(pbn)(CO)_3(PCy_3)]^+$.

Structure of Mass-Size Selected Nanoparticles by Scanning Transmission Electron Microscopy

LDRD Project 07-030
Michael G. White

PURPOSE:

The purpose of this project is to demonstrate the feasibility of measuring the atomic structure of small, supported nanoclusters utilizing high-throughput electron diffraction in a scanning electron transmission microscope (STEM). This project addresses the critical need to understand how the atomic structure evolves from small clusters containing tens of atoms to larger particles whose structure mimics the bulk material. Small nanoclusters (1-2 nm) are typically non-crystalline (amorphous) and cannot be imaged with atomic resolution by conventional transmission electron microscopy (TEM) or by scanning tunneling microscopy (STM). Our approach involves the novel coupling of mass-selected deposition, in which every nanocluster has precisely the same size (mass), and single-particle electron diffraction measurements using a STEM instrument. The specific technical challenges involve (1) the development of a vacuum load-lock system that allows transfer of air-sensitive samples between the deposition instrument in Chemistry and the STEM in Biology, and the development of a high-speed, 2D detector and software that enables high throughput, single particle diffraction. If successful, this program would demonstrate a new approach for probing the atomic structure of non-crystalline nanomaterials that could have significant impact on current nanoscience programs at BNL and future instrumentation developments at the Center for Functional Nanomaterials.

APPROACH:

We have recently developed a new instrument for depositing size-selected metal and metal compound (oxide, sulfide) nanoclusters onto solid supports as models for supported heterogeneous catalysts. By independently controlling the size of the particle, its chemical composition and the substrate material, size-selected cluster deposition provides a powerful approach for investigating the electronic structure and reactivity of small nanoparticles [1]. Our ability to understand and model the reactivity of such nanoparticles, however, is severely hampered by the lack of direct structural information, either in the gas-phase or deposited on surfaces. In large part, this is due to inherent limitations in STM (or AFM) for imaging the atomic structure of small (< 2 nm) particles deposited on surfaces. The latest generation of aberration-corrected TEM's is very promising for direct structural imaging, however, coupling of a cluster deposition apparatus and a commercial TEM is impractical. Furthermore, the limited flexibility of the sample mounting and transfer systems in most TEM instruments also precludes the study of air sensitive samples. This is particularly important for the study of reactive nanoparticles of interest for catalytic applications that often have exposed metal atoms on the surface that are readily oxidized.

In this project, we intend to combine the unique capabilities of the size-selected deposition apparatus discussed above with the imaging capabilities of the BNL scanning electron microscope facility (STEM) in collaboration with Joe Wall of the Biology Department. Wall's group has extensive experience with imaging small metallic clusters and has also developed an in vacuo transfer system for loading moisture sensitive samples into the STEM instrument. Our approach is to develop and install a compatible transfer system onto the cluster deposition apparatus in Chemistry so that samples can be moved to the STEM facility under high vacuum.

The samples will then be loaded into the STEM for imaging and structural characterization by single-particle, convergent beam electron beam diffraction (CBED). We intend to take advantage of the fact that every nanoparticle on the surface is identical and develop software to automatically search for nanoparticles and acquire single-particle diffraction images. Acquiring diffraction images for a large number of randomly oriented nanoclusters is key to reconstructing their precise atomic structure.

TECHNICAL PROGRESS AND RESULTS:

To date, we have performed feasibility experiments in which size-selected nanoclusters ($Mo_{46}O_{132}$ clusters) were deposited onto a supported carbon film, transported to Biology in an inert atmosphere and imaged with the STEM. Dark field images and mass measurements showed that the STEM has sufficient contrast and mass sensitivity to identify small nanoclusters that are of interest in this project. We have also designed most of the hardware required to adapt the STEM vacuum transfer system for mounting on the Chemistry deposition apparatus. Machining and acquisition of other vacuum hardware needed for the transfer system is currently underway.

A first generation pixilated silicon detector (32×32), developed at BNL Instrumentation, was recently installed on the STEM1 instrument and is in its beginning stages of testing. This detector replaced the current bright-field and small-angle scattering detectors and will allow CBED patterns to be collected with very high signal to noise and data transfer rates (10^3 spatial elements at 10KHz).

During the next year, we intend to finish assembling the Chemistry vacuum transfer system and perform preliminary STEM imaging experiments on a series of air sensitive metal sulfide and carbide nanoclusters for which we have prior knowledge of the free particle structure. The goal of these experiments is to establish the optimum conditions for deposition, e.g., ion deposition energy, cluster coverage, and to demonstrate the ability to acquire single-particle diffraction patterns. It is expected that these first diffraction experiments will make use of the recently installed multi-element silicon detector (32×32 pixels). New software for manipulating the data and automating the search and acquisition of CBED of individual clusters will also have to developed. In the final stages of the project, we expect to upgrade to the next generation of silicon detectors (512×512) that have significantly higher sensitivity and spatial resolution. In principle, the high rate of data transfer and high signal-to-noise ratio of the new detectors will make it possible to automate the data recording process and characterize roughly 100,000 individual clusters per hour.

Synthesis of Conjugated Polymers for Fundamental Questions in Solar Energy

LDRD Project 07-032
John Miller and Xiao-Qing Yang

PURPOSE:

This project intends to create conjugated molecular materials, "molecular wires" to test whether charges and excitons can migrate efficiently over long distances within such "wires." It is specifically focused on transport within single, long chains as distinguished from transport that requires hopping from one chain to another. If efficient, such transport could be utilized to design new, highly efficient solar cells.

APPROACH:

Polythiophenes are one of the most widely used materials at present for organic photovoltaic cells. Short-term targets were synthesis of polythiophenes having appended groups that could capture either electrons or excitons in the polymers: We hoped to create dual-purpose molecules in which different experiments could probe both questions. The appended groups (traps) would be distributed randomly along the polymer chains with one such trap group for each ~20 repeat units. That number would then be adjusted.

A second goal was to create such molecules with enhanced solubility in non-polar media to facilitate experiments there.

Following synthesis we aim to perform two initial types of experiments, both in fluid solution: a) Electrons would be attached to polymer molecules at the LEAF accelerator while monitoring formation of polymer anions and their disappearance by transient absorption

b) Photoexitation of the polymers would be performed, Transport of excitons to the traps and their capture there would be measured by quenching of fluorescence.

The first targets were synthesis of polythiophenes having radicals attached. These radicals were intended to function as either electron of exciton traps.

TECHNICAL PROGRESS AND RESULTS:

The first target was synthesis, to occur in two steps:

1. Synthesis of monomer groups having long or branched alkyl chains to confer enhance solubility and monomer groups having traps attached.
2. Polymerization of monomers into polymers a) polymers with traps. and b) without traps for use in reference experiments needed to quantitatively evaluate charge capture.

Several molecules were synthesized and characterized by NMR. Abbreviated schemes are shown below for synthesis of monomers and for polymers with dinitrobenzene groups.

Synthesis of thiophene monomers with functional groups.

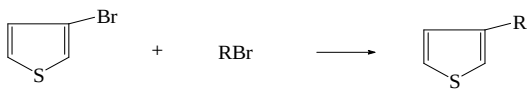

$Ni(dppp)Cl_2$

R = Hexadecyl **(9)**, 2-Butyloctyl **(10)**, 3,7-Dimethyloctyl **(11)**, 3,5,5-Trimethylhexyl **(12)**

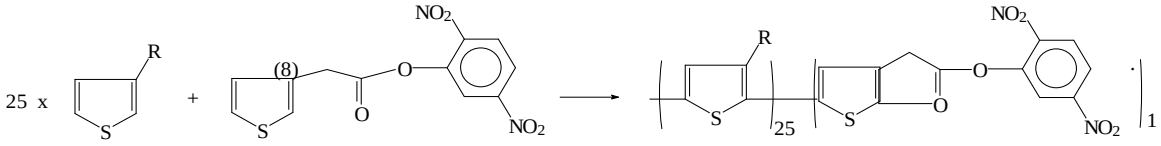

Scheme IV Synthesis of copolymers with dinitro-group
R = 2-Butyloctyl **(16)** R = 3,7-Dimethyloctyl **(17)**

Electrons were attached to native polythiophenes (having no trap groups) and those copolymerized with monomers with appended TEMPO free radicals or dinitrobenzene groups. In both cases the transient spectra obtained were those of polythiophene negative ions ($pT^{-\bullet}$), identical to those found in the native polythiophenes. Furthermore the decay in time of the $pT^{-\bullet}$ spectra was the same for polymers with and without copolymerized traps. Even if charges were immobile on the pT chains, bimolecular reactions of $pT^{-\bullet}$ with the trap groups on other pT molecules would have caused decay if the trap groups were present. Similarly the fluorescence spectra of the TEMPO and dinitrobenzene copolymers were identical to those of the native polymers.

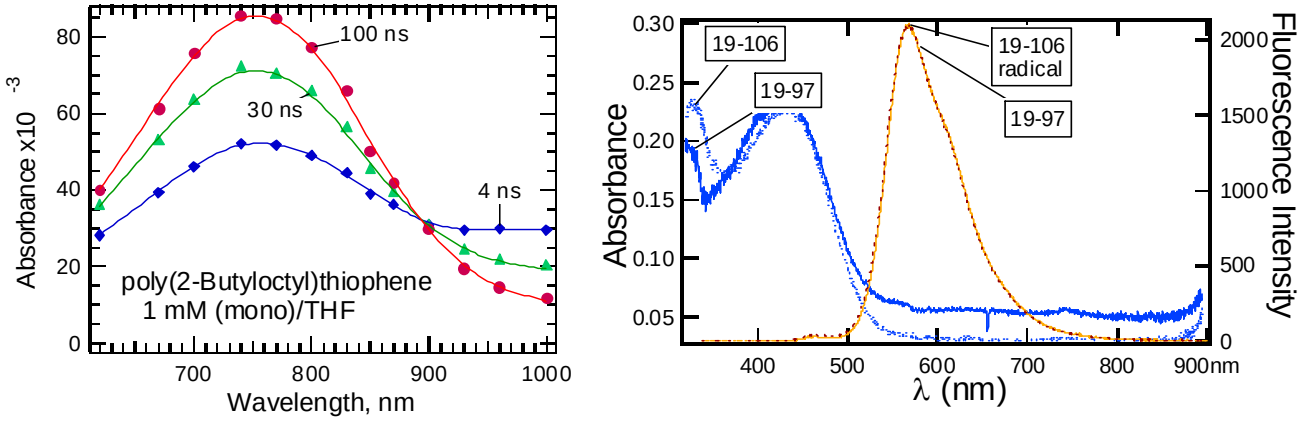

Figure 1 Spectra of poly(2-butyloctyl)thiophenes in tetrahydrofuran (THF) solution: a)(left) transient absorption spectra of the anions; b) Absorption (blue) and fluorescence of the neutral molecules without and with copolymerized TEMPO radicals.

The conclusion is that the trap groups, known to be present in the monomers, were damaged during the polymerization.
A summary of work to date is:

1. Seventeen compounds were synthesized including both monomers and their polymers; nine of these were new polymers.
2. We did not yet succeed at creating polymers containing groups that can act as traps for electrons and excited states.
3. We did create polythiophenes of unprecedented solubility in non-polar fluids.

Production of very highly soluble polythiophenes will enable much faster measurement of charge mobilities when we obtain molecules with active trap groups. New synthetic procedures are being employed to produce those molecules. It is our intent to obtain these and results on them within the next six months. We will evaluate long distance electron and exciton transport and then move to the second novel phase of this project.

Ultra-Thin Graphite Analog Compounds

LDRD Project 07-035
Tonica Valla

PURPOSE:

The purpose is to develop methods of synthesis of ultra-thin graphene layers, to probe their transport and spectral properties and to explore possibilities of modifying those properties. The ultimate goal is to "magnetize" graphene or to induce spin-polarization in the graphene bands, to measure magneto-transport and spectral properties of such magnetized structures and to explore possibilities of making spin-polarized transport devices that could be used in spintronics applications.

APPROACH:

We have spent some time on developing different methods of obtaining graphene layers. Two synthesis methods have shown the best results and have been pursued since Jun/July 2007:

1. high temperature annealing of SiC(0001) in an ultra-high vacuum
2. mechanical exfoliation of HOPG on SiO_2/Si

Spectral and transport properties of both systems have been measured and ways of modifying those will be explored in order to find the optimal system for applications in devices.

TECHNICAL PROGRESS AND RESULTS:

The growth of high-quality 1-4 graphene layers on SiC has been demonstrated at the NSLS and samples were characterized by ARPES and LEED. Unfortunately, the Dirac point in graphene grown on SiC is always ~0.5 eV below the Fermi level, indicating heavy electron doping. The exotic transport properties that stem from the "masslessness" and particle-hole symmetry near the "neutrality point" (E_D~E_F) are lost in such a system. Therefore, the SiC grown graphene does not have the potential to become a basis for (spin)electronics devices.

The "exfoliation" method produces samples that are much closer to the "neutrality point" and any departure can easily be balanced by field doping. Therefore, we have focused on these samples and in a very short time, we have perfected the synthesis to a level at which our samples are larger than those produced by World leading groups in the field (see Fig. 1). We can routinely produce samples ~50×100μm^2, 1-5 layers thick and we have already demonstrated their high quality by using Raman and ARPES studies. The field doping studies in Raman have shown that our single-layer samples (on SiO_2) have the Dirac point intrinsically within 10 meV from the Fermi level. On a thicker sample (~8-9 layers), prepared in air and introduced in the UHV chamber, we have performed ARPES studies, after a slight annealing (~200C) in vacuum. We have demonstrated that such a simple recovery procedure gives extremely sharp dispersing

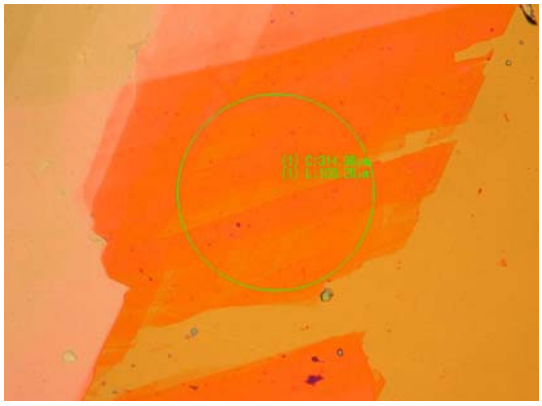

Fig. 1 Large (~200X150μm) flake of four and five-layer graphene on 400 nm thick SiO_2. Circle (ϕ=100μm) represents a typical spot size of the photon beam in an ARPES experiment.

graphene states with the Dirac point exactly at the Fermi level (see Fig. 2). The momentum width of Dirac point was essentially resolution limited.

These two results: 1) the proximity of the Dirac point to the Fermi level ("neutrality point") in real samples on SiO_2/Si and 2) extremely well defined electronic states, in conjunction with the robustness of graphene samples, are extremely important for the successful progress of our second graphene-related project, the Tech Maturation Project, funded on the basis of our successes in this LDRD. These results open the possibility for spin-polarized transport by inducing a spin polarization of graphene states as outlined below.

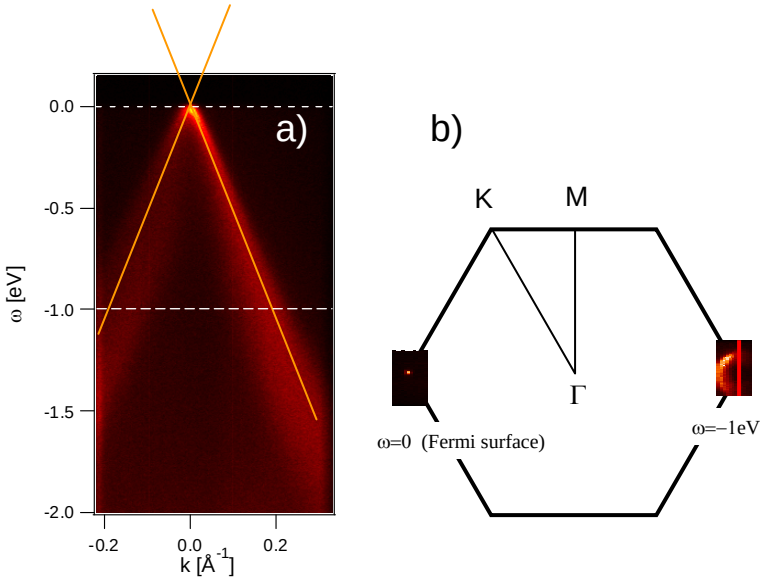

Fig. 2. a) Photoemission spectrum from a thick graphene flake (~8 layers) on SiO2 from the momentum line going through K point of the Brillouin zone as indicated in b) by the orange line. Linear dispersion indicates massless Dirac Fermions that give rise to exotic transport properties of graphene. b) Brillouin zone with the spectral contours at the Fermi energy (left) and at 1 eV bellow the Fermi level (right). Notice that the Fermi surface collapses into a (Dirac) point)

We first intend to reproduce the spin injection from ferromagnetic leads (Co, permalloy, etc) into the graphene layers. Different thicknesses and widths of ferromagnetic leads will control their coercive fields, enabling different configurations of polarizations. We will also explore the possibility of inducing the spin polarization in the graphene bands by "magnetic proximity" – by overlapping the graphene states with spin-polarized states in ferromagnets. Various ferromagnetic metals and insulators will be deposited on graphene layers and transport properties will be measured for different polarizations. In the case of metallic overlayers, transport must not occur through the overlayers (the polarizing metal has to be in the form of isolated clusters), while for oxides it is crucial that the graphene is not damaged in the oxidation process. Ferromagnetic oxides might also act as acceptors and even render the SiC grown graphene applicable.

The easiest and the most promising approach is to exfoliate graphene layers directly on a ferromagnetic insulator (candidates are EuO and GdN with T_C~60K and Co-doped CeO_2 T_C~750K) and measure their magneto-transport and spectral properties.

Absolutely crucial for the success of this LDRD and TM program will be the role of the CFN as the user facility where most of our contact patterning and some transport, structural and spectral studies (nano-lithography, STM, AFM, Kerr, Raman, 4-probe in-situ transport) will be done. We have already established numerous collaborations with different CFN groups and have obtained full support of the CFN director Emilio Mendez.

Lipid-Coated Nanoparticles and Their Interactions with Lipid Membrane Surfaces

LDRD Project 07-036
M. Fukuto, L. Yang, and O. Gang

PURPOSE:

Exploring methods to render inorganic nanoparticles (NPs) both bio-compatible and bio-functional is important for facilitating biomedical and biomimetic-device applications of NPs. One method that is likely to be highly effective and versatile is to coat NPs with lipid bilayer or monolayer membranes. Lipid membranes provide a natural environment for membrane proteins and also have the potential to endow NPs with the ability to adhere to and penetrate into the cells by means of membrane fusion. This project aims to (I) explore methods for coating NPs of various sizes with simple lipid mono- or bilayer membranes, and (II) investigate the interactions of lipid-coated NPs with simple model lipid membrane surfaces.

APPROACH:

There already exist well-developed techniques for depositing lipid layers on *planar* solid substrate-aqueous solution interfaces (e.g., vesicle fusion method). We will apply these to the highly curved surfaces of NPs and examine the effect of surface curvature on the ease and uniformity of lipid-layer coatings. NPs to be used are gold NPs (5-15 nm dia.) and commercially available silica spheres (dia. > 40 nm). Preparation and surface modification of gold NPs will be carried out in collaboration with Mat Maye, a Goldhaber fellow in CFN.

Part II of our study will elucidate the interactions between the lipid-coated NPs (LCNPs) and other lipid membrane surfaces, which include: (A) a single lipid bilayer or monolayer at planar substrate-buffer or buffer-vapor interfaces, (B) unilamellar lipid vesicles, and (C) neighboring LCNPs. Lipid mixtures will be used to explore and tune the interactions that are based on, e.g., protein-mediated binding and electrostatic forces. Establishing expertise with these membrane surfaces is also an important aspect of this project. These systems will be characterized by various structural probes based on imaging (fluorescence microscopy, AFM, and electron microscopy) and scattering (synchrotron x-rays and neutrons). Flat membranes (A) are well suited for initial studies because of their simple geometry and because we have the infrastructure for appropriate in-situ characterization tools (optical microscopy, AFM, synchrotron x-rays).

TECHNICAL PROGRESS AND RESULTS:

Our efforts in FY07 were focused on gaining experience with lipid membranes that consisted of binary mixtures of a neutral lipid and another lipid possessing a special property, e.g., a protein-binding ligand or a charged head group. Two summer students contributed to the following progress.

Using Brewster-angle microscopy (BAM) and grazing-incidence x-ray diffraction (GID), we studied the effects of biotin density within a lipid monolayer on the lipid-assisted 2D crystallization of soluble proteins streptavidin (SA) at the aqueous buffer-vapor interface. Biotin is a ligand that binds to SA. The surface density of biotin was adjusted through the composition in binary lipid mixtures of DMPC (neutral) and DPPE-x-biotin, while keeping the area per lipid fixed and using a buffer that promoted 2D crystallization. Both BAM and GID results (Fig. 1) indicate that 2D crystallization of SA occurs only if the surface density of biotin is comparable to or higher than twice that of the protein density in the 2D crystal, such that each SA is bound to 2 biotin lipids. This new result highlights the importance of well-defined protein orientations to 2D crystallization. It also provides insights to how the biotin-SA binding may be utilized to control the LCNP-lipid membrane interactions in Part II-A.

As another candidate for lipid membranes, binary lipid monolayers of dipolar DMPC and positively charged DMTAP on water surface were studied in order to gain insights on how the internal properties of membranes would be influenced by surface charge density. It has been known that at room temperature, the monolayers of both pure DMPC and pure DMTAP remain liquid-like at all surface pressures below the collapse pressure. However, our isotherm and BAM measurements (Fig. 2) indicate that a film consisting of a mixture of the two undergoes a first-order transition from 2D liquid to 2D solid-like phase upon lateral compression. The significance of this observation is that it provides evidence that mixing lipids with dipolar and charged head groups causes the lipid chains to pack tighter and, for this particular mixture, makes a solid-like phase more stable at high surface pressures.

We have hired a postdoctoral associate, Sumit Kewalramani, who arrived in October 2007 who will help initiate efforts to coat NPs with lipid membranes. The milestones that we aim to achieve in FY08 are: (1) to establish a method to reliably produce at least one type of LCNPs; and (2) to carry out AFM and x-ray scattering measurements to probe the adsorption of these LCNPs onto a lipid membrane at substrate-buffer or buffer-vapor interfaces.

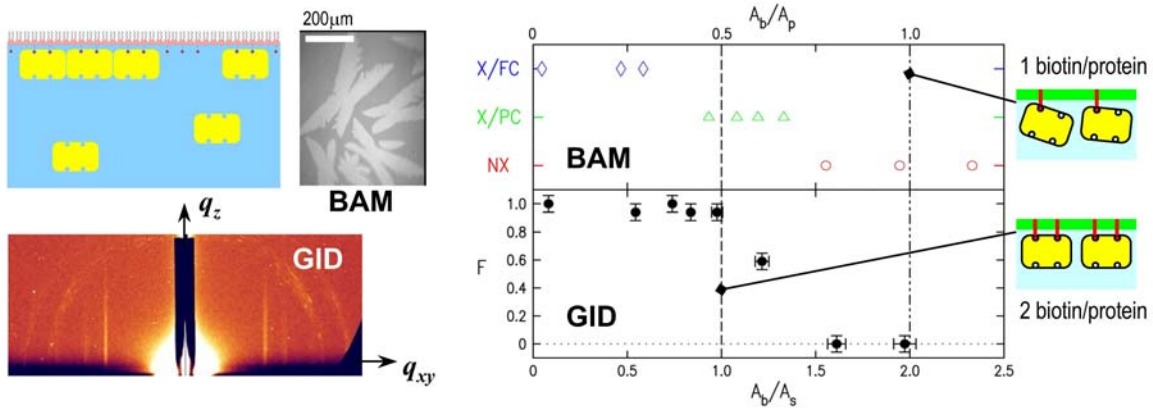

Fig. 1. (Left) Illustration of streptavidin (SA) bound to a biotin-labeled lipid monolayer of binary DMPC/DPPE-x-biotin mixture on water; an BAM image of growing 2D SA crystal domains; a GID pattern from 2D crystals of SA. (Right) A_b = area/biotin; A_p (A_s) = area per protein (per upward binding site) in 2D SA crystal, where $A_p = 2A_s$ = 3220 Å^2; from BAM (top), X/FC = full surface coverage by 2D SA crystals, X/PC = partial coverage, NX = no crystallization observed; from GID (bottom), F = fraction of illuminated spots showing 2D crystal peaks.

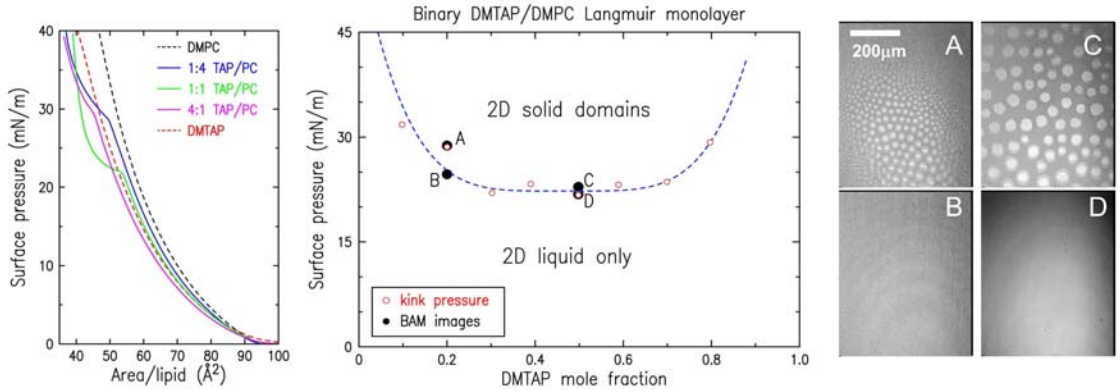

Fig. 2. (Left) Isotherms from Langmuir monolayers of binary lipid mixtures of DMPC (neutral/dipolar head) and DMTAP (positively charged head) on water at 23 °C. (Middle) Binary phase diagram showing observed kink pressures vs. DMTAP mole fraction. (Right) BAM images taken at points A-D in the phase diagram.

Angle-Resolved Time-of-Flight Ion Scattering Spectroscopy from MBE-Grown Oxide Thin Film Surfaces

LDRD Project 07-038
Adrian Gozar

PURPOSE:

We investigate the possibility to determine surface properties (composition, crystallography and electronic structure) of atomically smooth films of superconducting oxides by means of low energy ion scattering and recoil spectroscopy. The problem of surface structure determination is generally valuable for epitaxy, atomic layer engineering, catalysis, electronics etc. and many other surface science related topics of interest to BNL. More specifically, our study could answer important questions for the high temperature superconducting (HTS) films: what is the structure of the topmost layers in HTS films? Knowledge of structure is essential for the determination of electronic band properties which in turn is the most basic starting point for any model that attempt to explain their properties.

APPROACH:

We use the state-of-the art atomic-layer-by-layer molecular beam epitaxy (ALL-MBE) system to synthesize atomically smooth HTS films, multilayers, and superlattices. A time-of-flight ion scattering and recoil spectroscopy (TOF-ISARS) setup enables us to shoot alkali ions (Na^+ or K^+) in the 5-15 kV energy range on the oxide target. Detection is realized by micro-channel plates and by a mass spectroscopy of recoil ions (MSRI) detector. The cross section is monitored for several orientations of the scattering plane with respect to the film surface.

Surface composition can be studied using a classical theory of successive binary collisions. Crystallography is realized by monitoring the magnitude of the scattering cross section as a function of angular scattering geometry. Solving the crystal structure implies the development of a computer code. The approach we use is a technique that treats scattering as a succession of elastic binary collisions. The computational question is whether the experiment can fully constrain the problem, i.e. is there a one-to-one correspondence between 3D angular scans and a certain surface termination?

TECHNICAL PROGRESS AND RESULTS:

- Composition (Fig.1): We found that for HTS the TOF-ISARS technique is sensitive to about 3-5 % of the surface covering. We systematically studied $La_{2-x}Sr_xCuO_{4+\delta}$ films by in-situ TOF-ISARS as a function of rare earth / transition metal atom coverage for various substrate materials. Data was corroborated with results of other in-situ layer deposition tools (quartz crystal monitor data and grazing angle electron diffraction).
- Angular dependence (Fig.2): We showed that for the case of atomically smooth $BaBiO_3$ films angular scans allows for clear identification of surface termination. Our data so far also proved that anisotropic surface neutralization effects are not crucially important and consequently the high resolution MSRI detector can be used for quantitative surface determination.
- Software (Fig.3): Preliminary code in Mathematica was written for simulating two and three body atomic collisions. The data is consistent with previous results in literature but, compared to previous studies, to what degree one can better eliminate the approximations of the theory is still to be determined.

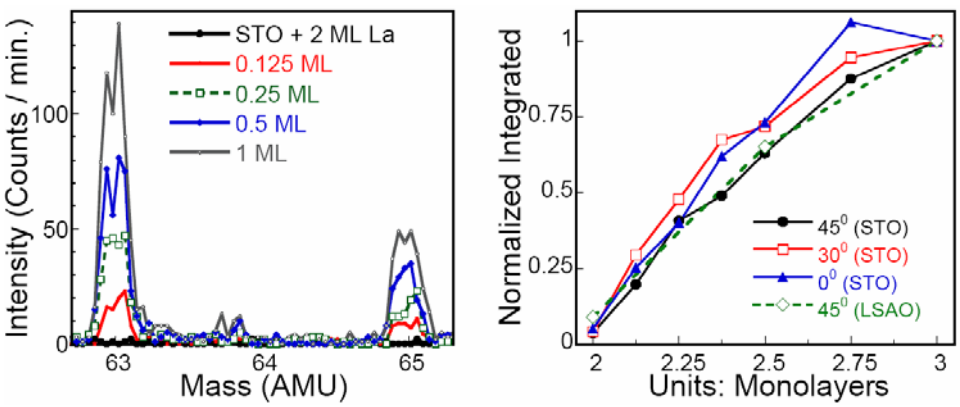

Fig.1: Evolution of the Cu MSRI peaks for 1/8, 1/4, 1/2 and 1 monolayer coverage during the growth of a La_2CuO_4 film on $SrTiO_3$ for several azimuths Φ. Data on the left is for Φ = 45°.

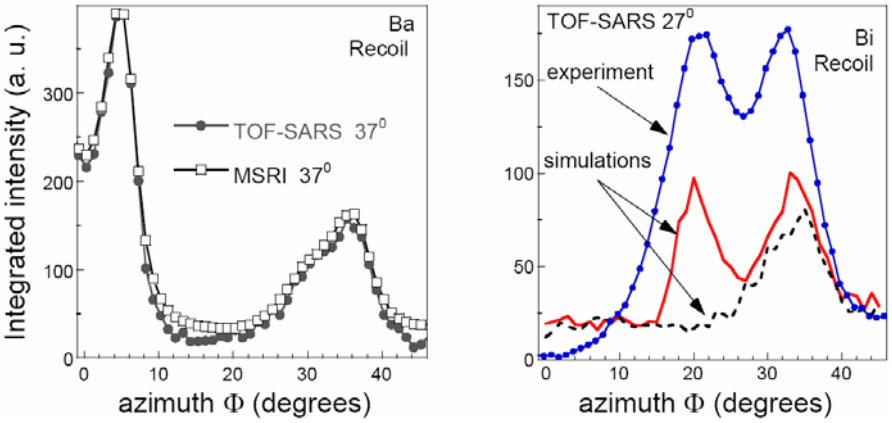

Fig.2: Right: azimuth (Φ) dependence of the intensity of the Ba recoil peak using MSRI and DRS spectra. Left: Φ dependence of the Bi recoil peak along with commercial SARIC code simulations assuming BiO (solid line) and BaO (dashed line) film terminations respectively.

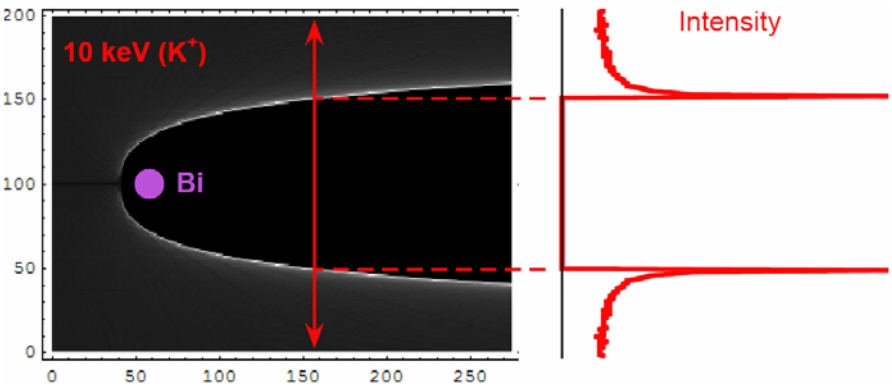

Fig.3: Simulations of the shadow cone generated by a uniform beam of K+ beam accelerated at 10 keV scattering from a single Bi atom. A cross section of the intensity profile behind the target atom is shown on the right.

Genome Analysis of Endophytic Bacteria that Promote Growth of Poplar for Biomass Production

LDRD Project 07-040
Safiyh Taghavi and Daniel van der Lelie

PURPOSE:
Along with crop residues, hybrid poplars are considered the front-runners as candidates for feedstocks for bioenergy production. We identified several endophytic bacteria that significantly increase the primary biomass production of their poplar host. The objective of this proposal is to identify functions used by endophytic bacteria to enter and stimulate the biomass production of poplar. This research should form the basis for a systems biology approach to study, model and engineer the interactions between endophytic bacteria and poplar in order to obtain increased and sustained biomass production of poplar on marginal soils.

APPROACH:
Poplar is considered as the model tree species for plant biomass production and carbon sequestration, two major missions of DOE. Plants, however, live in close association with symbiotic microorganisms which form complex microbial communities that are comprised of many cultivable and non-cultivable microorganisms including mycorrhizal fungi, rhizosphere and phyllosphere bacteria, and endophytic bacteria which live within the transport system and within the plant intercellular spaces. All actively affect overall plant growth and health.

Endophytic bacteria have several mechanisms by which they can promote plant growth and health. The most important mechanism is the production of phytohormones or enzymes involved in growth regulator metabolism. In addition, endophytic bacteria can assist plant growth via the fixation of nitrogen (diazotrophy). We recently showed that endophytic bacteria isolated from poplar are able to stimulate the growth of their host plant. However, nothing is known about the precise mechanism via which these plant growth stimulating compounds are produced, and how their synthesis is regulated. It is also unknown how endophytic bacteria select and enter their host plant.

To identify functions used by endophytic bacteria to enter and stimulate the biomass production of poplar, we propose, in collaboration with the Joint Genome Institute, to sequence the genomes of four endophytic bacteria, to perform data mining in order to identify endophytic functions involved in plant colonization and stimulation of plant growth, and to use directed mutagenesis for confirmation of gene functions. This directed engineering approach will form the basis of a research program to increase the potential and application of endophytic bacteria for improved biomass production.

TECHNICAL PROGRESS AND RESULTS:
Screening for metabolic functions: In order to better understand their plant growth promoting properties, we screened selected endophytic bacteria for properties related to phytohormone production and metabolization of plant growth regulating compounds, as well as the utilization of different carbon sources, including plant biomass derived sugars and plant metabolites. These compounds included: indole-3-acetic acid (IAA) production from tryptophane, metabolization of phenyl acetic acid (PAA), metabolization of 1-aminocyclopropane-1-carboxylic acid (ACC)

produced by plants as a precursor of stress ethylene, and metabolization of 4-amino-butyrate (4-AB). The non-endophytic *Burkholderia vietnamiensis* Bu61 was included for comparison with *Burkholderia cepacia* Bu72. None of the bacteria tested was able to grow autotrophically or able to fix nitrogen. The *Burkholderia* strains and *Serratia proteamaculans* 568 showed ACC-deaminase activity and were able to grow on ACC as sole nitrogen source. The *Burkholderia* strains as well as *Pseudomonas putida* W619 were also able to metabolize PAA and 4-AB. All strains IAA, with the highest levels observed for *P. putida* W619 and *Methylobacterium populi* BJ001. Some interesting differences were observed when comparing the *Burkholderia* strains: in contrast to the environmental strain *B. vietnamiensis* Bu61, *B. cepacia* Bu72 was able to utilize arbutin, salicin, pectin, trehalose and cellobiose, compounds typically found in poplar and willow. Also the other endophytic strains tested were well adapted to utilize plant derived compounds as carbon sources.

Preliminary analysis of the genome sequences of endophytic bacteria for plant growth promoting functions: Genome sequencing of *Enterobacter* sp. 638, *Stenotrophomonas maltophilia* R551-3, *P. putida* W619 and *S. proteamaculans* 568 was initiated. Draft genome sequences were exploited with emphasis on the properties related to phytohormone production and metabolization of plant growth regulating compounds.

In *Enterobacter* sp. 638, a copy of a putative ACC deaminase gene related to the D-cysteine desulfhydrase family was found. A similar gene was identified in *P. putida* W619 despite the fact that both strains were unable to use ACC. This observation suggests a primary role for these genes in sulfur metabolism rather than ACC deaminase activity. Consistent with growth on ACC, *S. proteamaculans* 568 and *B. vietnamiensis* Bu61 contained putative ACC deaminase genes while this gene was absent in *S. maltophilia* R551-3.

All strains, with the exception of *Enterobacter* sp. 638, possessed a copy of a Gamma-amino-butyrate permease or a closely related aromatic amino acid transport protein. This corresponds to the observed growth for these strains on 4-amino-butyrate. *S. proteamaculans* 568, *P. putida* W619 and *B. vietnamiensis* Bu61 were also able to grow on phenyl acetic acid, and this is consistent with the presence of a *paa* operon on their genomes.

IAA production was the most pronounced for *P. putida* W619. IAA synthesis from tryptophan requires two enzymes, a tryptophan 2-monooxygenase (IaaM) that oxidizes tryptophan to indole-3-acetamide, and an indoleacetamide hydrolase (IaaH) that produces IAA. Genome analysis revealed that although a putative indoleacetamide hydrolase gene was present in all strains, the putative tryptophan 2-monooxygenase could only be found in *P. putida* W619 and *B. vietnamiensis* Bu61. In addition, *P. putida* W619 lacks the tryptophan 2,3-dioxygenase, thus driving the conversion of tryptophan to IAA synthesis.

The complexity of the phyto hormone balance points towards the existence of a complex mechanism that fine-tunes the interaction between endophytes and their poplar host.

Structural Features of the Oxygen Tolerant Hydrogenase from *Thermatoga Neapolitana*

LDRD Project 07-041
Daniel van der Lelie

PURPOSE:
Sensitivity to O_2, the narrow scope of acceptable electron donor molecules, and the moderate range of temperature and pressure under which most hydrogenases are known to function, limit the practical applications of hydrogenases either for heterologous H_2 production systems or for their integration in hybrid devices intended for H_2 production. Our objective is to characterize the [FeFe]-hydrogenases present in *Thermatoga neapolitana*. It is expected that knowledge gained from this research will support development of new concepts and strategies for the protection of hydrogenases against inactivation by O_2. The results from this proposal will be used to further develop a research program at BNL that aims at characterizing, modeling and engineering of [FeFe]-hydrogenases from hyperthermophilic, H_2 producing organisms.

APPROACH:
Hydrogenases from thermophylic bacteria belonging to the order *Thermatogales* have unique features that might help expand the range for how these organisms or catalysts can be exploited for H_2 production. In addition, our preliminary data shows that certain members of this order have evolved unique mechanisms that allow them to grow and produce H_2 under conditions where O_2 is present. We will develop and apply methods for the purification of recombinant [FeFe]-hydrogenases for biochemical, biophysical and structural characterization. This should allow future use of protein engineering tools combined with heterologous protein expression in *Escherichia coli* to functionally characterize the [FeFe]-hydrogenases from *T. neapolitana* and the novel functions that protect these [FeFe]-hydrogenases from O_2. This work will provide the necessary tools for future investigations that will seek a more basic understanding of: (i) the structure-function of the *T. neapolitana* [FeFe]-hydrogenases with respect to their interactions with cellular electron-donors and the roles of the accessory subunits HydB and HydC; (ii) how the catalytic domain HydA1 alone or in a complex accomplishes electron-transfer with NAD^+/NADH as acceptor-donor during H_2 activation; (iii) the properties of the novel [FeFe]-hydrogenase HydA2 in *T. neapolitana* and; (iv) the mechanism responsible for O_2 protection of [FeFe]-hydrogenases in *T. neapolitana*.

TECHNICAL PROGRESS AND RESULTS:
Heterologous expression of the *T. neapolitana* [FeFe]-hydrogenase HydA1 catalytic subunit: A prerequisite for the structural characterization of the *T. neapolitana* [FeFe]-hydrogenase is that sufficient functional enzyme can be produced and purified. At this moment, an efficient genetic system does not exist for thermophylic bacteria from the order *Thermatogales*. We successfully expressed, albeit at low levels, a functional *T. neapolitana* [FeFe]-hydrogenase HydA1 subunit, which catalyzes H_2 production and whose activity was measured by a H_2 production assay, in a recombinant *E. coli* system that co-expresses the *hyd*EFG genes from the mesophyle *Clostridium acetobutylicum*. The *hyd*EFG genes encode for maturation proteins necessary to obtain expression of functional [FeFe]-hydrogenase HydA subunits, and are found in all organisms (prokaryotes and eukaryotes) possessing [FeFe]-hydrogenases. It is suggested that the hydrogenase accessory proteins synthesize an H-cluster

precursor that can be quickly transferred to the hydrogenase enzyme to effect activation. HydA activity is observed to be dependent on the protein fraction containing all three accessory proteins expressed in concert and cannot be accomplished with addition of heat-treated extract or extract filtrate, suggesting that the activation of the hydrogenase structural protein is mediated by interaction with the accessory assembly protein(s). Our results support the possibility for a directed mutagenesis and phenotypical analysis strategy of the *T. neapolitana* [FeFe]-hydrogenase.

Genetics of the *Thermatoga* [FeFe]-hydrogenases: The *T. neapolitana* DSM5068 and *T. maritima* MSB8 genomes have been sequenced at The Institute for Genomic Research. We performed a first comparison between these genome sequences and found that both species have two similar but not identical [FeFe]-hydrogenases that consist of three different subunits (HydABC). Sequence analysis of the genes indicated that:

- The HydA1BC [FeFe]-hydrogenase complex of *T. neapolitana* (TnHydA1BC) is homologous to the *T. maritima* HydA1BC complex (TmHydA1BC). TmHydA1BC has six [4Fe-4S] clusters, two [2Fe-2S] clusters, and a Flavo Mono Nucleotide (FMN) cofactor for interaction with the preferred electron carrier NAD^+/NADH. Based on free-energy calculations, the reaction coupling NADH oxidation to proton reduction and H_2 evolution is disfavored, therefore a kinetic parameter of the electron-transfer mechanism might be expected to dominate. The FMN moiety of HydB is necessary for electron-transfer to occur between TmHydA1BC and NADH, providing a structural clue to how electron-transfer kinetics might have evolved to overcome the unfavorable thermodynamics. Developing an understanding of the kinetic and thermodynamic parameters of electron-transfer in the multisubunit TnHyd1ABC [FeFe]-hydrogenase complex will support research efforts to enhance H_2 production metabolism in model systems.
- The catalytic Fe-S cluster resides within the alpha-subunit, which is equivalent to the single subunit that constitutes most mesophilic [FeFe]-hydrogenases. However, the most striking difference between the alpha-subunits of the thermophiles compared to their mesophilic counterparts is that they contain an extension at their C-terminus in which a putative [2Fe-2S] cluster is located. The role of this second [2Fe-2S] cluster is unclear. This unique feature of the thermophilic [FeFe]-hydrogenases and the observed differences in amino acid composition surrounding the [2Fe-2S] clusters in *T. neapolitana* DSM5068 and *T. maritima* MSB8 merits further research, as it might contain the key to the observed differences in O_2 tolerance of the H_2 production of both species.
- *T. neapolitana* DSM5068 and *T. maritima* MSB8 contain a second *hydA*-like gene *hydA*2. In the *T. neapolitana* genome, *hydA*2 is not associated with homologues to *hydBC.* HydA2 has not yet been purified or characterized, and it is unclear whether it forms a multi-subunit complex similar to TnHydA1BC and TmHydA1BC.

Characterization of *E*nzymatic *O*-acylation to Facilitate Biomass and Bioenergy Production

LDRD Project 07-047
Chang-Jun Liu

PURPOSE:

Acyl-CoA dependent enzymatic *O*-acylation is one of biochemical reactions involved in post modification of plant cell-wall lignocelluloses and in the biosynthesis of a variety of wood-forming required secondary metabolites in tree species. *O*-acylation of cell-wall polysaccharides prevents the enzymatic break down of biopolymers, thus negatively affecting bio-degradability of plant lignocellulosic feedstock, and reducing efficiency of bioconversion of plant biomass to ethanol. The addition of acyl groups on non-structural secondary metabolites alters chemical stability and solubility, and influences their subsequent sequestration and storage. Despite the wide occurrence of *O*-acylation in plant metabolism, biochemistry of this process remains largely elusive. The specific enzymes involved in lignocellulosic biogenesis and modifications need to be characterized.

The goal of this project aims at genome-wide identification of plant acyl-CoA dependent acyltransferases and characterization of the specific enzymes that are involved in cell-wall lignocellulosic acylesterification and that are responsible for the formation and modification of wood-forming metabolites. Systemically characterization of acyl-CoA dependent acyltransferases will provide available molecular tools for further exploring the biochemical mechanism and biological function of lignocellulosic acylesterification. Therefore, studies in this project implicate significant biotechnological applications in genetic modification of the physical and structural features of cell wall lignocelluloses thus to facilitate industrial bio-degradation of wood materials for biofuel production. This project will contribute to BNL and DOE's mission in energy security by improving biomass quality and promoting biomass production.

APPROACH:

Several bacterial polysaccharide acyltransferase genes were characterized but all share no homologous to the genes from plant origins. A few families of putative plant acyl-CoA dependent acyltransfer genes existed in plant genomes, but so far no specific gene encoded enzyme was functionally characterized for plant cell wall lignocellulosic modification. We proposed to combine an integrated biochemical genomics approach by analyzing model plants *Arabidopsis* and poplar genome sequences to identify all the putative acyltransferase genes in the genomes; followed by bioinformatics and transcriptional profiling analysis and *in vitro* enzymatic assay to systemically characterize the genes involved in cell wall biogenesis and modification. As a complimentary approach, the corresponding *Arabidopsis* T-DNA insertion mutant lines will be analyzed to monitor the composition changes of plant cell wall and to dissect the corresponding genes' biological functions.

TECHNICAL PROGRESS AND RESULTS:

To identify cell wall *O*-acylation responsible genes and enzymes, we took the advantage of genomics and functional genomics projects of poplar and *Arabidopsis* and based upon the highly conserved sequence motifs of plant acyltransferase superfamily members and conducted comprehensive sequence blat searching and data mining analysis. A large number of poplar and

Arabidopsis acyl-CoA dependent BHAD superfamily enzymes were isolated from both genomes. In addition, three other families of putative acyltransferase genes that are weakly similar to bacterial polysaccharide acyltransferase genes were also identified from *Arabidopsis* by low stringency blast search with bacterial polysaccharide acyltransferase sequences. Subsequently, each encoded putative polypeptides of the identified gene models were subjected to sequence alignment and computation analysis to predict their potential function and the potential transmembrane helices, protein sorting signal, and the subcellular localization site in cells by using web-based bioinformatics programs. "*in silico*" digital northern analyses were carried out based on the publicly available poplar Expression Sequence Tag databases (populusDB, http://www.populus.db.umu.se/), and the abundant cell wall biogenesis microarray datasets (UPSCBASE, https://www.upscbase.db.umu.se/); and the publicly available microarray datasets for *Arabidopsis*. To further dissect gene expression profiling, solid reverse transcription polymerase chain reaction was conducted for all of the identified putative poplar genes by using RNAs prepared from poplar leaf, root, developing stem, apical bud, cortex of bark, phloem, developing wood (2 months) and lignified wood (>1 year). This led to the recognition of a number of acyl-CoA dependent *O*-acyltransferase genes that are preferentially expressed in secondary cell wall biogenic tissues (stem, hypocotyls, and xylem). In order to systemically characterize encoded enzyme functions, a rapid biochemical procedure was developed, and about 50 protein expression vectors were constructed and a large number of recombinant proteins were produced. The functional characterization is ongoing.

In addition, more than 60 *Arabidopsis* T-DNA insertion mutants were identified and the homozygous lines are being screened and the analytical procedure for chemical analysis of mutant cell composition were established and validated.

Functional Neurochemistry

LDRD Project 07-048

Dardo G. Tomasi

PURPOSE:

Functional magnetic resonance imaging (fMRI), the method of choice for mapping brain function, is sensitive to unwanted contributions from large blood vessels, is not quantitative, and does not provide neuronal markers to study the dynamics of metabolic events during neuronal activation. Quantitative proton magnetic resonance spectroscopy (1H-MRS), on the other hand, can accurately determine metabolite concentrations and provides important information for the study of brain metabolism, which could validate fMRI measures and help understanding brain function at the chemistry level. Thus, we aim to develop functional 1H-MRS (1H-fMRS) to measure metabolites changes during brain activation, a technique that could be a powerful tool to study synaptogenesis, neurogenesis, or processes involving structural changes in the brain.

APPROACH:

Brief, as well as, prolonged blocked visual stimulation will be used to induce measurable changes of metabolite concentrations in primary visual cortices, while fMRI and fMRS will be acquired in an interleaved fashion. Novel RF surface coils will be developed for improved MRS acquisition. Accurate spectral analysis, with increased sensitivity, will be developed for the detection of metabolic activation changes that cannot be determined in conventional fMRS approaches.

TECHNICAL PROGRESS AND RESULTS:

We have developed novel RF coil prototypes, new methods for data acquisition and analyses, and stimulation paradigms, and were able to get encouraging preliminary data as detailed below:

<u>RF coil development</u>: We developed a novel slot-and-hole surface coil operating at 170.2 MHz, the resonance frequency of protons at 4-Tesla magnetic field. Images acquired with this probe have higher SNR ratio and better uniformity than standard surface coils what makes this RF coil design a good candidate for different MRI and MRS applications (Fig 1).

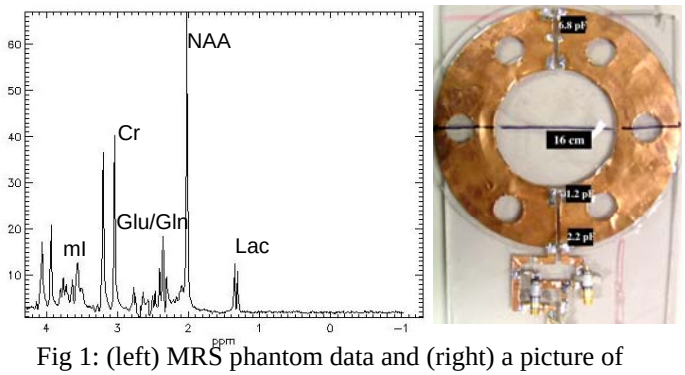

Fig 1: (left) MRS phantom data and (right) a picture of the coil and its passive tuning circuit.

<u>Data acquisition:</u> We adapted a single, voxel double, spin-echo sequence (PRESS) with short echo time (TE/TR = 30/2000 ms) to collect time series of water-suppressed spectra. Figure 2 demonstrates that this technique provides quantifiable concentrations, with good temporal stability, for the major brain metabolites (total acquisition time = 40 minutes).

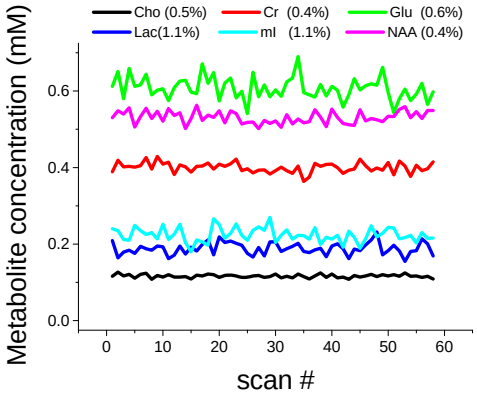

Fig 2: Temporal stability of the MRS phantom measures. Numbers in labels are concentrations errors

Automatic LC data analysis method: We implemented an automatic metabolite quantification approach using a spectra database of brain metabolites at 4-Tesla magnetic field, the commercial LC software package, and the Matlab software that allows us to determine time-varying metabolite concentrations from MRS time series (Fig 2).

Stimulation paradigms: We developed flickering checkerboard paradigms for brief and prolonged visual stimulation using the Matlab, Visual Basic, and Visual C languages. Stimuli are presented to the subjects on MRI-compatible LCD goggles connected to a personal computer. A trigger signal from MRI console precisely synchronizes the stimuli with the fMRI/fMRS acquisition, allowing the use of time-locked 1H-MRS techniques. Specifically, the brief (3 minutes) stimulation paradigm has a 30-seconds flickering (5-Hz) checkerboard vs. 30-seconds baseline (black screen) blocked design. This paradigm robustly stimulates the occipital cortices during fMRI (Fig 3). The prolonged visual stimulation uses a similar flickering checkerboard (12-minutes long; Fig 3, gray) that starts after 5 minutes of resting baseline. An additional 15 minutes long resting baseline follows the stimulation block.

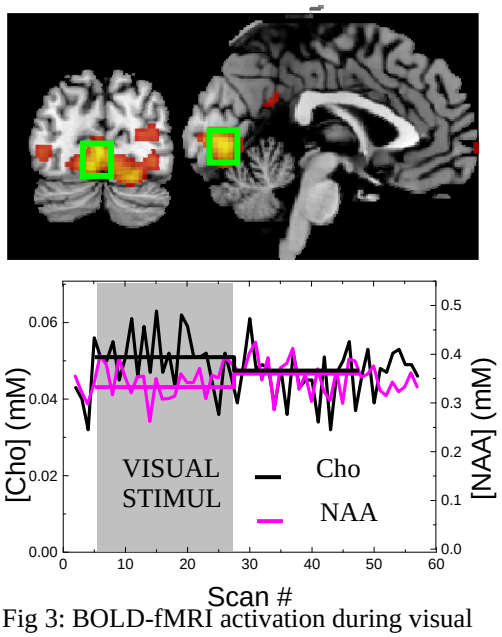

Fig 3: BOLD-fMRI activation during visual stimulation and associated MRS-time courses

Preliminary studies in humans: Six healthy volunteers were evaluated with our fMRI and fMRS techniques. The fMRI scan was done first and the corresponding activation pattern (Fig 3, top panel) was used to identify brain regions in the occipital cortex that were stimulated by the 5-Hz flickering checkerboard paradigm. This information was used for planning individual locations and sizes of the MRS voxels (green square in Fig 3, top panel). MRS spectra were acquired every 2 seconds using a short TE (30 ms) and averaged in groups of 16 to increase SNR. Thus, time series with 57 spectra resulted from each of the 29 minutes long fMRS acquisitions. The time-varying MRS data was fitted to our spectra database using our automatic LC model approach. The preliminary data indicates that visual stimulation increases choline [Cho], GABA, glutamine [Gln], and lactate [Lac], and decreases N-acetyl-aspartate [NAA] and glutamate [Glu] in activated areas of the occipital cortex. Fig 3 (bottom panel) shows an example of these changes. These preliminary observations support previous findings on Lac increases, probably reflecting excess of glycolysis over respiration in the visual cortex during visual stimulation. Our data additionally suggests that brain activation is associated to changes in more than a single brain metabolite. However, these results need to be carefully interpreted because concomitant time-varying changes in local magnetic susceptibility during activation produced by blood oxygenation level dependent (BOLD) effects can alter the resonance frequency and line width of MRS peaks as well as the baseline and phase of the spectra. These preliminary results also suggest that studying the coupling of fMRI and fMRS can help understanding the complex interrelations between metabolic and hemodynamic events in the stimulated brain, and that our ability to explore the dynamics of metabolic brain responses during visual stimulation could complement the power of fMRI to study brain function.

Miniaturized RF Coil Arrays for MicroMRI

LDRD Project 07-054
S. David Smith

PURPOSE:

Our project's goal is the development of novel, high performance radio frequency (RF) coil arrays for improved imaging on the Medical Department's 9.4 Tesla (400 mhz) micro MRI system. We will design and build several coil arrays, specifically for use in the 'parallel imaging' mode. The greatest challenge in designing array coils for high field small animal MRI systems, is in the fabrication of the ***highly miniaturized*** RF coil arrays that are fully integrated with their associated electronics. Independent receiver chains and tuning circuitry are required for each coil element and maximum performance can be achieved only if the early stages of the receiver chains, such as the tuning circuitry and signal pre-amplifiers are incorporated into the construction of the coil array itself. Coil arrays, when used in the parallel imaging mode, can dramatically improve imaging performance in terms of increased signal to noise ratio (SNR), reduced image acquisition time and image coverage. The benefits provided by array coils are based on the fact that smaller coils will provide a better sensitivity (i.e. increased SNR) over a smaller imaging volume or "field of view" (FOV). The reduced field overlapping views of the multiple coils are then combined into a single image, providing further benefits of increased FOV, SNR and acquisition speed. Realization of the goal of providing increased SNR will benefit every aspect of the Medical Department's Micro MR Imaging research program, yielding the same increased performance as might be obtained in a much more costly fashion by upgrading to a higher magnetic field strength.

APPROACH:

Parallel imaging is the recently developed technique, widely applied in the most advanced commercial clinical MRI systems. Comparable devices are not yet commercially available for small animal Micro MR imaging systems. Since an essential element of *Translational Imaging Research* is the direct comparison of human studies, obtained using standard clinical protocols, to those performed on research animals, it follows that such devices need be developed. The much smaller size of research animals compared to humans has led rather naturally to the use of higher magnetic field strengths in animal research *vis a vis* clinical imaging. The reduced imaging volume required for animal subjects, makes higher field strengths attainable at reasonable cost, while at the same time, smaller subjects allow the use of smaller gradient and RF coils, which can be more easily made to work at the correspondingly higher bandwidths and frequencies. Taken together, the result is increased performance in the form of increased spatial resolution, as is necessary for the imaging of the smaller volumes. For our work, however, the small size of the imaging volume leads to more difficult requirements for miniaturizing and more exacting tolerances in coil construction and assembly. Expertise is these areas is being provided through collaboration with the Central Shops' Tom Lambertson and the Instrumentation Division's Sergio Rescia.

TECHNICAL PROGRESS AND RESULTS:

During the first two quarters of FY 2007, a detailed R&D outline was developed and the search for suppliers of critical components was undertaken. A determination of necessary equipment purchases and the software development needs was also made at this time. Bench top evaluations of potential component and design changes were made using the BNL built coil shown in figure 1. Orders for some of the longer lead time components were placed upon completion of the evaluation. While design studies for the front end electronics continued, the plan for the Data Acquisition system was finalized and the purchase of an appropriate computer and necessary development software licenses was made in the final month of FY 2007. As a result of these efforts and purchases, the necessary tools and information are now in hand to complete the preliminary design and testing (Phases I and II of our proposal) by the end of the 2nd quarter FY 2008. At the same time, software development is underway, as will be necessary for the completion of Phase III the final quarters of the Fiscal year. In addition to the purchase of components, computer equipment and software test fixtures were constructed in the Central Shops to allow a careful measurement of the inductive couplings between individual coil elements in an array in order to better understand the complexities of tuning multiple coil arrays.

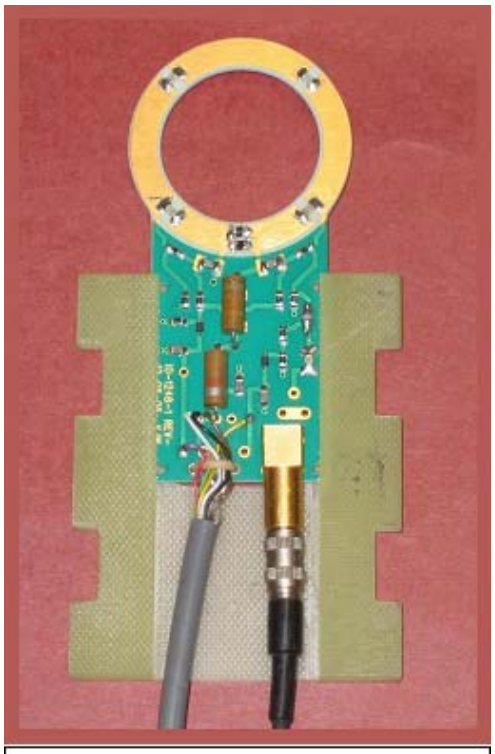

Figure 1. Three cm diameter surface coil fabricated by BNL Instrumentation Division.

The final Phase IV of the project, will produce a 16 element coil array that is fully integrated with the Bruker 9.4 Tesla MRI system. Our expectation is that we will be able to design several geometrical variants of the same basic design, each of which will be optimized for particular types of studies. We believe that all of the goals contained in the original proposal are achievable within outlined timeframe.

Neurocomputation at BCTN: Developing Novel Computational Techniques to Study Brain Function in Health and Disease

LDRD Project 07-055
Rita Goldstein

PURPOSE:
The Brookhaven Center for Translational Neuroimaging (**BCTN**) houses three important tools for in-vivo brain imaging: positron emission tomography (***PET***), functional magnetic resonance imaging (***fMRI***) and event-related potentials (***ERP***). The BCTN also acquires the functional assessment of cognitive brain processes with neuropsychological (***NP***) examinations. The present project is a cutting-edge effort at both the conceptual and computational levels to model and study the human brain in health and disease through the integrative use of these multiple data sets. This effort, therefore, furthers the central role of the BCTN as a meaningful integrator of multiple data sets (all from dynamically changing biological systems) toward current DOE initiatives of establishing BNL as a leader in the fields of Brain Health and Computational Biology.

APPROACH:
The current proposal bridges PET, fMRI, ERP and NP technologies to develop a state-of-the-art neurocomputational platform supporting multi-dimensional computational analysis of the human brain (chemical, metabolic, anatomical and psychologically functional). In our analyses, we resolve incompatibilities between PET, fMRI and ERP acquisitions (note different time scale from minutes, to second, to milliseconds, respectively); and use the newly emerging field of neurocomputation to set these multiple measures into a common database that allows the valid modeling of brain function. Our NP models guide the questions we pose.

TECHNICAL PROGRESS AND RESULTS
An integrated source for multiple datasets: We have been consolidating all datasets inside a flexible, well-supported and extendable database for each human subject. This work is now in progress necessitating the capture of a multitude of data fields that are acquired during each procedural encounter. Data entry tools enforce error-checking and facilitate specialized and compartmented control of data entry and access. The populated neurocomputational database is being developed to assemble records vectored across domain fields in response to user-definable queries. A mapping key strategy has been implemented to uniquely identify related records across NP, fMRI, ERP, PET domains. The mapping key strategy provides a clear link for relating data records and has proven to be a reliable and robust mechanism for relating elements across the variety of protocol encounters. Automated mapping key generation has been implemented inside our existing fMRI and NP protocol records, and supports the automated linking and import of data into the neurocomputational network.

Combined fMRI-ERP developments: To further the consolidation of fMRI and ERPs, Muhammad Parvaz, our Ph.D. student from SBU Biomedical Engineering Department, has attended a highly competitive 2-week workshop on combining fMRI and electrophysiological recordings at UCLA. He is now integrating ERP source analysis mapping with separately acquired fMRI activations, and preparing for simultaneous fMRI-ERP acquisitions.

Combined fMRI-PET developments: Samuel Asensio, a graduate student from Valencia, Spain, has been integrating the dopamine receptor availability PET data with our fMRI results to answer the first question that we posed in our original application: "Are impairments in immediate and sustained responses to monetary reward driven by decreased levels of dopamine?". To further this question we have also integrated the administration during our fMRI studies of methylphenidate, a dopamine agonist. We have now received IRB approval for implementation of this pharmacological intervention in treatment seeking cocaine addicted individuals. Thus, we plan to integrate into our studies treatment approaches based on our current results (e.g., NP exercises for brain regions known to be implicated in drug addiction; and enhancement of the brain regions underlying inhibitory control by other methodologies, including repeated transcranial magnetic stimulation to decrease craving).

NP task development (to equalize acquisition across modalities): We are continuing to develop new tasks designed for application across imaging modalities and to enable task-synchronized analyses. For example, we have been adapting the PET developed cocaine videos to the fMRI environment, and a new collaboration with Uri Hasson of NYU, an expert in this specific data analysis for fMRI (real-time complex intercorrelational datasets), has been established to further this goal. In addition, Scott Moeller, a Ph.D. student at Univ. of Michigan, has been working with us for the past two summer semesters to develop two additional tasks that tap into objective measures of reward processing and decision making in an emotional context. These same tasks will be used across all acquisition modalities after their behavioral validation. Here is of mention another collaboration we have established with Greg Hajcak, Ph.D., an Assistant Professor at the Department of Psychology from SBU, with whom we acquire and analyze ERP-fMRI markers of error processing in addiction.

Computer Science Applications: We have recruited three graduate students from the SBU Computer Science Department: Alex Panagopolous, Jean Honorio Carillo and Tejo Chalasani. These students are validating and extending the data-driven algorithms developed by our previous computer science student, Lei Zhang, Ph.D., which demonstrated highly sensitive and selective discriminations between fMRI responses to reward in subjects with and without histories of addiction. This pattern recognition discrimination software is now being validated across other tasks, imaging modalities, and samples of drug addicted individuals; it is also being assessed in more brain regions and studied for further optimization of the classifier network parameters. Together, these efforts help us answer the second question in this proposal "What are the neural features that best discriminate cocaine users from non-users when processing reward?"

Future developments: We plan to keep integrating these parallel yet disparate data sources using our multidimensional approach (unified database, tasks, and analyses across all imaging modalities) to advance our understanding of the brain networks underlying healthy and impaired inhibitory control and decision making. We are also developing new objective tools to tap into the brain regions underlying emotion. For example, we will use the facial discrimination algorithms developed by Dimitris Samaras, our computer science USB collaborator, to automatically and objectively identify craving. This will have a high impact in the field of drug addiction (and other disorders of uncontrollable behavioral) as to date craving has only been identified using self-report. Our objective algorithms will increase prediction of treatment outcome measures such as drug abuse and relapse while offering a cutting-edge scientific tool to identify, diagnose and predict hitherto subjective human emotions.

A Non-Fermentation Route to Convert Biomass to Bioalcohols

LDRD Project 07-059
Devinder Mahajan

PURPOSE:

The biomass "Fermentation route" to ethanol though inefficient is commercially practiced. An alternative pathway, the "thermochemical route", can process biomass through synthesis gas or synags (primarily a mixture of carbon monoxide and hydrogen) directly into ethanol but low turnover numbers and low ethanol selectivity results in process efficiency that is marginal to be of commercial interest. This proposal seeks to develop an alternate "thermochemical route" in which the first product is more efficient methanol that in a separate step, is efficiently converted to ethanol via catalytic homologation in an aqueous medium. A successful development of this pathway, i.e., though intermediacy of methanol, would allow high carbon conversion to bioalcohols and other fuels and allow utilization of more abundant biomass such as lignocellulose. The project goals align well with the BNL strategic goal to develop biofuel technologies.

APPROACH:

Background. Biomass is readily converted to ethanol via fermentation, a route labeled as "Sugar Platform" or 'Biochemical", that presently is a major commercial effort. Fermentation to ethanol requires glucose (Equation 1) and cellulose, generally the largest fraction (40-50%) of total biomass, and lignin-rich woody biomass remain underutilized with present technology.

$$C_6H_{12}O_6 \rightarrow 2\,CH_3CH_2OH + 2\,CO_2 \quad (1)$$

Equations 2 and 3 are collectively known as the alternate "Thermochemical route" (or Syngas Platform) through which biomass from a variety of sources can be converted into useful fuels and chemicals. In this two-step route, the first step is biomass gasification to yield synags. The second step follows with catalytic conversion of syngas into alcohols such as ethanol though total carbon utility remains a challenge.

$$\text{Biomass} \rightarrow x\,CO + y\,H_2 \quad (2)$$

$$2\,CO + 4\,H_2 \xrightarrow{\text{Catalyst}} C_2H_5OH + H_2O \quad (3)$$

Whereas the fermentation route produces 2 moles of undesirable CO_2 wasting 2 C atoms for every 6 C atoms processed (Equation 1), the syngas route (Equation 3) can theoretically utilize all the reactant C atoms and produce 1 mole of water as a byproduct per mole of ethanol synthesized making the latter a superior non-CO_2 producing alternative. However, studies reported in the literature show that thermodynamically, direct conversion of syngas to ethanol pose opposing requirements for C-OH bond formation and C-C coupling in a single reactor. The best known catalyst is Rh-based that operates in a liquid medium at T ~ 200^{o}C under high pressures and the turnover numbers (TO) and selectivity to ethanol is low. The approach here is to decouple the two steps and develop highly catalysts for each that can form the basis of a very efficient and selective process to produce ethanol. An additional requirement is the use of water as reaction medium for which metals containing water-soluble ligands is utilized.

Methodology. The planned runs operate in moderate temperatures and pressures and for these, a Parr batch unit consisting of a 300 mL constant stirred tank reactor (CSTR) was customized. A general procedure involved a shakedown run to check for any leaks in the system followed by a baseline run. For the baseline run, 100 mL methanol was poured into the 300 mL vessel, pressurized with 2 MPa N_2 gas, stirred and heated to 150°C for 3 hours. The system was cooled to room temperature, gas and liquid phases were analyzed by gas chromatographs (GCs) and mass balance was performed on each run.

Our initial study focused on testing two potential catalysts, Rhodium on alumina (Rh/Al_2O_3) and triruthenium dodecacarbonyl ($Ru_3(CO)_{12}$) for methanol to ethanol conversion. The former was purely for reference purposes. During a typical run with 1 mmol of catalyst and 100 ml methanol in a 300 mL Parr batch reactor under 2 MPa pressure of N_2 gas, the solution was heated to 150°C with constant stirring. Pressure began to rise steadily, then equilibrated where it was held for 3 hours. The contents were then cooled to room temperature and the pressure was noted. The infrared (FT-IR) spectrum of gas phase was recorded to identify any gaseous species present. Since no reaction appeared to occur with either catalyst at 150°C, a second set of runs at 200°C holding other parameters constant.

The work is being carried out in collaboration with Drs. K. Ro and P. Hunt of the Agriculture Research Service (ARS), U.S. Department of Agriculture (USDA), Florence, South Carolina.

TECHNICAL PROGRESS AND RESULTS:

The performance data of supported Rh (Rh/Al_2O_3) and unsupported trinuclear Ru precursor, $Ru_3(CO)_{12}$), with methanol reactant were collected in a batch reactor through a series of runs. The liquid analysis of the final solutions showed the absence of ethanol signature peaks in GC. The analysis of gas phases of the reactor showed the presence of CO, H_2, and CO_2 in the 1-3% range. Of these, CO and H_2 originated directly from methanol decomposition under the reaction conditions (Equation 4). The presence of trace amount of water will promote water-gas-shift (WGS) reaction (Equation 5) accounting for CO_2 in the product. But it was the recognition of additional peaks in the GC and the infrared for methyl and ether groups that was of interest. These peaks were attributed to dimethyl ether (DME) that constituted 0.8% and 1.3% of the gas phase with Rh and Ru catalysts respectively, and seems to be formed by dehydration of methanol (Equation 6):

$$CH_3OH \rightarrow CO + 2\,H_2 \quad (4)$$

$$CO + H_2O \rightarrow CO_2 + H_2 \quad (5)$$

$$2\,CH_3OH \rightarrow CH_3O\,CH_3 + H_2O \quad (6)$$

The formation of DME is of interest in its own right as this molecule is being considered as a diesel substitute.

For FY 2008, we plan to further probe the origin of DME formation and test conditions that may lead to increased yield. In addition, experimental conditions will be varied to promote ethanol formation from methanol.

Fate and Reactivity of Carbon Nanoparticles Exposed to Aqueous Environmental Conditions

LDRD Project 07-062
Barbara Panessa-Warren

PURPOSE:

The increase in the academic, industrial and research laboratories designing, developing, and manufacturing engineered nanoparticles for applications in energy storage, cosmetics, clothing, paints, optical devices, diagnostics, biosensors, drug delivery systems, and structural materials, has produced global concerns about environmental nanoparticle contamination. Little is currently known about the behavior of nanoparticles in the environment but it is obvious that disposal of these nanomaterials in sanitary landfills and down drains, increases the probability of nanoparticle contamination in our ground water, estuaries and coastal shorelines. This proposal attempts to experimentally determine how carbon nanoparticle (CNP) inherent characteristics (morphology, charge, reactive groups and composition), may change following aqueous exposure to specific simulated environmental conditions (i.e. light, pH, salinity, & natural organic matter called NOM). In this investigation, following these different types of aqueous exposure CNPs are incubated with human lung and skin cells (representing two possible routes of exposure: inhalation and surface contact) to determine if nanoparticle binding, cell processing and toxicity are altered when compared to exposure to non-environmentally treated controls. Probing these changes in CNP physicochemical properties and processes to elucidate the nature and mechanisms of environmentally-induced CNP alterations, and how they may alter CNP reactivity and fate, provides very specific information about whether groundwater CNP contamination poses potential environmental risks to living cells. Measuring CNP physicochemical and morphological changes will be challenging and require utilizing some of the state-of-the-art instrumentation now available at the Center for Functional Nanomaterials. This would be one of the first studies to verify how carbon nanotubes in an aqueous environment may change their surface reactivity, and determine how these measurable changes pose specific threats to living cells in terms of CNP binding, entry and altered ultrastructural cellular processing. To examine the longer term effects of CNP aqueous exposure to water and salt, we have some 2-7 yr carbon nanotube stored preparations, which offer the unique possibility to study long term physical CNP changes, and how aqueous CNP exposure may transform surface structure and reactivity of the Nanoparticles, which in turn would alter their environmental interactions with biota.

APPROACH:

This study examines two forms of a commonly used source of single walled carbon nanotubes (SWCNT):'as prepared' Carbolex SWCNTs (Carbolex, Inc., Lexington, KY) containing graphene, carbon black, Ni and Y, as well as cleaned carbolex SWCNTs. Although we planned to also investigate fullerenes in this study, we have focused primarily on SWCNTs due to the extensive use of carbon nanotubes in commercial products, and the comparative paucity of environmental fate and aqueous reactivity published data. In this LDRD, these CNP materials are being characterized using FT-IR, zeta analysis, and Uv-vis with the help of the Soft & Bio Nanomaterials Group at the CFN (Dr. Oleg Gang's laboratory). Raman spectroscopy, field emission scanning electron microscopy and x-ray microanalysis of both 'as prepared' and aqueous-treated CNPs are being done at BNL in the laboratories of Dr. Triveni Rao (Instrumentation Division laser laboratory) and Dr. John Warren (Instrumentation Division,

microscopy nanomaterial lab). Human cell experiments and TEM and SEM specimen preparation are currently being done in Dr. Panessa-Warren's laboratory at BNL. Eventually the cell culture experiments will be moved to the Eukaryotic cell culture facility at the CFN in the Soft & BioNanomaterials area of Dr.Van der Lelie. Experiments exposing CNPs to various aqueous environments (pH, light, NOM) are being done at Dr. Kenya Crosson's new laboratory at the University of Dayton (Dayton, Ohio), and eventually more of the nanoparticle characterization will be done at her lab under her direction, and in the EENS lab here at BNL.

TECHNICAL PROGRESS AND RESULTS:

(I) We have identified (a) available instrumentation at BNL for this project, and (b) supplies to be purchased for the various experiments. The needed supplies were purchased and all received by Sept.1 for this study. Discussions began in June with the project directors of the newly opened Center for Functional NanoMaterials (CFN) at BNL which resulted in our access to FT-IR, zeta analysis, UV-vis and human cell culturing facilities at the Nanocenter. We are now completing a formal Jumpstart Grant to the CFN for submission on Nov. 26, 2007 to extend this collaboration to also include access for work to be done using the analytical electron microscopy facilities and the Focused Ion Beam system for imaging and analysis.

(II) Dr. Crosson began to set-up the laboratory in EENS to do the physicochemical experiments with the nanotubes in June and July. We wrote the Experimental Safety Review documents according to all safety requirements at BNL, and wrote the additional Activity Safety Review documents for the portion of the research experiments that would be done in the Nanoparticle and Cell culture laboratory area Dr. Panessa-Warren has setup in the Division of Instrumentation here at BNL.

(III)When Kenya Crosson finished her post doctoral fellowship in August at BNL in the Dept. of Energy Sciences & Technology, she moved to the University of Dayton Department of Civil & Environmental Engineering & Engineering Mechanics, where she is now an Assistant Professor. Dr. Crosson is continuing to collaborate on this LDRD doing specific experiments and subsequent nanoparticle characterization, and she will return to BNL as a Guest Scientist (3 times during the fiscal year as part of this LDRD) to continue analyzing samples with Dr. Panessa-Warren at BNL and to continue jointly interpreting the data.

(IV) Our preliminary data has shown that extended aqueous exposure (both fresh water and buffered saline) of CNPs (and especially SWCNTs) may alter the composition and reactivity of the carbon nanotubes. Initial Raman spectroscopy suggested that following six or more years of aqueous water exposure, SWCNTs showed significant changes in composition with an increase in graphite and a loss of SWCNTs. Experiments done with lung cells exposed for 3 hrs to carbon nanoparticles incubated for 2.5 yrs in buffered saline (pH 6.8), showed that the saline-aged 100uM CNPs produced a 1.6% increase in cell necrosis compared to a 4.5% increase in cell necrosis following 3 hr incubation with freshly prepared 100uM suspended CNPs. This suggests that degradation of CNPs following fresh and saline water exposure over time may decrease reactivity, and subsequent cytotoxicity of these nanoparticles, to living cells.

Development of Room-Temperature CdMnTe Gamma-Ray Detectors

LDRD Project 07-073
Yonggang Cui

PURPOSE:
The goal of this project is to develop a new room-temperature gamma-ray detector based on CdMnTe (CMT) crystals. Its wide band-gap, high resistivity, and good electron-transport properties make it a viable candidate for detecting gamma rays. In addition, its relatively low-temperature growing process ensures good compositional uniformity and fewer impurities, potentially resulting in a high yield of the crystals in making detectors and large-area detector arrays.

In this project, we investigate the required characteristics for CMT as a material for gamma-ray detectors. The success of this work will lead to increased availability of new radiation-detection devices for many applications.

APPROACH:
Recently CMT crystals were proposed as potential gamma-ray detectors. Mycielski *et al*. (2005) discussed the current state-of-the-art of CMT crystals specifically grown for nuclear-detector applications. Indium (at ~10^{17} cm^{-3})-doped $Cd_{0.87}Mn_{0.13}Te$ crystals grown at the Institute of Physics, PSA (Warsaw, Poland) exhibited resistivity and mu-tau products exceeding 10^{10} Ω-cm and 10^{-5} cm^2/V, respectively. These crystals were used to fabricate devices that could detect 5.5-MeV alpha particles from an ^{241}Am source, and gamma radiation from ^{241}Am and ^{57}Co sources. The present electron mu-tau value of $Cd_{0.87}Mn_{0.13}Te$ detectors (~10^{-5} cm^2/V) is too small to assure good spectral performance for long drift-length detectors. This project seeks to improve the transport properties of CMT materials to produce a new class of solid-state gamma detectors for spectroscopy and imaging.

In this activity, we will characterize and improve CMT crystals for nuclear-radiation detectors. The crystals are provided from our collaborators with different composition $Cd_{1-x}Mn_xTe$ (x = 0.05 ~ 0.15) and different doping methods.

For each crystal, we conduct IR transmission mapping to locate and quantify Te inclusions. If needed, scanning and transmission electron microscopy (SEM and TEM, respectively) are used to identify the secondary phases present in the bulk and surface of the crystals. We also conduct EPD measurement and high-energy transmission x-ray diffraction using synchrotron radiation to understand the structural properties of the material. These measurements can reveal the quality of crystalline CMT and its relationship to the detector response, and provide an understanding of how extended structural defects affect device performance.

We process the crystal surface and develop contacts using electroless method. New fabrication methods were developed, which rely heavily on BNL's current fabrication processes used for cadmium zinc telluride (CZT). Modification of the CZT fabrication steps is needed to account for the material differences between CZT and CMT. I-V curves are measured after surface processing and electrode deposition.

High resistivity crystals are selected to fabricate planar radiation detectors. In addition to characterization and standard tests with sealed sources, we also use x-ray beams at NSLS to characterize the electrical-, structural-, and transport- properties of CMT on a micron scale. These properties can be correlated with other material properties to understand nonuniformities and improve surface preparation processes.

Depending on the success of the growth experiments, we plan to pursue developing unipolar devices, such as the BNL-patented modified Frisch-ring configuration that has shown impressive performances for CZT detectors.

Other investigators involving in this project include A. E. Bolotnikov, G. S. Camarda, P. Vanier, and A. Hossain.

TECHNICAL PROGRESS AND RESULTS:

In FY 2007. We focused on finding high-quality crystals and developing experimental setup, crystal processing and detector fabrication methods.

We designed and upgraded new hardware for an infrared transmission mapping system, including installation of new stages and controller. This upgrade improved the quality of IR images. New software was written to control the system. With this system, we scanned crystals in three dimensions very quickly and obtained IR images on a micrometer scale.

There are a few scientists growing CMT crystals today. We developed a fruitful collaboration with one important source: Prof. Andzej Mycielski at Institute of Physics PAS, Poland. In this fiscal year, he provided BNL with 12 CMT samples. We also purchased 3 samples from Cleveland Crystals, Inc.

Eight of Mycielski's crystals have been tested and presented low resistivity (less than $5x10^8$ Ω·cm), which made them too noisy for high-resolution spectra. However, one sample showed few Te inclusions in the IR transmission images, which was very encouraging. WXDT (white x-ray diffraction topography) images showed that most of these samples have a single domain. All these results indicted that CMT is a good material for radiation detectors. However, we need more growth experiments and analyses to attain a higher electrical resistivity.

All the samples were polished manually in our lab. One sample (No. 4495-6) was etched for EPD measurement. We tried to establish the right method to process the CMT crystals. Basically we found that the surfaces of CMT crystals can be easily damaged by the polishing process, as compared to CZT crystals. Chemical polishing using Bromine in methanol was not adequate to remove the damaged layers. Significant process was also made to develop suitable fabrication steps for producing planar detectors.

In FY 2008, we will continue our work by acquiring more samples and testing them. We will continue this collaboration with Prof. Mycielski to obtain CMT samples as needed. Right now, Prof. Mycielski is upgrading his technology and will be able to grow much better crystals. We will also ask him to grow crystals with specific composition and doping (e.g., indium).

Developing a New Framework for Investigating Earth's Climate and Climate Change

LDRD Project 07-075
Yangang Liu

PURPOSE:

The overarching goal is to develop a new framework for studying Earth's climate and climate change, with two major objectives. The first objective is to examine the role of entropy (budget) in shaping Earth's climate and its change. The second objective is to seek simple guiding principles that govern Earth's climate as a whole without knowing the "microscopic" details. The two objectives are complementary to each other as the state of a large system is likely constrained by entropy-related principles such as maximum entropy principle for equilibrium systems, minimum entropy production principle for near-equilibrium systems, and maximum entropy production principle for systems far-from equilibrium. This work will shed new light on many crucial issues regarding Earth's climate and climate change, and enhance our ability to predict them. Specifically, the work will lead to improved quantification of the role of entropy in shaping Earth's climate and new understanding of climate forcings from aerosols and greenhouse gases. The success of this work will give BNL an edge in competing for funding in ongoing and future programs (e.g., ARM, ASP, CCCP and SciDac) because understanding and modeling Earth's climate and human induced climate change is a central part of DOE science mission. The results from this proposal will also find additional applications in studies of complex systems (e.g., ecological and biological systems) in general. The proposed task is directly tied to the BNL strategic areas of computational sciences, and basic and applied sciences, and indirectly related to that of energy sciences.

APPROACH:

Climate involves (infinitely) many interacting subsystems that themselves consist of further smaller units, and a proper theoretical framework is central for virtually all climate-related scientific issues targeted by the DOE mission. Despite of its successes over the last few decades, the current mainstream framework suffers from two major deficiencies. First, current climate studies center on the concept of energy but overlook entropy, especially in studies of climate change. This neglect of entropy is problematic because any change of a system is related to entropy no less than to energy. Second, current climate models such as general circulation models are built upon the idea of breaking down Earth's system into ever-smaller interacting subsystems, which, in a sense, is like trying to describe the behavior of a gas by tracking every molecule. Despite the advantages of being able to have detailed investigation into individual processes, accurate representation of increasingly detailed subsystems, their interactions/feedbacks, along with the increasingly high demand for computer resources, poses both theoretical and practical challenges to such reductionism approach.

A major thrust of this proposal is its focus on entropy and entropy-related principles (e.g. second law of thermodynamics for nonequilibrium systems) in addition to energy (budget). Theoretical studies, model simulations, and analysis of both observational data and model simulations will be carried out in parallel to achieve the objectives**.** Theoretical studies will start with a simple system, and gradually increase the level of model complexities. I intend to use the analogy with thermodynamics and statistical mechanics and take advantages of the development in these fields to explore the new theoretical framework. Theoretical analysis can be used to assist examination of data from observations or model simulations. A major motivation to analyze model

simulations is to discern the model problems and to determine if the problems are related to the neglect of entropy-related issues.

TECHNICAL PROGRESS AND RESULTS:

In this fiscal year, progresses were made on two fronts. First, a new "zero-dimensional" climate model that considers the Earth-atmosphere as a whole system and accounts explicitly for energy and entropy budgets was established, and was applied to examine the global climate. As shown in Fig. 1, there is an optimal climate state whereby the total production of the entropy in the Earth-atmosphere reaches the maximum and occurs most probably. Furthermore, the details of the most probable state depend on the relationship between the shortwave albedo and long-wave emissivity of the Earth-atmosphere system. This new theory provides a physical explanation for the long-standing puzzle of why the observed shortwave albedo tends to be around 0.3, underlines the importance of clouds in determining the Earth climate, and sheds new light on the issue of climate change under global warming due to greenhouse gases and global dimming due to aerosols. A post doc, Dr. Wei Wu, was hired 5 September, 2007. She has been reviewing the relevant publications in literature, clarifying the concept and calculation of radiation entropy, and preparing herself for extending the "zero-dimensional" climate model to a one-dimensional climate model and calculating global distribution of radiation entropy.

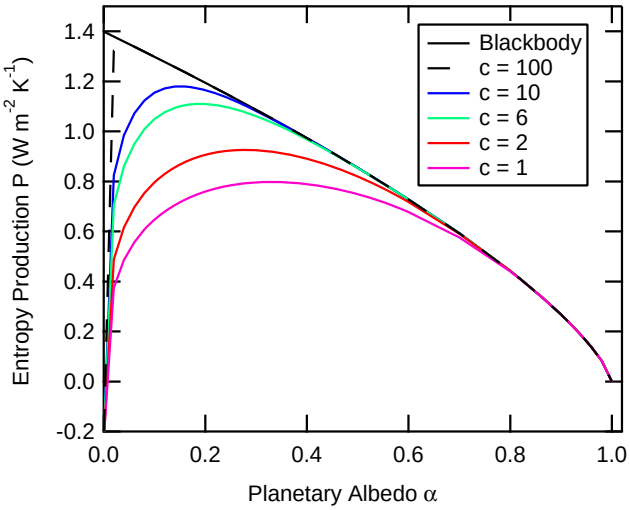

Figure 1. Relationship of the total entropy production to the shortwave albedo at different values of c (The value of c determines the relationship between shortwave albedo and longwave emissivity). It is evident that for a given c, there is an optimal albedo at which the Earth-atmosphere produces the maximum amount of entropy possible.

A Novel Approach for Efficient Biofuel Generation

LDRD Project 07-080
Dev Chidambaram

PURPOSE:

The objective of this work is to create a functionally-bioactive microorganism encapsulated polymer fiber material for the first time. Traditional methods of immobilizing microbes have not had much success in terms of survival rates of immobilized bacteria. One of the drawbacks has been the solid nature of materials used; solid materials provide bacteria with no channels for respiration or for obtaining nutrients.

APPROACH:

Although microorganisms have been used in industrial and niche application for ages, successful immobilization of microbes while preserving the desired functionality has been elusive. This work aims to create polymer fibers containing bacteria, for the first time, through a novel process that allows the formation of pores on the fibers as shown in Figure 1. These pores are essential for the respiration of the bacteria. Application for such a functionally bioactive material ranges from biosensors, biofuel cells, environmental remediation, ground water decontamination, biocatalysis and is only limited by imagination. In short, these biohybrid materials can act as living membranes.

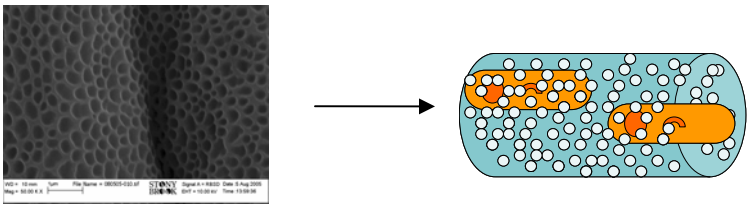

Fig 1: (a) A high magnification (50000 times) scanning electron microscopy image of a polymer fiber with pores (b) A schematic for proposed porous polymer (blue) encapsulation of microbes (orange)

Since this is an original work, we have a multistep approach that starts from simple polymeric materials and progressively leads to the final complex system, which is outlined below. To commence, we aim to create fibers of a biocompatible polymer (for compatibility with microbes) using the fiber process developed by researchers at Stony Brook University. This in turn poses certain restrictions such as use of non-toxic solvents, water soluble polymers, non-toxic concentrations of polymers, etc. Since the microorganism will be exposed to process conditions, another major issue is the survivability of the bacteria under the conditions of the process. In this work, we start with aerobic bacteria, *P. fluorescens*, and test its survival conditions during the process. Upon creation of these fibers, we test to see whether the microbes were successfully encapsulated in the fibers and whether the fibers are porous. Then, the survival of the microbes inside these fibers itself will be tested including a temporally based survival study that will provide us valuable data on the maximum shelf life of these materials. The system will then be modified accordingly to test for biofuel production and to increase

efficiency. The final step would be to optimize the process conditions to obtain the most dense and effective bioactive system.

Bacterial staining and fluorescence microscopy are used to identify, confirm the presence and determine the survival rate of microbes. Scanning Electron microscopy (Dr. J. Quinn) and atomic force microscopy (AFM) in conjunction with direct counting of stained bacteria using epifluorescence microscopy yields crucial quantitative data regarding the density of the bacteria in the polymer filaments. The bacterial growth curve is obtained using absorbance at 600nm. The bioactive system is produced at by Y. Liu and X. Ba (graduate students) under the advice of Dr. M. Rafailovich.

TECHNICAL PROGRESS AND RESULTS:

We used a blend of polymers to create a biocompatible mat of filaments. These filaments were stable. The process conditions were optimized to create filaments, over 95% of which were in the preferred 500-1000nm range as shown in Figure 2 (left). The polymer blend was then used to immobilize microorganisms. Confocal imaging showed that the

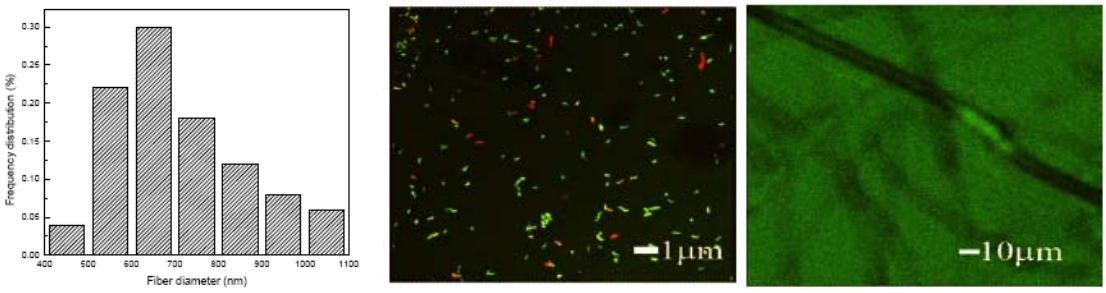

Figure 2: Diameter distribution of fibers indicates over 95% of fibers to be in desired size range 500-1000 nm (left). Confocal images show the presence of bacteria inside the fibers (center) and magnified image showing a single strand of polymer encapsulating a fluorescing microbe (right). Dead cells are indicated by red fluorescent stain, while live cells are indicated by green fluorescent stain.

microbial cells were aligned longitudinally with the fiber axis (Figure 2 right). Most importantly, the bacteria survived the process conditions. These can be seen in Figures 2 (center). This is a major technical milestone and successfully answers our first hypothesis.

In the current and next fiscal year, we plan to study the survivability of the microbes in the fibers immediately after creation and their shelf life. Then the system will also be tested for functionality. Finally, the conditions will also be optimized.

Investigations of Hygroscopic Growth and Phase Transitions of Atmospheric Particles by Noncontact Atomic Force Microscopy

LDRD Project 07-084
S. E. Schwartz

PURPOSE

Aerosol particles (nanometer to micrometer sized particles suspended in air) affect atmospheric radiation and cloud microphysics. A correct description of their behavior in the atmosphere is essential to accurate climate modeling. The processes of *aerosol "aging"* (a phenomenon in which non-hygroscopic particles become hygroscopic) and *aerosol deliquescence* (the uptake of water by hygroscopic aerosols and their eventual transition to liquid state) are important but not well understood at a fundamental level. ***The objective of this LDRD is to demonstrate the ability of Atomic Force Microscopy (AFM) to provide a better understanding of these processes on the nanoscale wetting and this will ultimately lead to improved climate models.*** Climate studies and fundamental understanding of processes on a nanoscale are both key strategic elements at BNL. This project brings together capabilities in the pertinent two directorates of BNL, EENS and BES.

APPROACH

Initial measurements and feasibility studies were carried out by Susan Oatis and Mathew Strasberg (SULI student) with guidance and participation from Antonio Checco, Ben Ocko. and Steve Schwartz, starting in June 2007. As described below, we have made great strides during the last few months. A new post-doc, Derek Bruzewicz (Ph.D. Harvard, Whitesides) is scheduled to start employment this December under support from this LDRD. We have carried out initial AFM studies to measure changes in morphology and hygroscopicity as a function of the relative humidity (RH) for sodium chloride aerosols, a well characterized aerosol, deposited on substrates with differing surface energies. Sodium chloride aerosols were atomized under ambient conditions and collected on a polished silicon substrate. The aerosol size distribution could be manipulated by varying the initial aqueous salt solution concentration in the atomizer. The salt nanoparticles were characterized with AFM in non-contact mode using a silicon cantilever. The AFM was calibrated against a 20 nm grating resulting in an uncertainty of ± 1 nm in all height measurements. The RH in the AFM chamber was controlled (±2%) using a feedback system that mixes dry and wet nitrogen. This system was developed over the summer.

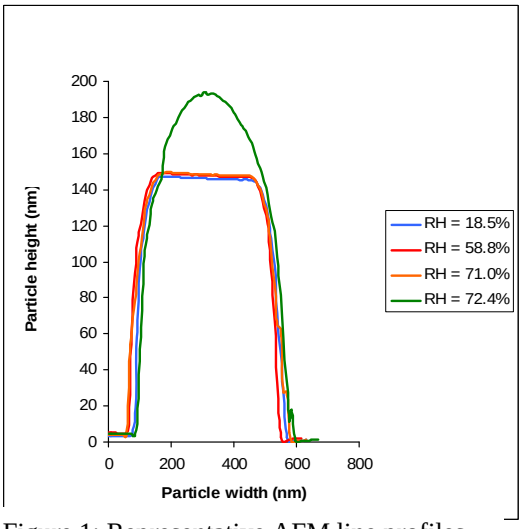

Figure 1: Representative AFM line profiles of a single NaCl salt nanoparticle at several different relative humidities.

TECHNICAL PROGRESS AND RESULTS

Initial experiments were carried out on NaCl aerosols of approximately 100-150 nm in height to validate the feasibility of the approach. The dry NaCl aerosols were nearly rectangular in shape, and the top of the particle could be flattened by allowing the aerosol to go through several humidified – dry cycles within the AFM chamber. This

"restructuring" of the aerosol allowed for more precise height measurements. A representative measurement is illustrated in Figure 1, where a particle with a height of 150 nm retains the same height as the relative humidity increases until it approaches the deliquescence relative humidity (DRH). Significant water absorption is observed at a RH = 72.4%.

The hygroscopic behavior of several, different sized particles was characterized by scaling the height (at a given RH) to the height at a low RH (typically below 10%, at which the particle is considered to be dry) as a function of RH (Figure 2). Water absorption or "pre-wetting" was observed prior to the DRH for all particles. For particles with height > 50 nm, DRH was observed near 75% (±2%) agreeing with the result of Tang and Munkelwitz (*Atmos. Environ.*, 27A(4), 467-473, 1993) relative to suspended particles. The 44 nm particle appears to have a DRH near 80%. Also for particles below 100 nm in height, significant "restructuring" of the aerosol, (illustrated by relative heights < 0.98) was observed between 50-60% RH. This indicates that, even at low humidity, there is enough water to allow for the smallest aerosol to minimize its surface energy. This effect might be enhanced by the presence of the substrate, although more data is required to support this hypothesis.

We have also explored a different method for synthesizing NaCl aerosols which rely on template-directed dewetting of salt solutions on chemically nanopatterned surfaces. Silicon wafers coated with a hydrophobic, self-assembled monolayer of octadecyltrichlorosilane (OTS) were locally oxidized through contact with a biased AFM tip under humid environment. The oxidized regions of the sample (~100 nm sized) exhibit carboxylic terminal groups and therefore hydrophilic properties. A saturated solution of NaCl was dropped onto the patterned surface and allowed to dry. Salt nanoparticles were observed on the hydrophilic patterns after the drying process. The hygroscopic behavior of these nanoparticles was found to be similar to that observed for particles deposited on the bare silicon surface. This result is not surprising because both surfaces exhibit OH terminal groups and therefore have a similar wettability.

These exciting, preliminary results demonstrate that environmental AFM is a viable probe for studying the hygroscopic behavior of salt nanoparticles on solid supports. These studies raise many interesting new scientific questions, such as the shift of DRH observed for particles of thickness < 50 nm. Further experimental and theoretical work is clearly required to address these issues.

In the 2nd year these initial studies will be extended to single- and multi-component aerosol particles of composition more directly relevant to ambient atmospheric aerosols, permitting a mapping out of these phenomena as a function of size and composition. Higher quality data is anticipated with a dedicated post-doc. At minimum, these findings will lead to a more differentiated picture of the deliquescence phase transition essential to representing this in atmospheric models, demonstrating the value of the AFM approach to such characterization, leading to publication and positioning us for gaining external support for this research.

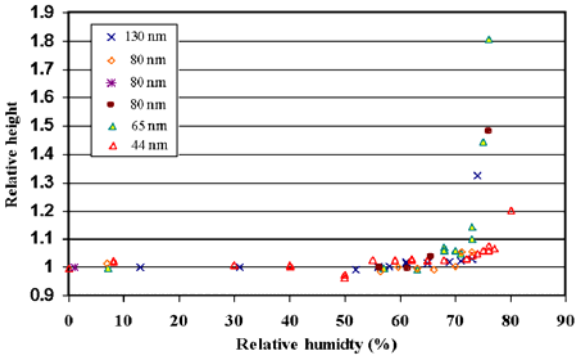

Figure 2 Relative height measured as a function of relative humidity for NaCl particles having dry diameter 44-130 nm.

Chemical Imaging of Living Cells in Real Time

LDRD Project 07-089
Lisa M. Miller and Roger Phipps

PURPOSE:
The objective of this work is to develop methods for high-resolution, chemical (infrared) imaging of living cells in real time. To date, infrared imaging of biological materials has primarily been performed on dried samples due to the infrared absorbance of water. In addition, most infrared microscopes are equipped with single-element detectors that hamper real-time imaging because the sample needs to be raster-scanned through the infrared beam. Here, we propose to develop a specialized incubator for living cells that is adapted for infrared microscopic imaging in real time. This incubator will be coupled to an infrared microscope with a new focal plane array detector system, where a 128x128 pixel array is used to image large areas quickly. This new technique will become a key element in the ongoing development of biomedical imaging programs at the NSLS that will take advantage of the high brilliance and stability of NSLS-II.

APPROACH:
Synchrotron-based Fourier transform infrared microspectroscopy (FTIRM) is a powerful method for sub-cellular spatial resolution imaging (2-10 μm in the mid-infrared region) of chemical components such as lipids, proteins, nucleic acids and carbohydrates, which are often altered in disease states or in response to external stimuli (e.g. drugs, radiation). One of the major drawbacks of FTIRM is the absorbance of water in the mid-infrared region. The O-H stretching mode of water spans from 3600 – 3100 cm^{-1} and the O-H bending mode overlaps the protein Amide I band (~1650 cm^{-1}). Due to this potential interference, most FTIRM data on biological cells and tissues published to date have been collected on dried samples.

In this work, we propose a series of developments so the technique can be extended to studying living cells in culture. The motivation behind this new technology is 4-fold: (1) The synchrotron infrared beam is non-ionizing and does not induce any heating effects so samples can be probed for weeks to months. (2) Since FTIR vibrational frequencies are sensitive to isotopic labeling, individual chemical components can be tracked spatially and in real time. (3) This technique can be used simultaneously with other optical-based imaging techniques such as epifluorescence or confocal microscopy and can compliment lower resolution, in vivo techniques such as Positron Emission Tomography (PET) and Magnetic Resonance Imaging (MRI). (4) As part of NSLS-II, infrared beamlines are proposed that will be optimized for infrared imaging. Development of this technology is expected to increase the user base dramatically.

The specific aims of this proposal are to (1) design an incubator for living cells that is compatible with infrared micro-spectroscopic imaging, (2) adapt the infrared imaging microscope with focal plane array detector to a synchrotron infrared beamline at NSLS and (3) apply the newly developed technology to study bone mineral production and the effects of a current, isotopically-labeled osteoporosis drug on this process.

TECHNICAL PROGRESS AND RESULTS:
A postdoctoral fellow (Dr. Imke Bodendiek) was hired and began work in September 2007. During the last two months of the fiscal year, Dr. Bodendiek began growing fibroblasts (human

Table I

Material	Solubility in Water	Spectral Range (1/cm)	Refractive Index (@2000 cm-1)	Living Cells	Dead Cells	Viability
CaF_2	3.45×10^{-11}	77000 to 1110	1.4	59	17	78%
BaF_2	1.84×10^{-7}	67000 to 870	1.45	16	3	84%
Ge	none	5000 to 560	4	46	15	75%
Si	none	83333 to 1430, 400 to 30	3.4	21	8	72%
ZnSe	3.6×10^{-26}	20600 to 5000	2.4	11	4	73%
AgBr	5.35×10^{-13}	22000 to 333	2.3	1	9	1%
KRS-5	3.71×10^{-6}	16600 to 285	2.38	2	5	3%

skin melanoma cells) on infrared-transparent materials. The first step of Specific Aim 1 is to identify the best infrared material for the incubator surface. The IR-transparent materials included calcium fluoride (CaF_2), barium fluoride (BaF_2), zinc selenide (ZnSe), zinc sulfide (ZnS), silver bromide (AgBr), KRS-5, germanium (Ge), and silicon (Si). Cells were grown on the bare substrate, and for instances where cells would not grow, the substrates were coated with sulfonated poly-styrene (SPS) and cell growth was tested again. Tests were performed for cell viability and adhesion and the results can be seen in **Table I**. As can be seen, CaF_2 and Ge had the fastest cell growth (i.e. largest number of cells) and good viability. Conversely, AgBr and KRS-5 had very low cell viability, likely due to their sufficient solubility in water that poisoned the cells.

The adherence of the cells is also an important factor for proper cell growth. Those cells that "ball-up" on the surface of the slide are not healthy fibroblasts. Thus, the adherence of the cells on various substrates was assessed through light microscopy. **Figure 1** shows the fibroblasts from culture dishes containing the 7 different substrates. Results show that the cells grown with CaF_2, Si, and Ge most resemble the control cells in shape, adherence, and density. Conversely, cells grown with AgBr and KRS-5 are all round (i.e. dead). Even coating the substrates with SPS did not enhance cell viability with these materials.

In FY 2008, parallel efforts will continue to grow mineralizing osteoblasts (bone cells) on the same materials to confirm viability. For the fibroblasts, we will proceed with CaF_2, ZnSe, and Ge as viable infrared transparent materials for our incubator. Crystals of these materials will be cut in an attenuated total reflection (ATR) configuration as trapezoids and hemispheres. An incubator will be built and it will be coupled to the synchrotron-based focal plane array IR microscope, which was recently funded by the NIH.

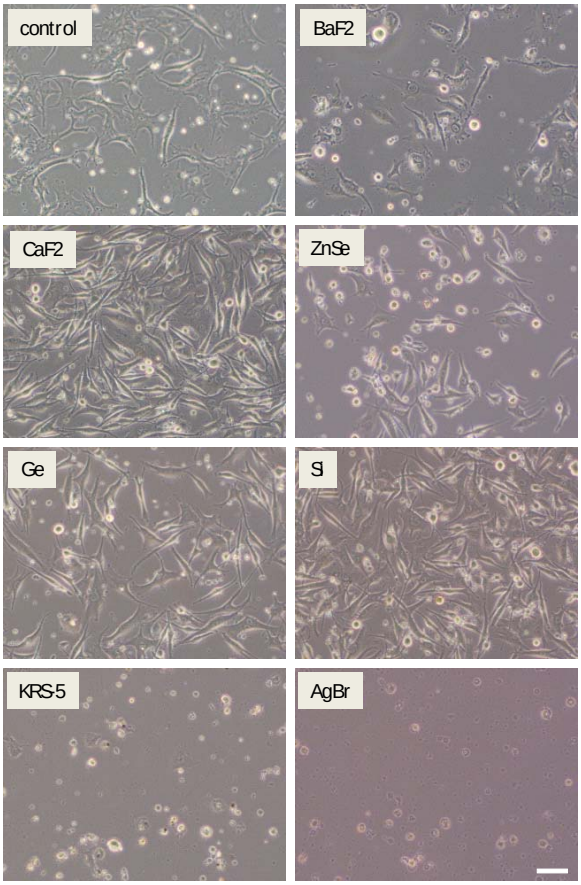

Figure 1. Light microscope images of human skin melanoma cells grown on various IR-transparent substrates. Scale bar is 20 microns.

Coherent Bragg Rod Analysis of High-Tc Superconducting Epitaxial Films

LDRD Project 07-090
Ron Pindak

PURPOSE:
The two goals of this LDRD are: (1) to develop a beamline facility at the NSLS for the implementation of the COBRA phase retrieval method and the development of user-friendly COBRA data acquisition and analysis software to facilitate the application of COBRA by as large a user community as available beam time allows and (2) to apply the COBRA method to obtain structural information on the high-temperature (high-Tc) complex oxide epitaxial systems prepared by Bozovic's group using their unique ALL-MBE growth facility. This structural information is crucial to achieving a complete understanding of the physics underlying the phenomena of high-Tc superconductivity.

APPROACH:
The combination of high brightness insertion device x-ray sources, efficient and precise surface x-ray diffraction measurements using new pixel array detectors, and new phase retrieval methods have resulted in model-independent structural determinations of a growing number of physical systems. The COBRA phase retrieval method, developed by two investigators on this LDRD (Pindak and Yacoby) together with R. Clark, is the only method that has succeeded in determining the structure of buried interfaces with sub-angstrom resolution. One of the investigators (Yacoby) has recently applied COBRA to discover the physical nature of three different phenomena observed in epitaxial thin films: (1) the striped to uniform ferroelectric domain transition as the thickness of ferroelectric epitaxial films is reduced, (2) changes in interfacial ordering at buried epitaxial interfaces as the result of metallic contact overlayers, and (3) the development of a 2D electron gas at the interface between complex oxide epitaxial layers.

Other investigators on the LDRD, I. Bozovic, A. Gozar, G. Logvenov, N. Bozovic, R. Sundling (CMPMSD) will prepare complex oxide epitaxial systems of various types that exhibit high-Tc superconductivity using their ALL-MBE growth facility and characterize the thermal and transport properties exhibited by these films.

TECHNICAL PROGRESS AND RESULTS:
A Post-Doctoral Research Associate, Hua Zhou, was hired and began work on October 22, 2007. Hua completed his PhD with Randy Headrick (University of Vermont) on “Ion-bombardment-induced self-organized nanostructures on sapphire”.

Prior to Hua's arrival, Yacoby and Pindak measured Crystal Truncation Rods (CTRs) for a 5 Unit Cell sample of $LaSrCuO_4$ on a $LaSrAlO_4$ substrate prepared by Bozovic's group. These preliminary measurements gave puzzling diffraction results that can only be fit using a model that has the in-plane lattice spacing of the epitaxial film evolve from being less-than to more-than the in-plane lattice spacing of the underlying substrate! One of Hua's first projects will be to see if these distinctive diffraction features only occur for the particular case studied or are characteristic for this class of epitaxial films.

Also prior to Hua's arrival, a proposal was submitted for beam time in the January-April cycle at the Advanced Photon Source (Argonne) to apply the COBRA method to obtain complete

structural information on the 2D high-Tc superconducting samples prepared by Bozovic's group [submitted to Nature]. The superconductivity in these samples is confined to the interface between metallic and Mott insulating complex oxide epitaxial layers.

On the agenda for the December NSLS SAC Meeting is a presentation regarding the purchase of the Psi 2+4 Circle Goniometer required for the implementation of COBRA on the NSLS X21 Wiggler Insertion Device (ID) beamline. There will be available space on this beamline when the X21 SAXS program is moved to the new NSLS X9 Undulator ID beamline in the fall of 2008.

Hua and the PIs will also collaborate with Randy Headrick to upgrade his existing surface diffraction chamber for accurate CTR measurements. This surface diffraction chamber is currently installed on the NSLS X21 Wiggler ID beamline

A meeting with Roy Clarke, University of Michigan, is planned for November 20 to discuss the formation of an NSLS phase-retrieval special interests group. Clarke has a Research Associate and two PhD students currently working in this area.

Development of a Planar Device Technology for Hyperpure Germanium X-Ray Detectors

LDRD Project 07-091
D. P. Siddons, I. Bozovic, and P. Rehak

PURPOSE:
The project aims to bring a mew manufacturing method for the fabrication of multi-element monolithic planar radiation detectors using germanium as the semiconductor. Manufacturing methods for this material have not followed the same development as that of silicon-based devices. As a result, multi-element detectors are not easily made, and more sophisticated devices such as drift-detectors are impossible to make. This program will open up a new range of applications for germanium detectors for use with synchrotron radiation sources.

APPROACH:
Synchrotron radiation experiments have steadily been shifting towards the harder end of the x-ray spectrum for a variety of reasons. Advanced detectors can be made relatively easily using planar silicon technology realized in high-resistivity silicon, but the absorption of x-rays by silicon drops rapidly above 10 keV for typical silicon wafer thicknesses. Of course, thick detectors can be made using lithium drifting techniques, but these do not allow complex detector configurations to be realized. Since the absorption of x-rays is proportional roughly to Z^4, it helps greatly to choose a semiconductor with higher Z than silicon. Germanium is eminently suitable for this task, and is capable of much better performance than some of the II-IV or III-V compound semiconductors which have been tried more recently. Thus, in spite of the need to cryo-cool germanium, it remains the material of choice for high-resolution hard x-ray and gamma-ray spectroscopy.

The techniques used to fabricate x-ray detectors from germanium have not changed in many years. They are essentially handmade in a small laboratory, and subject to the variability one might expect from such an approach. We were motivated to try to develop a technology which is closer to the planar mass-production technologies used in silicon to allow us to make efficient detectors with similar sophistication to those we currently make in silicon. This implies the need to develop doping recipes, passivating and insulating layers to prevent surface currents, and convenient cryo-cooling systems. Given these components we believe we will be able to do so.

TECHNICAL PROGRESS AND RESULTS:
There were delays in getting appropriate visas for the excellent Postdoctoral candidate that we succeeded in attracting. He finally was able to start on November 12th. In the meantime we have done some searching of literature, and purchased some raw material (a non-trivial exercise, since the number of companies growing hyperpure germanium is not large).

Now that the postdoc is on board, we hope to make rapid progress with the first stages of the project, which is to evaluate ion implantation recipes suitable for germanium, and the development of implantation mask materials to allow lithographically patterned implants. The second year will see us fabricating and testing real detector systems using these elements.

Study of Epigenetic Mechanisms in a Model of Depression

LDRD Project 07-096
Fritz Henn and Allison Liu

Purpose:

The goal of this project is to determine the control genetic background has over the magnitude of epigenetic effects using an animal model of depression. This model as developed in rats over the last decade has excellent face validity, pharmacological response and exhibits all the measurable physiological changes seen in depression. Two lines have been created through selective breeding one of which is susceptible to stress and develops the depressive like features while the other is resistant to a similar degree of stress, and does not exhibit depressive behavior. It is known that poor maternal care early in life will lead to an increased risk of depression in children as they become adults. We wish to look at the epigenetic changes caused by poor maternal care, determine which gene expression patterns are altered and determine if this is different between the two lines of animals when exposed to the same degree of maternal care. This will be the first demonstration of the degree of genetic control over environmental factors and will provide methodology to pursue such questions not only in human disease models but even when looking at the effects of environmental changes on plant growth. The development of rapid CHIP methodology to determine which genes change expression is the tool which can result from this project and which will aid in both medical and plant research.

Approach:

The demonstration that maternal care altered both rodent and human adult affective behavior suggested that epigenetic factors played a major role in depressive illnesses. There has been no clear demonstration of which gene expressions are altered nor to what degree genetic factors can influence epigenetic change. We see the opportunity to begin to understand both issues using the animal models available at BNL. This requires developing fast methods for screening gene expression and we have chosen to look at changes in methylation of DNA as a marker of epigenetic changes. To rapidly and reproducible assess this we have been working with Nimblegene, a gene technology firm, to create microarrays specific to this task. Concurrently behavioral studies were carried out to look at maternal care behaviors of our breeding mothers to design a controlled maternal deprivation paradigm. The major effort in microarray design and implementation was done by Dr. Liu who was hired to carry out the microarray portion of this LDRD.

Technical Progress and Results:

The project had to begin with the hiring of Dr. Liu, subsequently a graduate student Greg Garafola joined the team. New laboratory space was found and a CHIP laboratory was designed and put into place. The animals were bred and the maternal behaviors were video taped and scored, giving us base line data on the mothers. The second round of breeding was begun and wild type animals were trained and tested in the behavioral paradigm. The first run to isolate DNA and look at methylation patterns will be carried

out this month. In the next fiscal year, we should collect sufficient data to write an NIH grant and produce the initial publications.

Polarized Electron SRF Gun

LDRD Project 07-097

Ilan Ben-Zvi

PURPOSE:

The purpose of the project is to carry out research on the feasibility of using a superconducting, laser-photocathode RF electron gun (SRF photoinjector) for the production of polarized electrons. We expect to show that a cesiated gallium arsenide photocathode (which is necessary for the production of polarized beams) maintains it quantum efficiency in an RF gun and that that the migration of cesium from the cathode to the SRF cavity is so small that the properties of the gun will not be affected. This is a most desirable result since SRF gun outperform DC guns for high brightness beams. The motivation of this research is twofold: First, demonstrate that a SRF photoinjector can be used at the International Linear Collider (ILC) to eliminate the need for an electron damping ring. Second, such a gun would be at the heart of the linac for eRHIC, thus have a large impact on the future of the QCD laboratory strategic initiative at BNL.

APPROACH:

State-of-the-art polarized electron guns rely on the use of direct band gap III/V semiconductor NEA cathodes. When illuminated with circularly polarized laser light the cathode emits polarized electrons. Cathodes made of strained GaAs have been especially successful. The laser excites electrons from the valence band into the conduction band. To achieve reasonable emission efficiency the work function of the material has to be lowered. This can be accomplished by adding a monolayer Cesium and oxide to the surface. This surface layer is subject to rapid aging, which leads to a decrease of quantum efficiency of the cathode.

In DC polarized guns, we recognize two main contributions to the cathode aging process: Oxidation through reaction with the background residual gas in the vacuum system and ion impact on the cathode surface will both lead to degradation of the quantum efficiency. Both effects are proportional the vacuum pressure in the gun. While DC guns typically have a vacuum pressure of 10^{-11} torr, a normal conducting RF gun reaches only 10^{-9} torr due to out-gassing caused by the RF field. Under such conditions the cathode life time can be as short as 10 seconds. In a superconducting RF gun the cryo-pumping of the cavity walls improve the vacuum and the pressure can match that of a DC gun. While in a DC gun all ions are accelerated towards the cathode, only ions generated at the correct RF phase will reach the cathode and the maximum kinetic energy is limited due their high masses. With identical vacuum conditions the ion back-bombardment in a SRF gun can be an order of magnitude lower. In an RF gun, electron back bombardment is an additional cause of concern. The source of these electrons is field emission in the gun. However, the same extensive cleaning procedures that are used to improve the quality factor (Q) of the SRF gun cavity have been proven to reduce field emissions significantly.

The experiment consists of three major parts: a cryostat containing a 1.3 GHz SRF electron gun with a beam transport system, vacuum system and diagnostics; a cathode preparation chamber for the development of a strained gallium arsenide, cesiated photo-cathode under ultra-high vacuum (10^{-11}torr or better) and a transporter system allowing to move the cathode between the two systems while maintaining an ultra high vacuum. We use parts that became available from other projects to the largest extent possible.

The goal of the experiment is the measurement of the quantum efficiency lifetime of the cathode and the SRF performance of the gun over sufficiently long time to demonstrate the compatibility of the cathode with SRF performance and the compatibility of operation of the photocathode in high RF field in the gun.

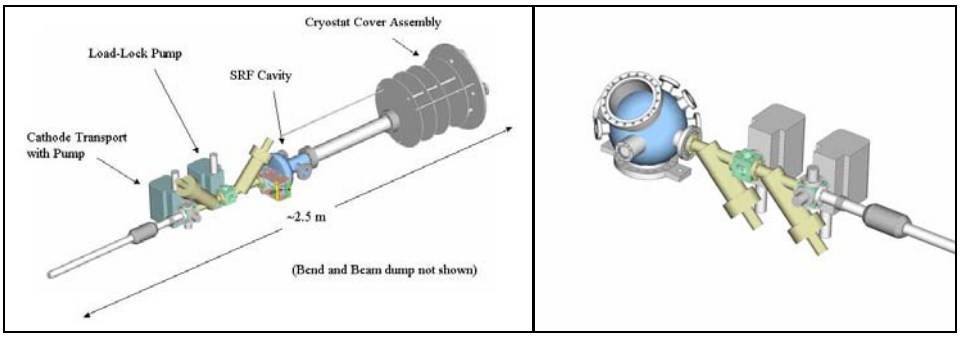

Figure 1: Gun assembly (removed from the cryostat) with attached transporter system and the preparation chamber with the attached transporter. Shown are also the valves and vacuum pumps that allow attaching and separating the transporter to both systems.

TECHNICAL PROGRESS AND RESULTS:

A detailed design for the transport system and the vacuum system was produced. A conceptual design for the beam transport, diagnostics and the preparation system was produced. Flow rates and pressure levels in the vacuum system were calculated. The cryostat and major parts of the vacuum system were purchased. A permanent magnet for focusing the beam was designed. A field compensation coil was designed. The field levels in the gun and the beam transport system were calculated with the computer code SUPERFISH. A 90° degree deflection magnet and a corresponding vacuum pipe with ports for diagnostic and the laser beam was designed. The beam transport from the cathode to the Faraday cup has been simulated with the computer code PARMELA. The existing 1.3 GHz gun has been cleaned and tested. The facilities at Jefferson Lab were used for this purpose. The gun reached a maximum gradient of 41 MV/m on axis, exceeding the requirements for this project. The cryostat was tested with liquid helium and the heat load was measured. Simulations were performed with PARMELA that show that is is feasible to replace the ILC electron injector and damping ring with a photo-cathode SRF gun and linac.

The time line for 2008 is as follows: Major components of the transporter system including the gate valves will be ready in FY09. The cavity modification will be done by 11/07, clamp system 03/08, transport assembly 05/08, cold mass assembly 09/08, focusing and bending magnets 04/08. A base line test of the cavity without modifications will be performed by 03/08.

New Approach to H_2 Production, Storages and Use

LDRD Project 07-098
Weiqiang Han

PURPOSE:

Hydrogen has great potential as an environmentally clean energy fuel and as a way to reduce reliance on imported energy sources. This requires safe and efficient hydrogen production, transportation, conversion and storage. In this project, we work on designing, synthesizing and characterizing new nanomaterials that have the possibility of meeting the criteria for high-efficiency hydrogen producing based on water-gas shifting (WGS) reaction and water splitting.

APPROACH:

Hydrogen can be produced from a variety of resources (water, fossil fuels, biomass) and is a byproduct of other chemical processes. In this work, we focus on WGS reaction. The WGS reaction ($CO + H_2O \rightarrow H_2 + CO_2$) is a critical process in providing pure hydrogen for fuel cells and other applications. The design and optimization of WGS catalysts are hindered by controversy about basic questions regarding the nature of the active sites and the reaction mechanism. A central challenge is the difficulty of characterizing the active state of the catalyst and the reaction mechanism. We have started a coordinated research program to understand the active sites and reaction mechanism for the WGS on promising metal (Au, Cu, Pt, Pd)/oxide (CeO_2, TiO_2, MoO_2), incorporating with extensive experimental efforts.

We also work on designing and synthesis of new oxide nanostructures (such as nanocavities and nanotubes) as the promising new routes for high efficiency absorbing solar energy for the photo-assisted WGS reaction and water splitting. Noble metals and Nobel metals containing bimetallic nanomaterials are important catalysts. We work on design and synthesis nano-noble-metals with different size, shape and chemical composition.

The major cooperators are Ping Liu (Department of Chemistry) and Xiaowei Teng (CFN).

TECHNICAL PROGRESS AND RESULTS:

A new method was developed to make anatase titania nanorods with dense regular nanocavities. Titanium oxide has been extensively used in photovoltaics solar-cells, water splitting catalysts for hydrogen generation and sunscreen. To improve the photoreactivity of TiO_2, several approaches, including doping and metal loading, have been proposed. The third route is to increase the photoreactivity of semiconductors. In this work, a simple novel approach is developed to produce dense regular polyhedral nanocavities in TiO_2 nanorods and found that these dense nanocavities significantly enhance the optical absorption coefficient of TiO_2 in the near-ultraviolet region, thereby providing a new approach to increasing the photoreactivity of the TiO_2 nanorods in the applications related to absorbing photons, such as photovoltaic solar-cell, water splitting and photo-assisted WGS catalysts for hydrogen generation.

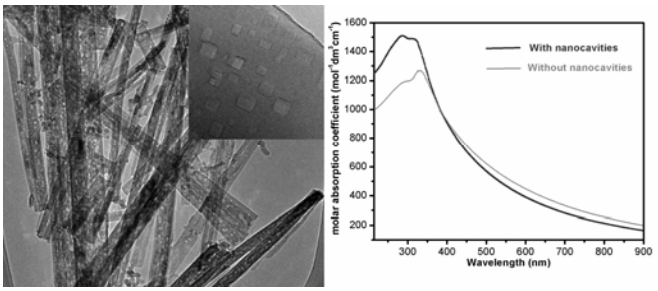

Figure 1 (a) TEM image of nanocavities inside titania nanorods; (b)titania nanorods with nanocavities have higher optical absorption than titania nanorods without nanocavities in the UV region.

Anatase TiO_2 nanorods supported palladium nanoparticles with loading of 0.5 %, 1%, 3% and 5% were prepared and the crystalline structure, size, bond distance, bond length disorder factor and catalytic activity towards WGS reaction were characterized and studied. We found good balance between particles size, loading, and stability might result in the best performance of the catalysts. The conclusion was evident by the fact that products with 3 % and 1% Pd loading were the most active in WGS reaction.

A new synthesis method is developed to make iron-doped titanate nanotubes with approximately 10 nanometers in diameter and up to one micrometerlong. These experiments were also aimed at improving the material's photoreactivity. It is demonstrated that the resulting nanotubes exhibited noticeable reactivity in the WGS reaction.

Using a phase transfer method, we succeeded in synthesizing ultrathin palladium and platinum nanowires (< 2.5 nm in width). Both nanowires show ferromagnetism up to room temperature. We developed a new synthesis route to prepare Au/Pd alloy nanostructure through the galvanic replacement reaction between Pd ultrathin nanowires (2.4 + 0.2 nm in width, over 30 nm in length) and $AuCl_3$ in toluene. We monitored both morphological and structural changes during the reaction for up to 10 hours. Continuous changing of chemical composition and crystalline structure from Pd nanowires to $Pd_{68}Au_{32}$ and $Pd_{45}Au_{55}$ alloys and Au nanoparticles was observed. These nano-noble metals are expected to have great potential as catalysts for hydrogen production.

Density Functional Theory (DFT) calculations is performed to investigate the WGS reaction on Au_{29} and Cu_{29} nanoparticles seen on CeO_2 (111) with STM. Figure 2 shows the calculated energy profile of the WGS reaction on Cu_{29}. Compared to Cu (100), water and CO bond to Cu_{29} more strongly by occupying the corner sites, which are generally considered more active than the terrace sites due to their low coordination. The water dissociation on the top of the cluster is also found to be more facile. The rate-limiting step for all these systems is the same, water dissociation. Within a micro-kinetic model based on the DFT calculations, WGS activity was estimated, which decreases in a sequence: Cu_{29} > Cu(100) > Au_{29} > Au(100). Our calculations agree well with the experiments (Au/CeO_2 > Cu/CeO_2 > $Cu/ZnO(000\bar{1})$ > Cu(100) >$Au/ZnO(000\bar{1})$ > Au(111)), where ZnO was found to act only as a support for the nanoparticles and did not participate directly in the reaction. This, however, is not the case for CeO_2, which appears to be directly involved in the reaction to facilitate the water dissociation. The behavior of Au/CeO_2 in the WGS illustrates the essential role that an oxide can have for the activity of supported Au nanocatalysts. The importance of cooperative effects cannot be overstressed. Similar studies was also carried out to investigate the WGS reaction on $Mo_2C(001)$ surfaces. Our results showed that the high WGS activity of Mo carbide observed experimentally is due to the formation of a Mo oxy-carbide in the surface of $Mo_2C(001)$ during the WGS reaction.

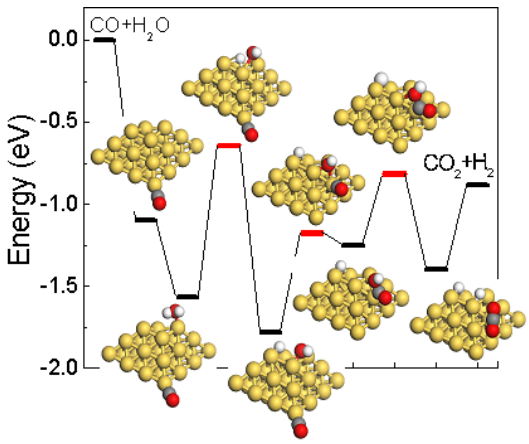

Fig. 2 DFT calculated energy profile for the WGS on a Cu_{29} nanoparticle. Cu: yellow; H: white; O: red; C: grey.

We will continuous to design, synthesize and characterize nano-oxide and nano-metals as the catalysts for high efficiency hydrogen producing. We will also work on synthesis of single-walled BN nanotubes, which have large potential for the application of hydrogen storage.

Increasing the Capability and Reliability of Small Diameter Direct Wind Multi-Layer Coil Magnets

LDRD Project 07-100
John Escallier

PURPOSE:
The goal of this LDRD was to characterize the thermal properties of compact small diameter Direct Wind superconducting coils designed for used in the Insertion Regions of various accelerators. Determining the precise quench threshold of coils built with this construction technique is a major priority and forms the goal of this development program

APPROACH:
With increasing frequency, accelerators are being proposed with greater demands on final focus magnets. These magnets are built very close to the interaction point, at times within the detectors themselves, and hence susceptible to energy deposition in the coil windings from beam loss. Coil construction is necessarily compact, with coils being wound directly on the beam tube or a concentric support tube. Prior work in this area limited the operation of such coils to a safe level below the capability of the superconducting cable, because of a lack of information on quench thresholds inherent in the assembled coil.

Beam loss calculations for the final focus ILC quads provide initial estimates of the thermal load within the magnets. No data exist regarding the quenching characteristics of direct wind multilayer magnets such as those proposed for the final focus magnets. Given the pulsed nature of the losses, standard quench heater elements cannot provide heat pulses of short duration, but rather, more of a steady state input. By embedding a low thermal mass heater within the coil pattern of a direct wind magnet, faster transient energy pulses can be provided to the superconducting wire. The transient heat pulses desired are consistent with beam loss simulations for low duty cycle high peak energy losses.

A detailed experimental program was conducted using strategically placed heating elements imbedded in dedicated test coils whereby safe limits for operation of the coils can be established. These energy threshold limits were explored by initiating quenches with the heaters at increasing current levels up to the known limit of the superconductor. This information then can be used to improve the design and reliability of these type of magnets which are the baseline magnets for the International Linear Collider (ILC) final focus quads, or for upgrades to the Large Hadron Collider at CERN (LHC).

The test coil package was designed by Dr. Brett Parker. It was comprised of 6 layers of 7 strand superconductor in the form of a quadrupole focussing magnet, of a diameter of 1 inch (24.5 mm) internally, and 6 inches (152 mm) long. This length allowed the use of an existing small cryostat system. Andrew Marone designed the physical package and the manufacturing process for the magnet. Dr. Muratore developed the test plan as well as implimented the cold tests of the magnet. Dr. Ghosh provided the test facility for

cool-down and operation of the magnet. Analysis of the results is currently being performed by Brett Parker and Joe Muratore.

TECHNICAL PROGRESS AND RESULTS:

1. Developed the low inductance high speed interleaved heater design used within the first layer of the magnet. It is a 4 ohm bifilar low inductance element to reduce coupling to the superconducting coil. An additional full length DC heater was placed under the entire coil of the magnet.
2. Designed and fabricated the heater fast pulse generator capable of 50 microsecond risetimes and falltimes while delivering sufficient energy per pulse to exceed the expected quench capability of the coilsets.
3. Designed and fabricated a tophat adapter to provide additional diagnostic capability for the existing magnet top hat design. This adapter allowed the use of all existing dewar/tophat hardware without dignificant modification. It delivers a 4 ohm heater stripline designed and built in house, the voltage taps, and all temp sensors to the magnet.
4. Wound the full, 6 layer, quadrupole test magnet with full instrumentation.
5. Successfully tested the quadrupole test magnet at 4.2 K with background fields ranging from 4 to 8 Tesla and under a variety of heater settings ranging from steady state (DC) heating, single pulse events, and fast (1 millisecond duration) pulses at 8 Hz repetition rate. The magnet's quench performance was quite consistent with no sign of training. We now have a large data set which we will analyze further to characterize the thermal properties of our direct wind coils.

We will undertake the detailed analysis of this data with a goal of relating these data to the expected energy deposition for the ILC IR magnets. As required we may consider making additional measurements with this apparatus as our understanding of the energy deposition requirements evolves. In particular the ILC repetition rate will be 5 Hz but with the available trigger pulser the slowest we could go was 8 Hz. With a different pulser it would be nice to replicate the actual ILC energy deposition time structure rather than scaling from a different repetition rate.

High End Scientific Computing

LDRD Project 07-101
James Davenport and Sam Aronson

PURPOSE:
The purpose of this LDRD is to establish at BNL, a laboratory competence in the efficient and effective utilization of large-scale, high-end computers in support of our multi-program research environment. The goal is to increase the number of applications which can take advantage of the new machines which are being deployed throughout the DOE complex.

We will accomplish this task by bringing together scientific expertise in laboratory mission areas with experts in computational science, applied mathematics, and computer operations.

APPROACH:
The current direction in high end computing is to build massively parallel machines with tens to hundreds of thousands of processors connected through complex communication networks. IBM's Blue Gene architecture is one example of such a machine, which currently is the world's fastest. In collaboration with Stony Brook University, BNL acquired a 100 teraflops Blue Gene/L during 2007. Called New York Blue, this machine contains 36,864 processors and is two orders of magnitude faster than a typical departmental cluster computer and one order of magnitude faster than the 10 teraflops quantum chromodynamics on a chip (QCDOC) machines currently in use at BNL. This unique resource enables investigations that are of a scale and complexity previously unavailable to BNL scientists. To further the goals, a CRADA has been established with Stony Brook University and the Research Foundation of SUNY.

Unfortunately, most codes and algorithms are not designed to take advantage of the immense power these machines offer. Typically, dividing a large problem among many processors does not lead to a comparable speed up in the calculation because of an imbalance between computation and communication. Therefore most codes need to be rewritten to be effective in this environment. This process requires a team approach with expertise in the scientific, mathematical and computational aspects brought to bear.

This project therefore involves a large number of collaborators in nuclear and elementary particle physics, nanoscience, computational biology, applied mathematics, fluid dynamics, and climate modeling. These teams are being formed, and in some cases have obtained early results.

TECHNICAL PROGRESS AND RESULTS:
In June 2007 the machine was installed and the operating and batch systems are working. A test run yielded the #10 position on the top500 computer list. More than 50 accounts have been set up. The CRADA with Stony Brook has been implemented.

For FY 2008 it is anticipated that the numerous additional projects will be brought to fruition and that the additional computing power of a Blue Gene/P with an additional 28 teraflops performance will be brought on line.